

SEARCH FOR RAPIDLY STAR FORMING GALAXIES
AT HIGH REDSHIFT

by

Richard Joseph Elston

A Dissertation Submitted to the Faculty of the
DEPARTMENT OF ASTRONOMY
In Partial Fulfillment of the Requirements
For the Degree of
DOCTOR OF PHILOSOPHY
In the Graduate College
THE UNIVERSITY OF ARIZONA

1 9 8 8

INFORMATION TO USERS

The most advanced technology has been used to photograph and reproduce this manuscript from the microfilm master. UMI films the text directly from the original or copy submitted. Thus, some thesis and dissertation copies are in typewriter face, while others may be from any type of computer printer.

The quality of this reproduction is dependent upon the quality of the copy submitted. Broken or indistinct print, colored or poor quality illustrations and photographs, print bleedthrough, substandard margins, and improper alignment can adversely affect reproduction.

In the unlikely event that the author did not send UMI a complete manuscript and there are missing pages, these will be noted. Also, if unauthorized copyright material had to be removed, a note will indicate the deletion.

Oversize materials (e.g., maps, drawings, charts) are reproduced by sectioning the original, beginning at the upper left-hand corner and continuing from left to right in equal sections with small overlaps. Each original is also photographed in one exposure and is included in reduced form at the back of the book. These are also available as one exposure on a standard 35mm slide or as a 17" x 23" black and white photographic print for an additional charge.

Photographs included in the original manuscript have been reproduced xerographically in this copy. Higher quality 6" x 9" black and white photographic prints are available for any photographs or illustrations appearing in this copy for an additional charge. Contact UMI directly to order.

U·M·I

University Microfilms International
A Bell & Howell Information Company
300 North Zeeb Road, Ann Arbor, MI 48106-1346 USA
313/761-4700 800/521-0600

Order Number 8906385

Search for rapidly star forming galaxies at high redshift

Elston, Richard Joseph, Ph.D.

The University of Arizona, 1988

U·M·I
300 N. Zeeb Rd.
Ann Arbor, MI 48106

SEARCH FOR RAPIDLY STAR FORMING GALAXIES
AT HIGH REDSHIFT

by

Richard Joseph Elston

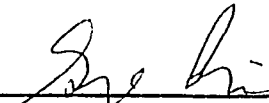

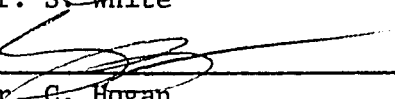
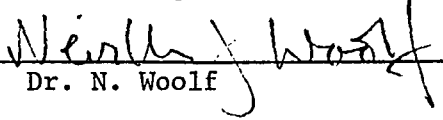
A Dissertation Submitted to the Faculty of the
DEPARTMENT OF ASTRONOMY
In Partial Fulfillment of the Requirements
For the Degree of
DOCTOR OF PHILOSOPHY
In the Graduate College
THE UNIVERSITY OF ARIZONA

1 9 8 8

THE UNIVERSITY OF ARIZONA
GRADUATE COLLEGE

As members of the Final Examination Committee, we certify that we have read
the dissertation prepared by Richard J. Elston
entitled Search for Rapidly Star Forming Galaxies at High Redshift

and recommend that it be accepted as fulfilling the dissertation requirement
for the Degree of Doctor of Philosophy.

 _____ Dr. G. Rieke	<u>11/18/1988</u> _____ Date
 _____ Dr. S. White	<u>11/18/1988</u> _____ Date
 _____ Dr. G. Hogan	<u>11/18/1988</u> _____ Date
 _____ Dr. N. Woolf	<u>11/18/1988</u> _____ Date
_____ Dr. R. Voight	<u>11/18/1988</u> _____ Date

Final approval and acceptance of this dissertation is contingent upon the
candidate's submission of the final copy of the dissertation to the Graduate
College.

I hereby certify that I have read this dissertation prepared under my
direction and recommend that it be accepted as fulfilling the dissertation
requirement.

 _____ Dissertation Director	<u>11/18/1988</u> _____ Date
Dr. G. Rieke	

STATEMENT BY AUTHOR

This dissertation has been submitted in partial fulfillment of requirements for an advanced degree at The University of Arizona and is deposited in the University Library to be made available to borrowers under rules of the Library.

Brief quotations from this dissertation are allowable without special permission, provided that accurate acknowledgment of source is made. Requests for permission for extended quotation from or reproduction of this manuscript in whole or in part may be granted by the head of the major department or the Dean of the Graduate College when in his or her judgment the proposed use of the material is in the interests of scholarship. In all other instances, however, permission must be obtained from the author.

SIGNED:  A handwritten signature in dark ink, appearing to be 'R. J. Et', is written over a horizontal line.

ACKNOWLEDGMENTS

It is such a great privilege to not only be allowed to do astronomy but to be paid to do astronomy that it is impossible to name just a few persons who have helped me. I thank my parents, Wolfgang and Lorraine, not only for their support but for giving me an interest in learning about the world. My best friend and love, Laurie Johnson, has made my world a better place to be during my graduate work. Steward Observatory has provided me with all the facilities any astronomer could want and the TAC has given me good access to them. Particular thanks to George and Marcia Rieke for not only providing me with the finest IR instrumentation but for also giving me their guidance and help. Lastly, all the other graduate students at Steward Observatory have given me both a stimulating place to work and a good supply of friends. I also thank those who helped pay for my fun, including a NASA Graduate Student Fellowship and a National Science Foundation Fellowship.

TABLE OF CONTENTS

	Page
LIST OF ILLUSTRATIONS	7
LIST OF TABLES	8
ABSTRACT	9
1. INTRODUCTION:	
OBSERVATIONAL LIMITS ON GALAXY FORMATION	1
2. DEEP 2μ IMAGING OF THE SKY.....	4
2.1 Introduction	4
2.2 Primeval Galaxy Models	5
2.3 Previous PG Searches	6
2.4 Identifying PG Candidates.....	8
2.5 Observations.....	14
2.6 R-K vs. K CM diagram and Red PG Candidates	27
2.7 Follow Up Observations of Red PG Candidates	31
2.8 Blue PG Candidates	40
2.8.1 Candidate Star Forming Galaxies at $z = 4$	41
2.8.2 Star Forming Galaxies at $z < 3$	46
2.9 Galaxy Counts in the Near IR	47
3. LYMAN α IMAGING OF $z = 3$ QUASAR ENVIRONMENTS	53
3.1 Introduction	53
3.2 Expectation for Lyman α emission from PGs	54
3.3 Observations	58
3.4 Discussion	69
4. THE STELLAR POPULATIONS OF	
BLUE RADIO GALAXIES	78
4.1 Introduction	78
4.2 Observations	79
4.3 The Case of 3C256	87
4.3.1 The Current Star Formation Rate	87
4.3.2 The Ratio of Past to Current Star Formation	88
4.4 Discussion	91
5. CONCLUDING REMARKS	96
LIST OF REFERENCES	99

LIST OF ILLUSTRATIONS

	Page
Figure 2.1. Number vs. K for PG Models	26
Figure 2.2. R-K vs. of Redshift for Galaxies	29
Figure 2.3. R-K vs. of K for Giant Elliptical Galaxies	31
Figure 2.4. Noise vs. Integration Time	37
Figure 2.5. Contour Plot of IR Image Pair.....	38
Figure 2.6. Photometry Errors	46
Figure 2.7. Observed R-K vs. K diagram	50
Figure 2.8. Observed R-K vs. R-I diagram	51
Figure 2.9. Optical Spectrum of Red PG Candidates	57
Figure 2.10. Spectral Energy Distributions of Red Objects	58
Figure 2.11. Surface Photometry of Red PG Candidates	63
Figure 2.12. Optical Image of of PG Candidates	64
Figure 2.13. Spectral Energy Distributions of Blue Objects	73
Figure 2.14. Optical Spectrum of 130527.1+294634	74
Figure 2.15. Galaxy K Corrections for the K band	83
Figure 2.16. Model and Observed IR Galaxy Counts	86
Figure 2.17. Model Redshift Distribution of IR Selected Galaxies	88
Figure 3.1. Lyman α Equivalent width vs. time	95
Figure 3.2. Photometric Color vs. Lyman α EW	96
Figure 3.3. Observed V-N Color Magnitude Diagram for Quasar Fields.	103
Figure 3.4. Distribution of V-N Colors	113
Figure 3.5. V-N vs. V for Line Excess Objects	114
Figure 3.6. Distribution of V Magnitudes for Companions	116

Figure 3.7. Distribution of Lyman α Flux	117
Figure 4.1. Spectral Energy Distributions of 3C Radio Galaxies	130
Figure 4.2. Model Spectral Energy Distributions	139
Figure 4.3. V Luminosity Evolution of a Star Burst	142
Figure 4.4. H-K vs. J-K Color-Color Diagram for Radio Galaxies	145

LIST OF TABLES

	Page
Table 2.1. Journal of IR Survey Observations	40
Table 2.2. Photometry of IR Selected Objects	41
Table 2.3. IR Photometry with the MMT	48
Table 2.4. Photometry of Red PG Candiates	53
Table 2.5. Photometry of Luminous Red Galaxies	55
Table 2.6. Photometry of Blue IR Selected Objects	71
Table 3.1. Quasars Observed for Lyman α Companions	99
Table 3.2. Narrow Band Excess Objects	102
Table 3.3. Comparison of Spectral and Photometric EW for Quasars ..	111
Table 4.1. Photometry of Blue 3C Radio Galaxies	127

ABSTRACT

We have conducted three surveys to try and locate distant star forming galaxies. The most general survey used deep 2μ images with optical CCD photometry to locate objects with peculiar SEDs. Using the IR data we should be able to locate rapidly star forming galaxies to $z = 25$. With a 3σ detection limit of 18.5 at K we have found no objects with $z > 5$ but we have found several blue objects at $z < 4$ in $16min^2$ of sky. This suggests that there is no extremely luminous early phase of galaxy formation.

We have found several blue objects at $z < 4$ in $10min^2$ of sky. Of particular interest is an object which has a flat SED from V to K but shows a strong spectral break between B and V and a weaker break at 5800\AA . We suggest these may be Lyman limit and Lyman α forest absorption at $z=3.8$ in a galaxy forming $\approx 400M_{\odot}year^{-1}$ of stars. A large sample of galaxies (100 objects) selected to have similar properties ($R - I < .5$, $B - R > 1$) has also been found. From this sample it appears this possible high redshift star forming phase only contributes 1/10 of the metal present in disks or spheroids.

We have also found 30 Lyman α emission line companions to 12 $z = 3$ quasars. These objects have Lyman α equivalent widths (50\AA) and luminosities ($V = 24$) consistent with galaxies forming $\approx 100M_{\odot}year^{-1}$ of stars. Also, 2 of the quasars have 8 companions and may be in cluster environments. Radio luminosity may be correlated with a richer environment.

A final survey analyzed optical to IR SEDs of luminous blue radio galaxies at $z > 1$. In these objects we find SEDs indicative of star formation rates between 10 and $100M_{\odot}year^{-1}$ but interpretation is difficult due to the AGN component of the sources.

While these data seem to suggest a significant star forming phase taking place in galaxies at $z \approx 3 - 4$, interpreting this result is difficult since we can not determine if we are observing disk or spheroidal populations. In the case of the quasar companions and the radio galaxies, consideration of their dense environments and current epoch morphology suggests that these may be spheroids but these galaxies may not be typical of galaxies in general.

Chapter 1

Introduction: Observational Limits on Galaxy Formation

This thesis is an investigation into the star-forming periods which punctuate the lives of galaxies. The question we would like to answer is "are there short periods of time when galaxies form the bulk of their stars?". The approach we adopt to attack this question is to try and directly observe distant galaxies which are in luminous star forming phases. The "how and when" of star formation is one of the central questions in studies of the stellar populations of galaxies. The when of galaxy formation is also central to the study of the formation of structure in the universe. Finally, an understanding of the star formation histories of galaxies is critical if one wishes to use galaxies as probes of cosmology.

The classic view of galaxy formation is the collapse and metal enrichment model presented by Eggen, Lynden-Bell and Sandage (1962). They found correlations between $[\text{Fe}/\text{H}]$ and the eccentricity, angular momentum and W velocity of the orbits of local sub-dwarf stars around the Galaxy and inferred that the Galaxy underwent

enrichment during a star-forming phase that lasted less than about 2×10^8 years, coincident with its collapse. A chemical gradient is a signature of star formation during such a dissipative collapse. But the evidence for such gradients in the halo of our galaxy is mixed. For globular clusters Zinn (1985) found marginal evidence for metallicity gradients, with little gradient for $R > 7 Kpc$ for low metallicity clusters. Norris (1986) found no correlations with kinematics for low metallicity dwarf stars in contrast to the results of Sandage (1986). The origin of this discrepancy is not clear. In M31, Mould (1986) finds a rather flat or nonexistent metallicity gradient in the halo. However, the bulge of our galaxy does appear to have a metallicity gradient (Blanco 1988, Terndrup 1988)

Much current research in galaxy evolution has focused on the effects of the environment on galaxies, especially interactions between galaxies and the resulting mergers or stripping of stars (see Dressler 1980 for a review). In this context galaxy formation would be a slow process of assembly and spheroids could be built up from shredded disks (Toomre 1977). It appears that interaction can lead to large "bursts" of star formation (Larson and Tinsley 1978, Cutri and McAlary 1983, Lonsdale et al. 1983, Schweizer 1982) but these appear to produce only a few percent of the stellar mass of a galaxy even in extreme cases (Rieke et al. 1985). Djorgovsky et al. (1987b) has argued that some of the structure seen in 3C radio galaxies at $z > 1$ may be due to dissipative mergers, but the recent finding that radio lobes and optical isophots are aligned in these sources (Chambers et al. 1987) does not

fit this picture well.

In the context of galaxy formation by mergers one would not expect a metallicity gradient but would perhaps expect multiple generations of stars if star formation accompanied the merger events. As noted above such mergers do appear to trigger large amounts of star formation. One could hope that spectral synthesis could address the problem of whether spheroids are single age populations or composite populations. The results of spectral synthesis on E galaxies appears to indicate significant star formation at recent times (about 5 Gyrs) (O'Connell 1976, Rose 1985, Pickels 1985). Taken at face value this would indicate multiple generations of stars if the oldest stars formed at times similar to globular clusters. Unfortunately, there is a great deal of uncertainty in how to convert the main sequence turn off color derived by spectral synthesis into an age. Renzini (1986) has pointed out that small corrections to the mixing length, metallicity and convective overshooting of the core can give last burst ages consistent with globular clusters, thus removing the need for multiple generations of stars.

The only spheroidal populations which can be studied in detail are the dwarf ellipticals of the local group and the bulge of our galaxy. For dwarf ellipticals, the presence of luminous carbon stars suggests that multiple generations are present in at least some cases (Fornax, Leo I and Carina, Azzopardi et al. 1985) but others show no such evidence. For the galaxy, Frogel and Whitford (1987) argue that the stars of the bulge are as old as those in globular clusters.

We are left with a rather unclear picture of how galaxies form their stellar populations. Evidence for star formation during dissipative collapses is provided by chemical gradients but it is not clear if chemical gradients are present. Formation by slow assembly would be supported by evidence for multiple generations of stars but this evidence is not clear except for the special cases of dwarf ellipticals where it is both supported and contradicted. Fortunately, galaxies during vigorous periods of star formation should be very luminous and thus one could hope to observe these star-forming episodes directly even at extremely large look back times (Partridge and Peebles 1967, Meier 1976). It is the approach of direct observations which we shall take in this thesis by trying to find and study star forming galaxies at several epochs.

In the next three chapters I will describe three studies aimed at finding and studying galaxies which are in the process of forming the bulk of their stars. Chapter 2 presents the results of a near IR survey for galaxies undergoing an initial collapse phase at redshifts up to $z=25$. Chapter 3 will discuss a survey of the environments of $z=3$ QSOs looking for Lyman alpha emission from galaxies near the QSOs. Chapter 4 will describe a study of high redshift radio galaxies with very blue optical colors which appear to be producing significant quantities of stars. Finally chapter 5 will try to tie this new information into our understanding of the formation of galaxies.

Chapter 2

Deep 2 micron Imaging of the Sky

2.1 Introduction

With the recent development of array detectors which operate beyond 1 micron (see *Infrared Astronomy with Arrays* edited by Wynn-Williams and Becklin 1987), it has become possible for the first time to investigate the sky to very low light levels in the near IR. We have made the first deep 2 micron images of the sky. These observations were made to try and detect very distant galaxies as they undergo a theorized luminous initial collapse phase at $z < 25$ (Partridge and Peebles 1967, Meier 1976). Also, deep 2 micron images should contain many distant galaxies with $z > 1$. These galaxies can be used to place constraints on cosmology and the formation epoch of galaxies.

The near IR is well suited to the study of high redshift galaxies for several reasons. Even in the rest frame, the spectral energy distributions (SEDs) of normal galaxies peak in the near IR. As galaxies become more distant the SEDs get shifted

further into the IR with redshift. High redshift galaxies are as easily detected at 2 microns as on deep optical CCD images (Walsh et al. 1985, Lilly et al. 1985). The infrared colors are relatively insensitive to the evolution of the stellar population because the near IR is dominated by the light from giant stars whose colors vary little with mass or age. Thus, for galaxy counts in the near IR the K corrections for almost all galaxy types are the same and the form of the evolution is simple. In addition, the near IR holds the promise of being able to detect objects which emit very little radiation in the visual. Such objects could be high redshift galaxies where the Lyman limit or Lyman alpha forest absorption lies above the visual or those reddened either by dust within the galaxies or in the intervening space.

Boughn, Saulson and Uson (1986) used a single-detector near IR photometer to look at the smoothness of the 2 micron background in a search for primeval galaxies. Although this study did place useful limits, it appeared possible to produce significantly better results with an infrared camera, even on a smaller telescope. In this chapter we shall review galaxy formation theories which predict luminous collapse phases. Then we shall take a brief look at other primeval galaxy searches, with an eye toward understanding how a near IR survey can advance the state of our knowledge. Finally, we shall describe our survey.

2.2 Primeval Galaxy Models

Before considering individual detailed models we will investigate what general limits can be placed on the collapse epoch of galaxies. The simplest limit that can be placed on the formation epoch of galaxies is by equating the present density of matter within galaxies with the matter density of the universe at the time of formation. This provides an upper limit on the formation epoch of about $z=30-40$ ($q_o=.5$) since galaxies could not have collapsed at an earlier time and have achieved densities as low as they now have.

An additional general constraint on the collapse epoch of galaxies can be gained from the spin parameter of Hoyle (1945);

$$\lambda = \frac{\sqrt{EJ}}{GM^{2.5}} \quad (2.1)$$

For self gravitating dissipational collapse $\lambda \propto r^{-.5}$. The initial value of Lambda for dissipative clustering is found to be near .05 for a large range of conditions (Barnes and Efstathiou 1987). For rapidly rotating spiral galaxies $\lambda = .4$. Such a large value implies a very large collapse of a factor of 100, which would require a collapse time greater than a Hubble time. To solve this problem one can place the dissipative material in a halo of dissipationless matter: then $\lambda \propto r^{-1}$. This reduces the collapse to a factor of 10 with a collapse time of a few times 10^9 years for a $10^{11} M_{\odot}$ galaxy. For elliptical galaxies and slowly rotating bulges the final $\lambda = .1$. This implies much smaller collapse factors and collapse times of only a few times 10^7 years. Thus, one

would expect E galaxies and slowly rotating bulges to form first at high redshift ($z=10-20$). If merging occurs (i.e. if spheroids are formed by mergers) there is no reason to believe that λ will be conserved.

Partridge and Peebles (1967) produced a PG model which seems to have been strongly motivated by the notion of a rapid collapse and enrichment model of the halo discussed by Eggen, Lynden-Bell and Sandage (1962). In order to collapse in a free fall time the model has no dissipation. This leads to a very short (3×10^7 year) bright phase in which most of the metals in a galaxies spheroid are produced. Also, the Partridge and Peebles PG is extended with rather uniform surface brightness. They demonstrated that the spectral energy distribution of a PG would be dominated by the hot O and B stars. Thus, the SED is like a hot black-body ($T=30000K$) with an abrupt drop of about 20 in F_ν at the Lyman limit. Partridge and Peebles also pointed out that the Lyman alpha line could have about 6% of the bolometric flux if there is a large hydrogen nebula to reprocess the Lyman continuum radiation into Lyman alpha emission. However, without dissipation it is not clear that galaxies with the proper density profiles will be produced.

Meier (1976) produced PG models based on the dissipative collapse models of Larson (1974). As a result of dissipation Meier's PGs have a longer bright phase (2×10^8 years) and a more compact core than those of Partridge and Peebles. The longer bright phase would result in fainter PGs than those described by Partridge and Peebles but the more compact core would give these objects higher surface

brightness and would make them easier to detect. Also, Meier constructed more detailed SEDs based on Kurucz (1979) stellar atmosphere models. These SEDs were very flat longward of the Lyman limit with a drop of about 10 at the Lyman limit. Using Larson's simple parameterization of the star formation rate these dissipational galaxy models produced galaxies with luminosity profiles and metallicity properties similar to elliptical galaxies.

Recently Baron and White (1987) developed an inhomogeneous dissipative collapse model for PGs. This model was motivated by hierarchical clustering models for the formation of structure in the universe. Their model produces galaxies slowly as preexisting clumps merge to produce the final galaxy. Baron and White's PGs form late with a long bright phase lasting a few times 10^9 years. The long bright phase of their model coupled with very extended morphology leads to PGs with very low surface brightness making detection very difficult.

The great diversity in PG models makes it very difficult to design a single search which would be effective for detecting all the predicted PGs, but the diversity of PG models also argues for the necessity of PG searches to constrain possible models. With our IR search we will target PGs with high luminosity (i.e. high star formation rates) at redshifts up to 20. Such objects could be large E galaxies and large slowly rotating bulges for which one would expect early formation times if merging is not important.

2.3 Previous PG Searches

The seminal paper by Partridge and Peebles (1967) stimulated a large number of primeval galaxy searches. A good review of these observations is given by Koo (1986a); here we shall only briefly review the searches so that we can try and understand their possible limitations and to illustrate how an IR search can overcome some of these. Basically, searches for discrete PGs can be broken into 2 classes. There are imaging searches where one either looks for objects morphologically similar to PGs or one looks for objects with unusual optical colors. Also, there are spectrographic searches where one looks for strong emission from a Lyman α line.

Partridge (1974) and Loh and Wilkinson (1979) used red imaging to look for red extended PGs but no PGs were found. Also, optical color surveys have been used to look for compact blue PGs but QSOs are the only product of such surveys (Koo 1985). Finally faint magnitude limited surveys of galaxies could locate PGs if they occurred at a bright enough level (Koo and Kron 1987, Ellis et al. 1987), once again none have been found.

Spectral searches have been carried out in several ways. Deep long slit spectra have been taken of blank sky looking for Lyman α emission (Koo and Kron 1980, Cowie 1985). While such surveys produce low flux limits if the Lyman continuum flux is converted into Lyman α flux efficiently and the Lyman α emission can escape, the areas covered are not large. Slit-less spectral searches have also been used but

they produce poorer flux limits (Koo and Kron 1980). Finally Pritchett and Hartwick (1988) have used moderate band width filters (100\AA) to image the sky looking for excess line emission in one band.

Another class of PG searches consists of attempts to detect the extragalactic background light due to PGs by making measurements of the brightness of large areas of the sky. Only limits have been derived for the optical background light but a possible detection has been reported at K by Matsumoto et al. (1988). The limitation of this technique is that it does not locate individual objects which can be studied in detail and requires the removal of the signal from stars and low redshift galaxies. Given the brightness of the K background it must have a large contribution from normal galaxies.

The failure of these searches suggests the constraint on PG models that "galaxies do not go through a bright PG phase". Due to limitations of the searches, such a constraint is not strong. It seems doubtful if any of these optical surveys could locate PGs where the optical lies below the Lyman limit in the PG ($z > 7$). Thus, the above constraint would be weakened to "PGs do not have a bright phase at $z < 6$ or 7 ". The addition of dust would weaken the constraint further. Also, all the spectral surveys which depend on line emission to detect PGs would not place useful constraints on PGs if the line emission from PGs was not strong. Indeed, Meier and Terlevich (1981) and Hartman et al. (1988) do not detect strong Lyman α emission from low metallicity star forming dwarf galaxies which should have conditions similar

to PGs. The strength of the Lyman α line seems to be correlated with metallicity such that one gets stronger Lyman α emission from lower metallicity galaxies. Thus, one would expect significant line emission from galaxies only until they pollute themselves with metals, only a few times 10^6 years. Such a short Lyman α bright phase would make the sky density of PGs so low that long slit spectral searches with their small sky coverage are doomed to fail.

A search for PGs by near IR imaging can overcome the above problems. First, the Lyman limit does not pass through the K band until $z=2.5$. Also, observing in the near IR would greatly reduce the susceptibility to dust absorption. Finally, IR imaging provides precise locations for candidate objects and combining optical with IR observations of objects facilitates the recognition of PGs. In the next section we shall discuss how one may identify a PG from an IR survey.

2.4 Identifying PG Candidates

Once a survey has been made the major difficulty lies in selecting PG candidates out of the sea of giant-dominated galaxies. To do this, one would like to use properties which are common to all PG models. In this section we shall review a few properties that all PG models predict. These properties can then be used to find good PG candidates.

The spectral energy distribution (SED) of a PG should be dominated by hot O

and B stars as pointed out by Partridge and Peebles (1967). The more complete spectral synthesis by Meier (1976) indicates that the SED will be very flat redward of the Lyman limit for much of the bright phase. Initially, the SED is Rayleigh-Jeans for the first 10^7 years; then it becomes flat until a few times 10^8 years when a red population begins to dominate. While it is agreed that there will be a drop in flux blue-ward of the Lyman limit, the exact amount is less clear. The depth of the Lyman limit will depend critically on the initial mass function and the amount of hydrogen in the PG, since hydrogen processes Lyman continuum radiation into line emission. Without hydrogen reprocessing in the nebula, Partridge and Peebles predict a drop in flux of about 20 over the Lyman limit while Meier predicts a depth of about 10. If there exists large amounts of hydrogen the PG could be nearly black below the Lyman limit but depending on the filling factor and geometry this need not be the case. Also, absorption by intervening Lyman α forest clouds could decrease the flux of the PG between its Lyman α line and the Lyman limit. Such absorption seems likely from the observed spectra of high redshift QSOs. Thus, it seems that any good candidate PG should have a fairly flat spectrum with a drop in flux into the blue. A PG with strong Lyman α forest absorption would not have the classic sharp break at the Lyman limit that is expected.

The number density of PGs on the sky should also be predicted by any PG theory. Unfortunately, this density is rather uncertain because it is very cosmology dependent. It also depends on the formation redshift and length of the bright

phase. We can derive an approximate relation for the number density on the sky by combining the volume element (2.2) with the relation between proper time and the redshift (2.3). For the case that the length of the bright phase is short compared to the Hubble time at the redshift we find the number density is given in equation 2.4 (Boughn, Saulson and Uson 1986).

$$\frac{dV}{dz} = \frac{4\pi c^3}{H_o^3 (1+z)^6} \frac{(q_o z + (q_o - 1)(\sqrt{1+2q_o z} - 1))^2}{q_o^4 \sqrt{1+2q_o z}} \quad (2.2)$$

$$t = \frac{\sqrt{1+2q_o z}}{(1-2q_o)(1+z)} + q_o (2q_o - 1)^{-3/2} \cosh^{-1} \left(\frac{1 - q_o(1-z)}{q_o(1+z)} \right) \quad (2.3)$$

$$N = 653h \left(\frac{n}{8 \times 10^{-3} Mpc^3} \right) \left(\frac{\Delta\tau}{10^8 years} \right) \left(\frac{(q_o z + (q_o - 1)(\sqrt{2q_o z + 1} - 1))^2}{(1+z) q_o^4} \right) deg^{-2} \quad (2.4)$$

Figure 2.1 shows the number of primeval galaxies for various cosmologies and formation epochs. Here we have assumed that the number of large E galaxies equals the number of PGs ($3 \times 10^{-3} Mpc^{-3} h^{-3}$, Davis and Huchra 1982, Ellis 1983). Another approach is to assume a value of M/L for the spheroidal component of galaxies and integrate the luminosity function to find the number of total number of galaxies with bright phases more luminous than a given value. We have done this in figure 2.1 using a Schechter(1980) luminosity function with $\alpha = -1.07$, $L_* = 10^{10} L_\odot h^2$ and $\Phi_* = 3 \times 10^{-3} Mpc^{-3} h^{-3}$. Here the major uncertainty is in the value one should

assume for M/L since the nature of dark matter in galaxies is unknown. For our calculation we have chosen a value of $M/L = 10$ which is both close to the inferred M/L for the inner bulges of galaxies and to theoretical values of M/L for an old stellar population. Due to the cosmological uncertainties and the lack of consensus on the length of the bright phase no firm prediction can be made as to what the density of PGs should be. What is clear is that any good PG candidates should be very numerous on the sky.

Cowie (1987) has pointed out that the sky brightness (eqn. 2.5) of PGs should be related to the current metal density of spheroids in a manner which is fairly independent of cosmology or the length of the bright phase. This comes about because we assume the SED is flat for a PG and thus has no spectral term in its K correction and because the cosmology dependence of the volume element cancels the luminosity distance of the PGs. We note that this assumption will be violated at large burst ages ($\tau > 10^9 \text{ years}$) and very young ages ($\tau < 10^7 \text{ years}$). Assuming a flat SED, all that remains is the amount of energy released by the PG which can be simply related to the amount of metals produced.

$$S_\nu = 4 \times 10^{-25} \left(\frac{\rho_z}{2 \times 10^{-34} g \text{ cm}^{-3}} \right) \text{ erg cm}^{-2} \text{ sec}^{-1} \text{ Hz}^{-1} \text{ deg}^{-2} \quad (2.5)$$

The major uncertainty is the current metal density of the universe which is appropriate to the bright phase of PGs. For stars in spheroids Cowie finds the metal density to be $5.6 \times 10^{-34} h^2 g \text{ cm}^{-3}$. If one considers an x-ray emitting cluster of

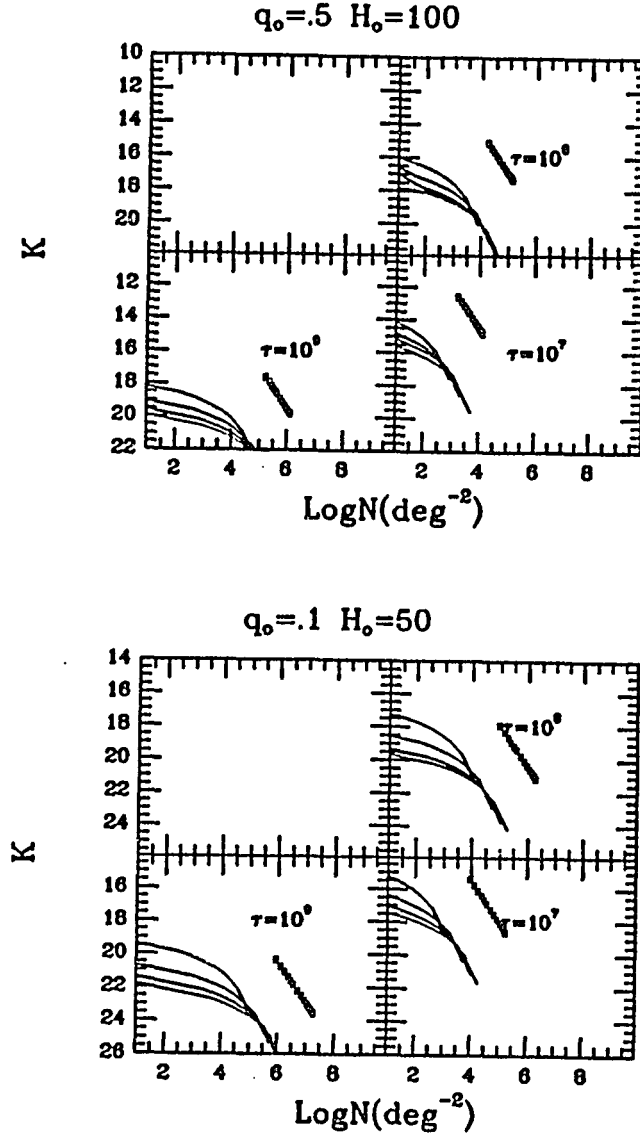


Figure 2.1: Predicted K magnitude and number density of primeval galaxies. Models are presented for a galaxy which processes $10^{12} M_{\odot}$ of hydrogen into solar metallicity stars with four different durations of the bright phase ($\tau = 10^7, 10^8, 10^9$ years). Points are given for formation redshifts of 5, 6, 7, 8, 9, 10, 12, 14, 16, 18, 22 and 24, with $z=5$ being the brightest point. Also, separate plots are presented for a very large ($q_0=0.1$, $h=0.5$) and a very small cosmology ($q_0=0.5$, $h=1$). Note that all models lie along a single line of constant sky brightness. Also shown are the integral galaxy counts for a Schechter(1980) luminosity function with $L_* = 10^{10} L_{\odot}$ and $M/L = 10$ for the spheroidal components of galaxies. Lines are for formation epochs of 5, 10, 15 and 20.

galaxies one would predict 2-3 times more metals for the observed stars because the metals in the gas dominate the metals in the stars. Since it seems possible that all galaxies would eject large amounts of enriched gas during rapid star forming phases this may well be the correct metal density and the cluster potential just retains this gas making it observable. Once again if star formation continues for longer then a few times 10^8 years the assumption of a flat SED will be violated because the spectra will become dominated by supergiants (Renzini and Buzzoni, 1986). In any case a population of luminous PGs should have a sky brightness consistent to within a factor of 3 of that given in equation 2.5.

Since optical surveys are most effective at finding low redshift PGs ($z < 6$) we decided to target our survey toward finding luminous high redshift PGs . A good way to proceed is to look for objects with redshifted Lyman limits between the near IR and the visual, which can be identified by their flux decrements between these spectral regions. Also, it is necessary to survey an area of about 10 square arcminutes to have a good chance of finding a PG. Lastly we must consider to what depth a survey should be conducted. From the spectral energy distribution of Meier (1976) we can predict the luminosity of a PG (eqn. 2.6). We will assume that a PG generates the metal contents of galaxy in a time which we shall parameterize in terms of 10^8 years.

$$L_{\nu} = 5 \times 10^{31} \left(\frac{M}{10^{12} M_{\odot}} \right) \left(\frac{\tau}{10^8 \text{ years}} \right)^{-1} \text{ erg sec}^{-1} \text{ Hz}^{-1} \quad (2.6)$$

For various values of cosmological parameters Figure 2.1 shows the K magnitude of a PG which produces $10^{12} M_{\odot}$ of solar metallicity material in a time τ . All the PG models lie along a single line in figure 2.1 which is a line of constant sky brightness as suggested by Cowie (1987). A survey to $K = 18$ should provide viable detection limits for PGs. A decrement of greater than 10 in F_{ν} between R and K gives $R - K > 4.5$.

A further problem at $K = 18$ is differentiating PGs with Lyman decrements of 10 from galaxies at $z=1$. To illustrate, we note that galaxies without ongoing star formation are the reddest galaxies at any redshift. Figure 2.2 shows the $R - K$ colors of model elliptical galaxy at various redshifts. We have plotted model E galaxies from Bruzual (1983). A 'c' model has no star formation after an initial burst of star formation at $z=5$, also shown is a ' $\mu = .5$ ' model galaxy which has exponentially declining star formation with half the stars formed during the first 10^9 years. We have also plotted the colors of a nonevolving elliptical since this may reproduce the colors of real galaxies better than Bruzual models. These colors were produced by convolving a spectrum obtained from observations of elliptical galaxies and spiral bulges with the filters. All these indicators show an envelope to the galaxy colors, with no galaxies expected redward of the envelope. The reality of this limit to the colors of galaxies at any redshift is confirmed by observations of high redshift elliptical galaxies (Eisenhardt and Lebofsky 1987, Lilly, Longair and Arllington-Smith 1985). From these curves it appears that galaxies with $z \geq 1$ can

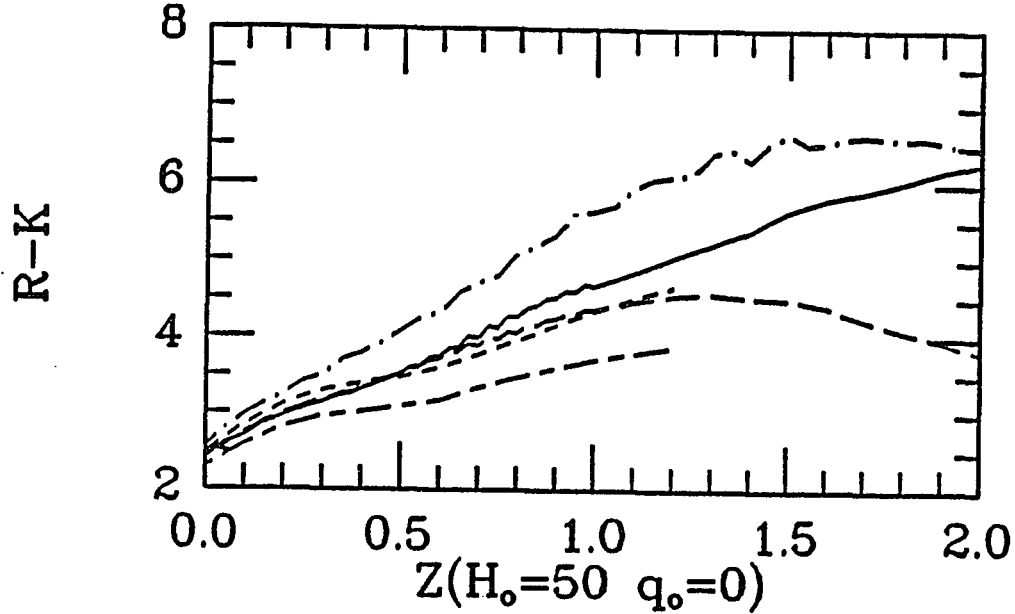


Figure 2.2: The predicted $R - K$ colors of various model galaxies as a function of z . The solid line and the long dashed line are for 'c' and ' $\mu = .5$ ' model galaxies presented by Bruzual (1983) respectively. The long dash-dot line is for an unevolving elliptical galaxy. The short dashed line and the long-short dashed lines are for unevolving red and blue spiral galaxies respectively (Sbc and Scd) using optical K corrections from Coleman, Wu and Weedman (1982). We note that until $z=1$ all the model galaxies rise monotonically in $R - K$ with z .

be easily confused with primeval galaxies. Also, figure 2.2 shows that the $R - K$ color can be used as a crude redshift indicator since there is little dispersion for varied galaxy types and the $R - K$ color is monotonic and steeply rising for $z < 1$.

Let us consider the above color redshift relation in a color-magnitude plane. Since the reddest galaxies are giant E galaxies which are also the most luminous galaxies, these can be used to define an observational red envelope in the $R - K$ vs. K color magnitude diagram. Figure 2.3 shows the $R - K$ vs. K color-magnitude diagram for brightest cluster ellipticals ($M_V = -22.4$, $q_0=0$) for the same model galaxies as

in figure 2.2. Ongoing star formation, as seen in the ' μ ' model mainly makes the galaxy bluer while brightening it only slightly. Thus, star forming galaxies will stay below our theoretical "red envelope". One possible exception to this behavior is due to the Bruzual models not including AGB stars which could be a dominant near IR component when the turn-off mass is between 2 and 5 solar masses (Renzini and Buzzoni, 1986). While there is no observational support for this AGB reddening, since the near IR colors of high redshift galaxies do not exceed the red envelope (Lilly and Longair 1984, Eisenhardt and Lebofsky 1987), this is not a major concern. But since previous observations only sampled a small number of specially selected galaxies the red envelope should be considered a prediction which needs to be tested.

The existence of this red envelope suggests a means to differentiate PG candidates from the sea of normal galaxies. Objects which exceed the red envelope can be considered PG candidates. PGs with Lyman break amplitudes greater than 10 ($R - K > 4.5$) can be differentiated from galaxies as long as their K magnitudes are brighter than 18 and $6 < z < 20$. At K of 18 to 19 the Lyman break must be greater than 30 to differentiate PGs from normal galaxies. At K fainter than 19 detection of galaxies at R fainter than 25 will present a problem. From the above discussion a survey to K of 18 to 19 and R of 24 seems appropriate. Deeper surveys will present a problem both for obtaining additional data on the sources and for differentiating normal galaxies from PGs.

For PGs with a redshift less than 6 the PG will appear very blue since the

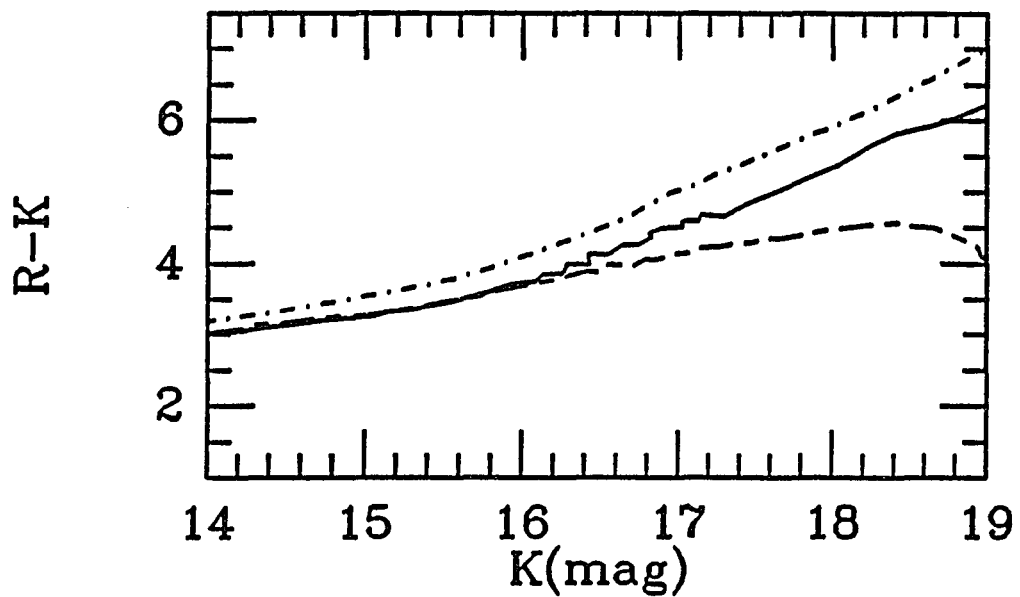


Figure 2.3: The predicted observational plane of $R - K$ vs. K for a brightest cluster galaxy. As in figure 2.2 the solid line and the long-short dashed line are for the Bruzual 'c' and ' $\mu = .5$ ' models. The dash-dot line is for the nonevolving elliptical galaxy. Since all other galaxies are either fainter or bluer than a brightest cluster galaxy they will all occur under the nonevolving elliptical galaxy in this observational diagram.

spectrum will be flat between R and K ($R - K = 2$). Here the problem will be differentiating nearby low luminosity star forming galaxies from luminous PGs. At photometric resolution, both of these types of galaxies have essentially the same SED and they can only be differentiated on the basis of luminosity, i.e. we need some redshift information. A PG with a redshift greater than 3 will have the Lyman limit within the optical. Since the Lyman limit is the only strong spectral feature in star forming galaxies the presence of a flux decrement into the blue along with a flat SED in the red can only be attributed to a high redshift star forming galaxy. Thus, a source with a flat spectrum in the red to IR but which get fainter into the blue must be a high redshift star forming galaxy (a PG). While these objects would primarily be found based on an optical selection the addition of the IR data will facilitate recognizing them.

To summarize this section, we have shown that a PG survey to K of 18 to 19 covering about 10 square arcminutes of the sky, could find high luminosity PGs with $2 < z < 20$ which would be missed by optical surveys. Also, by making an $R - K$ color magnitude diagram we can differentiate high redshift ($z > 6$) PG candidates from normal galaxies.

2.5 Observations

To make our deep 2 micron survey we used several HgCdTe IR arrays made by Rockwell International Science Center. The IR array is fully described in Rieke, Rieke and Montgomery (1987). The device consists of an array of HgCdTe photodiodes which are then bonded to a four phase CCD which is used as a read out. The CCD has a well depth of about $4 \times 10^6 e^-$ and a read noise of about $600 e^-$. Thus, when we allow the photocurrent to accumulate until the CCD wells are full we are background noise limited. Also, when operated at 2 microns the dark current is negligible.

The fields for the deep survey were selected in Leiden-Berkeley deep survey areas which already had deep multi-color 4 meter plates and radio continuum observations. Additionally, we needed a nearby star brighter than about 12^{th} magnitude so that we could offset guide the telescope under "bright time" conditions. Two sets of fields were selected near guide stars in Lynx and SA57.

The Steward observatory 61" telescope was selected to make the observations since it provided a large plate scale of $1.2''$ per pixel and since several weeks of time could be obtained on this telescope. The first observations were made with a 32×32 array during two one week observing runs during the spring of 1986. While there were only 3 photometric nights we did learn a great deal about how to flat field images so that we can detect objects at $1/20000$ the level of the background.

During the spring of 1987 we observed an additional two weeks with a 64x64 array. Since this array had just gone into operation there was some less than optimum performance. During the first run there was a light emitting diode in the array which created a 10% gradient across the chip. This was removed by subtracting a dark exposure with an exposure time equal to the images from the images. During the second run the light emitting problem had been fixed. Data were taken on a total of 6 nights but it was found that only data for 4 fields was of good quality. Finally, we observed for 10 nights during the spring of 1988 using a second 64x64 array. 5 nights of data were taken under good conditions. It was found that during the first run a bit in the A/D was stuck and a great deal of quantization noise resulted, making the data useless. Only one additional night of good data was taken during the spring of 1988. Thus, we surveyed a total of 5 pairs of fields covering about 15 arcmin^2 of sky.

The greatest challenge in making a deep survey in the near IR is flat fielding images to 1/20000 of the level of the night sky. During the spring of 1986 we found that the background across the chip was highly time variable. Thus, in the following observing runs we used a chopping mode of observing. During the observations a background limited exposure was taken of the field (60-120sec) and then the telescope was offset to the reference field where another background limited exposure was taken. In all about 200 images of the field and reference field would be taken during a night. When the data were reduced, the offset field observations

were used to flatfield the field exposures. The final technique for flattening the field observations was to divide it by the normalized average of the offset field observations from before and after the field observation. The flattened image was then cleaned of cosmic rays using a program written by the author. The average of the pixels in a 5x5 box was taken and then pixels more than 10 sigma from the mean were pruned until a stable mean was obtained. The remainder of the image reduction was done under IRAF ¹. The cleaned images first had their zero levels aligned. Since the telescope guiding was not perfect due to flexure of the offset guider, the centroid of a star was measured in each frame. The images were then shifted so that the stars registered. Finally, all 100 flattened images were combined by taking a median of all the frames to yield the final image. The final image has the sources from the field as positive flux deviations and objects from the reference field as negative flux variations. A second version of the image was made by convolving the image with a 2.5pixel FWHM gaussian. Such filtered images are useful for locating faint extended objects.

The dominant noise source in the images is the statistical uncertainty in the sky (i.e. the photon uncertainty in the sky brightness of any pixel). This enters in two ways: 1) the flat field, 2) the image pixel. A full well image with $3 \times 10^6 e^-$ has a statistical uncertainty of $1700 e^-$ in the value of any pixel. This dominates

¹IRAF is distributed by the National Optical Astronomy Observatories, which is operated by the Association of Universities for Research in Astronomy, Inc., under contract to the National Science Foundation.

the $600\ e^-$ readout noise of the CCD. A divided pair of images will thus have an uncertainty of $2400\ e^-$ per pixel or 4ADU RMS of pixel to pixel variations. If we are truly dominated by photon statistics and not by systematics the signal to noise of an image should decrease as the square root of the number of images. To test this I measured the RMS deviations of pixel to pixel variations for a series of images taken of the field SA57-3 during the course of a single night. As more images are combined the noise should decrease by the square root of the number of images. In figure 2.4 we show that this expectation is nearly realized, and that there appear to be no serious systematic effects. The product of square root of the number of images and the RMS of the image does rise a small amount initially indicating there is some additional source of nongaussian noise. This noise source could be slight variability of the sky gradient and intensity between the field and the reference field but this effect is very small. Thus, in theory by integrating longer one could achieve higher signal to noise. We also do not appear to be running into any confusion limit as one might expect if the sky were covered by numerous faint sources at K.

An additional source of uncertainty is the flux calibration of the IR images. We would observe 3 or 4 photometry standards from Elias et al. (1982) on each night data were taken. From these we would derive the photometric zero points. A standard extinction correction of $.1\text{mag}\ \text{airmass}^{-1}$ was applied. The standards showed a scatter of about .05 magnitudes. This scatter coupled with the fact that no color corrections were derived probably limits the ultimate photometric precision

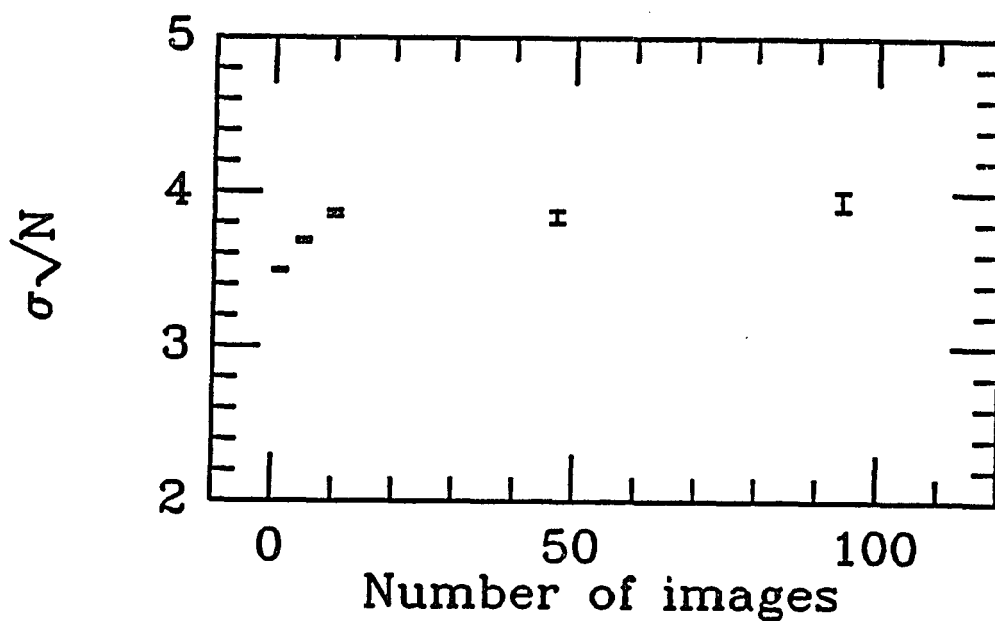


Figure 2.4: The product of image noise (pixel to pixel standard deviation) and the square root of the integration time versus the integration time, for flattened images of S3. If the noise were fully dominated by photon statistics, as in the ideal background limited case this relation should be a flat line. This photon noise limited performance is nearly realized, indicating that the noise can be reduced further simply by integrating longer.

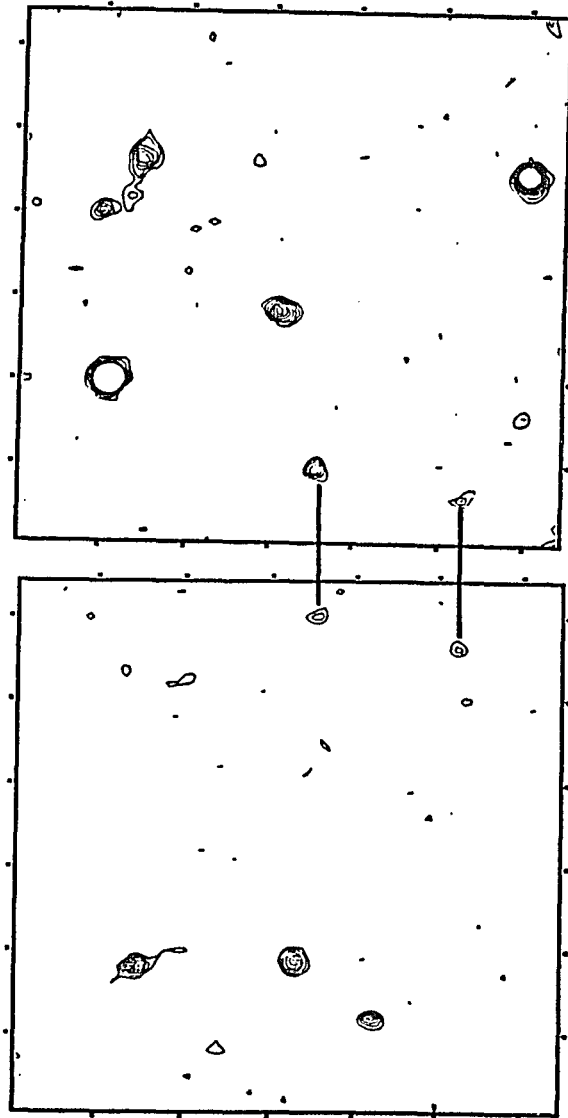


Figure 2.5: Contour plot of the field and reference field for S3. The contours start at the 2 sigma level and are equally spaced in intervals of 1 sigma. The sources connected by lines are faint galaxies observed in both the field and offset field as reliability checks. We note that source crowding is not significant even with the doubling of sources from the field and offset field.

to .05 magnitudes.

Table 1 gives the log of observations for this project. Observations were made under conditions varying from photometric to very light cirrus. Latter it was found that even light cirrus caused variations in the sky structure making flat fielding noisy. Thus, we eliminated all data taken under non-photometric conditions. Figure 5 shows a typical pair of images taken of the field SA57-3. Note that even with doubling of objects from the field and reference field the crowding is minimal. Table 2 gives positions and K magnitudes of all sources as measured from the IR camera frames.

The positions were measured in a 2 step process. The positions of optical sources in the fields were measured from the POSS using the NOAO GRANT measuring machine. These coordinates, which were bootstrapped from 10 SAO stars, are generally good to about .5". These objects were then used to generate a coordinate grid for optical CCD frames taken of the same region. The optical counterparts to the IR objects were found on the optical image and its position was measured. If no optical counterpart could be found, the IR objects with positions would be used to generate a coordinate grid for the IR image and the object's coordinates would be measured. The final coordinates should be accurate to about 1.5" arcsecond.

Photometry of all sources was obtained in 9" circular apertures using the IRAF *APPHOT* task. The sky was measured in a local annulus between 10" to 20" from the source. Since the *APPHOT* task was experimental we tested its photometry

Field	Band	Date (UT)	Phot	Number of Images	r (sec)	Scale "/pix	σ per pix	σ (gauss) per pix
L1a	K	2/15/87	Y	40	75	1.15	21.2	22.6
		2/18/87	Y	64	75	1.15		
	R	2/16/88	Y	3	600	.297	28.6	
		3/18/88	Y	2	600	.297		
	B	3/18/88	Y	3	900	.297	29.7	
	V	3/18/88	Y	3	600	.297	29.2	
L1b	K	2/19/87	Y	51	75	1.15	21.8	22.9
		3/11/87	Y	19	85	1.15		
		4/13/87	Y	25	70	1.28		
	R	2/16/88	Y	3	600	.297	28.6	
		3/18/88	Y	2	600	.297		
	B	3/18/88	Y	3	900	.297	29.7	
	V	3/18/88	Y	3	600	.297	29.2	
SA1	K	4/12/87	Y	45	70	1.28	21.6	22.9
		4/13/87	Y	78	70	1.28		
	R	2/16/88	Y	2	600	.297	28.2	
		2/25/88	N	2	900	.297		
		3/18/88	Y	1	600	.297		
	V	3/18/88	Y	2	900	.297	28.9	
	B	3/18/88	Y	2	900	.297	30.0	
SA2	K	4/14/87	Y	115	80	1.28	21.5	23.1
	R	2/16/88	Y	2	600	.297	28.3	
		2/25/88	N	2	900	.297		
		3/20/88	Y	2	600	.297		
		3/18/88	Y	1	600	.297		
	V	2/25/88	N	4	900	.297	29.7	
		3/18/88	Y	2	900	.297		
	B	2/25/88	N	3	900	.297	30.0	
		3/18/88	Y	2	900	.297		
	I	3/20/88	Y	2	600	.297	27.8	
SA3	K	3/9/88	Y	95	120	1.20	21.5	23.0
	R	3/18/88	Y	3	600	.297	28.3	
	V	3/18/88	Y	1	900	.297	29.0	
		4/12/88	?	2	900	.297		
	B	3/18/88	Y	2	900	.297	29.8	
		4/12/88	?	2	900	.297		
	I	4/12/88	?	4	600	.297	27.8	

Table 2.1: Journal of Observations

Table 2.2: Photometry of IR Selected Objects

Name	RA(1950)	DEC(1950)	K	$\sigma(K)$	R-K	$\sigma(R-K)$	R-I	$\sigma(R-I)$	V-R	$\sigma(V-R)$	B-V	$\sigma(B-V)$	Comment
sal-1	130516.12	+294627.9	15.87	0.07	3.59	0.07			0.89	0.01	1.33	0.02	Galaxy
sal-2	130516.39	+294609.0	15.35	0.05	3.66	0.05			0.70	0.01	1.14	0.01	Galaxy
sal-3	130515.22	+294532.2	15.72	0.30	5.66	0.30			0.56	0.09	1.88	0.31	8" from sal-2, Badly contaminated, Galaxy
sal-4=8	130519.85	+294552.8	17.50	0.18	2.54	0.18			0.36	0.02	0.35	0.02	Star?
sal-5	130521.16	+294645.8	16.39	0.11	3.53	0.11			0.91	0.02	-0.23	0.04	Galaxy
sal-6	130523.61	+294553.6	17.62	0.37	5.05	0.47			0.77	0.58	1.91	0.71	Galaxy?
sal-8=4	130519.86	+294552.3	17.88	0.33	2.17	0.33			0.35	0.02	0.35	0.02	Near edge of optical image
sal-9	130523.77	+294538.8	17.71	0.28	7.11	1.53							Near edge of optical image

Table 2.2: Photometry of IR Selected Objects

Name	RA(1950)	DEC(1950)	K	$\sigma(K)$	R-K	$\sigma(R-K)$	R-I	$\sigma(R-I)$	V-R	$\sigma(V-R)$	B-V	$\sigma(B-V)$	Comment
sa2-1	130527.58	+294340.2	16.28	0.05	2.96	0.05	0.76	0.03	0.50	0.01	1.11	0.01	Galaxy. Confused by sa2-2
sa2-2	130527.46	+294334.3	14.80	0.02	3.72	0.02	0.83	0.01	0.69	0.00	1.90	0.01	Galaxy. Confused by sa2-1
sa2-3	130526.75	+294323.0	17.35	0.18									Near edge of optical image
sa2-4	130526.05	+294333.7	17.77	0.28									No optical ID, very extended IR, probably not real
sa2-5	130527.06	+294354.9	17.91	0.31	6.15	0.43			1.46	0.50			Galaxy?
sa2-6	130528.93	+294352.0	17.19	0.17	4.45	0.18	1.05	0.12	0.55	0.06	0.85	0.06	Galaxy
sa2-7*	130529.70	+294318.9	16.94	0.14									Near edge of optical image
sa2-1b	130526.39	+294511.9	16.60	0.10	4.13	0.10	1.83	0.12	0.69	0.03	1.50	0.04	Galaxy
sa2-2b	130528.07	+294513.1	16.73	0.11	3.51	0.11	0.90	0.04	0.56	0.02	1.97	0.03	Star?
sa2-3b	130528.91	+294504.2	16.76	0.15	5.13	0.16	0.68	0.15	0.75	0.07	1.89	0.14	Galaxy
sa2-4b	130527.45	+294459.5	18.58	0.57	4.81	0.60	1.78	0.22	0.47	0.22	1.07	0.24	Galaxy
sa2-5b	130525.67	+294424.1	17.85	0.30									No optical ID at R=23.5

Table 2.2: Photometry of IR Selected Objects

Name	RA(1950)	DEC(1950)	K	$\sigma(K)$	R-K	$\sigma(R-K)$	R-I	$\sigma(R-I)$	V-R	$\sigma(V-R)$	B-V	$\sigma(B-V)$	Comment
sa3-1	130526.20	+294614.6	15.19	0.03	2.08	0.03	1.16	0.00	0.74	0.00	1.73	0.00	Star
sa3-2	130526.14	+294638.6	17.38	0.18	2.64	0.18	1.01	0.02	0.73	0.02	1.49	0.02	Star
sa3-3	130526.40	+294639.6	17.19	0.16	5.37	0.50	1.12	0.14	0.89	0.16	-0.43	0.14	6" from sa3-2, badly contaminated, Galaxy
sa3-4	130526.55	+294645.6	16.74	0.10	5.08	0.17	1.54	0.14	1.44	0.18	1.36	0.20	Galaxy
sa3-5	130527.75	+294645.5	18.42	0.36									No ID
sa3-6	130527.98	+294623.9	16.62	0.09	5.32	0.11	1.36	0.09	0.92	0.11	0.84	0.11	Galaxy
sa3-7=5	130528.39	+294601.4	18.09	0.35	3.75	0.36	1.71	0.08	0.45	0.09	1.02	0.07	Galaxy
sa3-8=4	130529.88	+294557.1	18.12	0.36	4.94	0.41	0.46	0.39	0.57	0.26	1.34	0.34	Galaxy
sa3-9	130530.55	+294608.1	18.06	0.34	2.96	0.34	0.51	0.06	0.27	0.04	1.01	0.03	Galaxy
sa3-10	130530.59	+294642.5	15.91	0.05	3.28	0.05	0.93	0.01	0.34	0.01	1.37	0.01	Galaxy
sa3-1b=s2-1	130526.39	+294511.9	17.33	0.10	3.40	0.10	1.83	0.12	0.69	0.03	1.50	0.04	IR CCD contaminated by sa3-1
sa3-2b=s2-2	130528.07	+294513.1	17.10	0.14	3.14	0.14	0.90	0.04	0.56	0.02	1.97	0.03	
sa3-3b=s2-3	130528.91	+294504.2	17.61	0.22	4.28	0.23	0.68	0.15	0.75	0.07	1.89	0.14	
sa3-4b=8	130529.88	+294557.1	18.08	0.36	4.98	0.41	0.46	0.39	0.57	0.26	1.34	0.34	
sa3-5b=7	130528.39	+294601.4	17.78	0.27	4.06	0.28	1.71	0.08	0.45	0.09	1.02	0.07	
sa3-6b=s2-4	130527.45	+294459.5	18.51	.37	4.88	0.41	1.78	0.22	0.47	0.22	1.07	0.24	

Table 2.2: Photometry of IR Selected Objects

Name	RA(1950)	DEC(1950)	K	$\sigma(K)$	R-K	$\sigma(R-K)$	R-I	$\sigma(R-I)$	V-R	$\sigma(V-R)$	B-V	$\sigma(B-V)$	Comment
11a-1	084224.62	+444704.4	13.28	0.01	2.79	0.01			0.39	0.01	2.29	0.01	Star
11a-2	084224.92	+444716.1	17.37	0.19	3.98	0.19			1.04	0.08	0.38	0.08	10" from 11a-1, Galaxy
11a-3	084226.60	+444736.7	15.74	0.06	4.14	0.06			1.09	0.02	2.41	0.03	Star
11a-5*	084228.36	+444725.8	17.51	0.30	5.75	0.35							IR not confirmed by MMT
11a-1b	084227.55	+444613.7	17.39	0.20									IR not confirmed by MMT, no opt ID
11a-2b	084226.95	+444626.9	17.92	0.59	5.17	0.61			1.41	0.46	-0.65	0.47	8" from 11a-3b, Galaxy
11a-3b	084227.55	+444631.5	15.80	0.06	3.60	0.06			0.97	0.01	1.58	0.02	Star
11a-4b*	084225.03	+444636.9	16.95	0.25	5.59	0.26			0.33	0.15	0.15	0.24	IR not confirmed by MMT, Galaxy
11b-1	084234.89	+444620.3	15.96	0.10	1.53	0.10			0.46	0.00	0.81	0.00	Star
11b-2	084233.77	+444624.4	15.07	0.04	2.49	0.04			0.64	0.00	1.07	0.00	Star
11b-1b	084234.62	+444714.7	16.96	0.17	3.64	0.17			0.94	0.04	0.67	0.04	Galaxy
11b-2b	084234.46	+444751.3	16.66	0.13	3.93	0.14			1.15	0.03	1.42	0.06	Galaxy
11b-3b	084230.89	+444745.1	16.02	0.14	3.12	0.14			0.56	0.01	0.97	0.01	Large Disk Galaxy

against photometry measured by DAO PHOT and GASP. The results indicated that *APPHOT* performed well. The photometry errors given in table 2.2 are computed from *APPHOT* based on the sigma of the sky within the annulus. Thus, they do not include systematic errors such as calibration.

The correspondence between objects on the IR images and the optical images provides good confirmation of the IR technique. As a further reliability check IR frames were overlapped by about $10''$ so that multiple observations would be made of some regions. These overlapped regions demonstrated that the IR images were reliable. No objects were spuriously detected on one image but not the other at the 3σ detection limit. Additionally several faint sources were observed on both frames. Figure 2.6 shows the difference the K magnitude which were measured on the two frames. This demonstrates both the reliability of detections and the photometric accuracy.

To identify PG candidates we took R CCD images of the fields. The initial CCD observations were made in the spring of 1986 at the SO 90" using a TI CCD. The data from this night were of rather poor quality due to poor seeing ($2 - 3''$) and uncertain photometric conditions. During the spring of 1987 we tried to take additional photometric observations at the 90" but we were unsuccessful due to poor weather and the nonlinear response of the then seriously damaged TI CCD. Finally, in the spring of 1988 we did get a second set of deep R band CCD images under photometric conditions with good seeing ($1 - 1.5''$). Additional CCD images in BVI

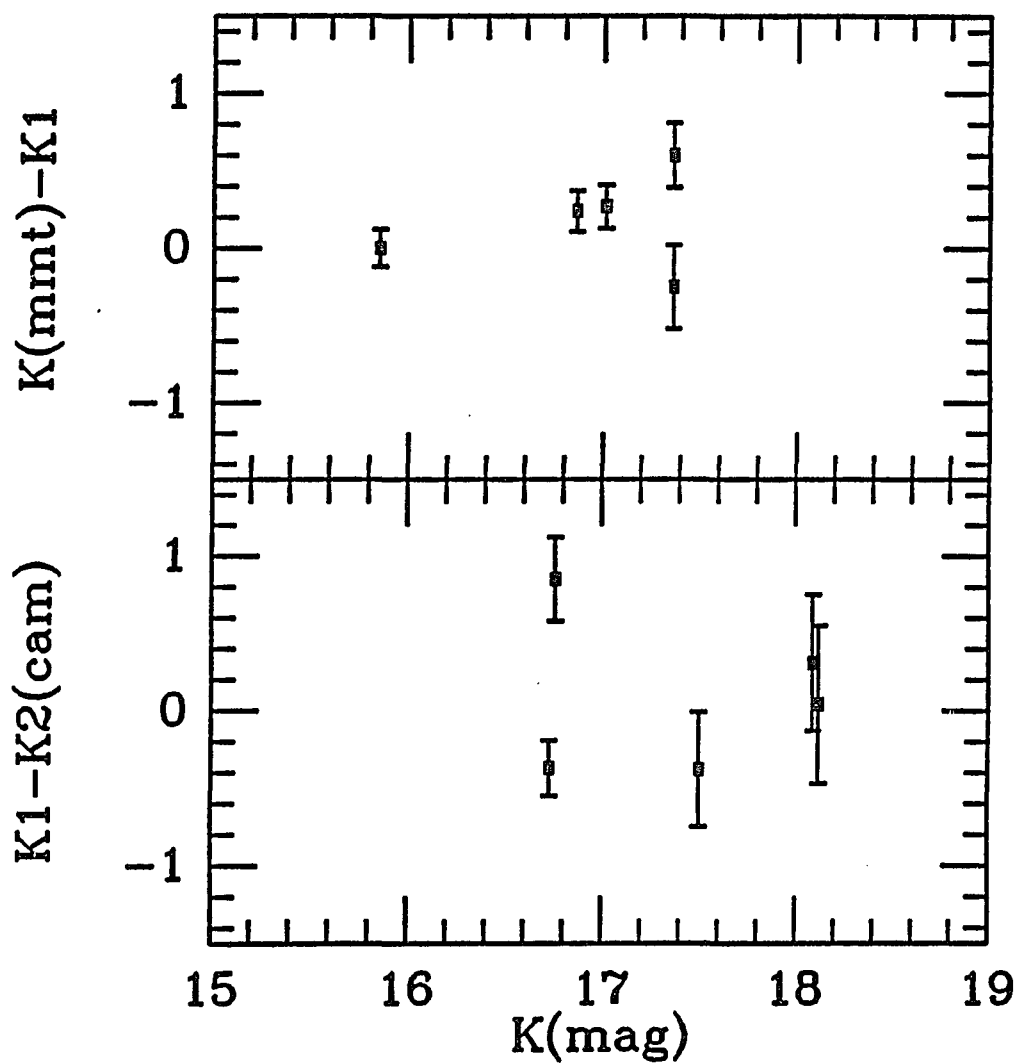


Figure 2.6: Differential photometry of sources observed with the IR camera. 2.6a displays the difference of photometry obtained for sources with the MMT IR photometer and the IR camera at the 61". 2.6b gives the difference in magnitude of sources observed in the overlap of IR camera frames. The photometry appears sound with only one point deviating a significant amount.

were taken at the 90" in the spring of 1988 to follow up PG candidates. Usually, about 4 exposures were taken in each filter for a single object.

All CCD images were reduced in the same manner. The high frequency "pixel to pixel" variations were removed by using the sum of about 20 dome flats with about the same background intensity as the night sky. After application of this dome flat, low frequency variations (large gradients) did remain in the images. These were removed by taking a median average of all frames, taken in a single filter, during the night. This "sky flat" which was devoid of stars was then median filtered using a 20x20 sampling box to remove noisy high frequency variations. After being shifted so that they registered the images were added. The final images were typically flat to .1% of the night sky over the entire image. The CCD images were primarily calibrated using the M67 standards of Schild (1983). The R and I observations are in the Kron-Cousins system normalized to a 1sec exposure with $M_o = 25$. The solutions of the standard observations are:

$$R = r - X (.121 \pm .015) - (1.329 \pm .012)$$

$$V = v - X (.169 \pm .011) - (.602 \pm .009)$$

$$B = b - X (.256 \pm .019) - (.4316 \pm .015) + (B - V) (.203 \pm .005)$$

$$I = i - X (.044 \pm .002) - (1.655 \pm .001)$$

Table 1 gives the log of the optical observations and the limiting magnitudes of the images.

Name	J-K	$\sigma(J-K)$	H-K	$\sigma(H-K)$	K	$\sigma(K)$
L1-4a					>18.0	
L1-5a					>18.2	
L1-1b					>18.2	
L1-3b					15.85	.10
L1-4b					>18.5	
S2-5a					17.95	.20
S2-3b	2.21	.27	0.85	.22	17.36	.15
S3-4	1.88	.12	1.03	.14	17.01	.09
S3-6	1.74	.14	1.31	.19	16.86	.09

Table 2.3: Photometry with the MMT

In the spring of 1988 we obtained confirming IR photometry of deep 2 micron imaging objects using the MMT². While we had a total of 7 nights only about 1.5 were photometric so these data are not extensive. Table 3 gives the MMT magnitudes for objects measured. All observations were made with the MMT LHe cooled InSb photometer. An 8.7" diameter aperture was used with a 10" chopper throw. These observations were also calibrated using the standards from Elias et al. (1982). Figure 2.6 shows a comparison of the MMT magnitudes and the camera magnitudes. Basically, the agreement is very good with the only major discrepancies existing at the faintest levels near the detection limit of the IR camera.

In the two discordant cases, objects appeared at the 3σ level on the smoothed IR camera frames but were not detected by the MMT. There are several possible causes for these spurious detections. First the 3σ detection limit only represents 99.7% confidence and one would expect three 3σ deviations on a frame with 1000

²Observations reported here were obtained with the Multiple Mirror Telescope operated by the Smithsonian Institution and the University of Arizona

pixels. This does not fully explain the spurious detections since they occupy several adjacent pixels. Since all of the spurious sources were on one image this could suggest some special conditions on this image. Indeed, this image did contain a bright star, $K=13$, which is about 300 times brighter than the sources we were searching for. Such a bright object could produce scattered light which would show up as faint extended sources. On the whole, the MMT observations confirm the validity of the IR camera observations but they suggest that extended objects detected near the limit should be treated with caution.

2.6 $R-K$ vs. K color magnitude diagram and Red PG candidates

Figure 2.7a shows the $R-K$ vs. K color-magnitude diagram for all sources detected in the IR survey. Figure 2.7b excludes confused sources with unreliable photometry and bright stellar objects. As discussed in section II this diagram can be used to locate PG candidates if there is a "red envelope" for the normal galaxies. Most of the objects do lie below the predicted red envelope. A locus of galaxies seems to run from $K = 16$ $R-K = 3$ to $K = 18$ $R-K = 5$. From the $R-K$ colors we would expect the galaxies which make up the ridge to have redshifts from $z=.2$ to 1.

To investigate the objects further we can construct color-color diagrams. An

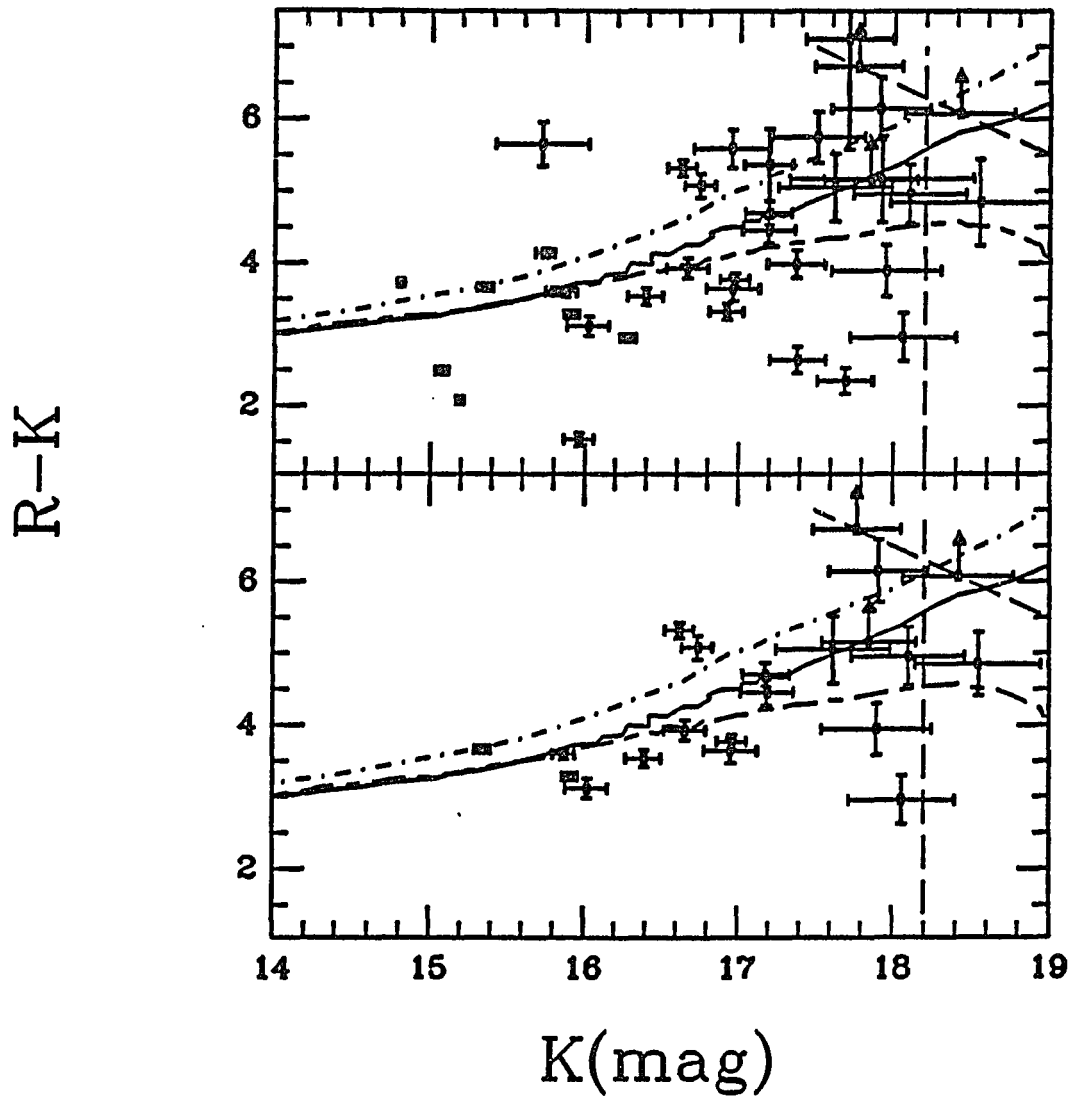


Figure 2.7: The observed color-magnitude diagram for sources detected in the 2 micron survey of 15 min^2 of the sky. 2.7a has all sources which were found at 2 microns. 2.7b has been cleaned of bright stellar sources and objects which were too crowded to obtain reliable photometry. The lines are the same as in figure 2.3. The bulk of the objects do seem to form a locus parallel to the model elliptical galaxies with others scattering toward the blue and to fainter magnitudes. Two sources lay about 1 mag above the galaxy locus in a region which should not be occupied by a large number of galaxies at any redshift.

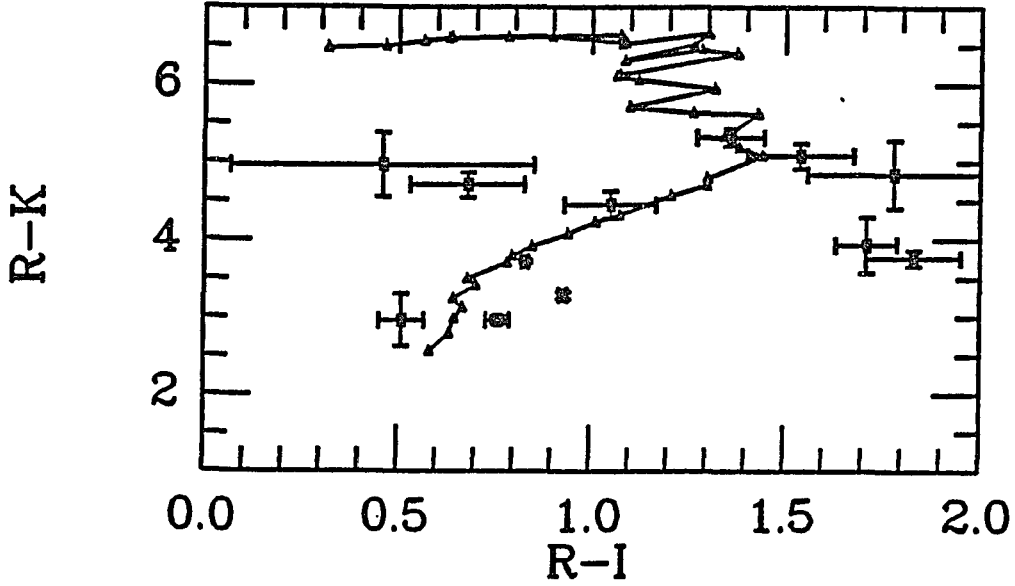


Figure 2.8: The $R - I$ versus $R - K$ color-color diagram for sources in 4 min^2 of sky. The solid line with triangles are the colors for a nonevolving elliptical galaxy at $z=0$ to 2 in intervals of .05. Above $z=1$ this prediction becomes very noisy. The diagram indicates that the bulk of the objects found follow the colors of normal galaxies from $z=.1$ to 1.

$R - I$ vs. $R - K$ color-color diagram is presented in figure 2.8. By using the reddest colors possible we remove much of the sensitivity to evolution of the stellar populations. The colors are dominated by the observed red-shifting of the giant branch. Figure 2.8 has the expected colors for an old stellar population. Our observed objects lie along this relation confirming that these are mostly normal galaxies with z between .2 and 1. Also, this supports the use of the $R - K$ color as a crude redshift indicator for galaxies near the red envelope.

In the initial survey four objects were found to lie outside of the region where we have argued that galaxies should be found. These objects are listed in table

2.4 . They are extended, have R-K colors of about 5 and K magnitudes of about 17. In the original survey these objects lay just a few sigma from the normal galaxy locus and could be outliers from the galaxy distribution . Thus, we obtained confirming observations with the MMT IR photometer. As a result of these observations (084225.0+444636) was found to be significantly fainter than indicated by the imagery, but the photometry of the three others was confirmed (Table 2.4). 130528.9+294504 moved near the locus of galaxies on the R-K vs. K diagram and is probably an L_* galaxy near $z = .75 \pm .2$. Cowie and Lilly (private communication) have obtained a spectrum that suggests a redshift of $z=.3$, in which case its colors are peculiar. A spectrum with higher signal to noise is needed to help resolve this dilemma.

The two remaining sources do lie outside the locus of normal galaxies in our $R - K$ vs. K diagram. The $r - K$ vs. K diagram by Lilly, Longair and Allington-Smith (1985) suggests that they could be similar to the reddest luminous radio galaxies at high redshift ($z=1$). Photometry of a large sample of 3CR galaxies obtained by us in the same photometric system as that of the new object confirms this conclusion, but only if the two sources are as red as the reddest 15-20% of the radio sample. As will be discussed in detail in the next section the probability of finding two galaxies with the luminosities of a brightest cluster galaxy (BCG) is about 1 in 10^4 in our 15 min^2 survey. This confirms our suggesting that these objects are not part of the normal galaxy distribution.

Name	RA(1950)	DEC(1950)	K(camera)	K(MMT)	R
11a-4b	084225.03	+444636.9	16.95 \pm .25	> 18.5	22.26 \pm .30
sa2-3b	130528.93	+294504.2	16.76 \pm .15	17.36 \pm .15	21.31 \pm .10
sa3-4	130526.55	+294645.6	16.74 \pm .10	17.01 \pm .09	21.81 \pm .12
sa3-6	130527.98	+294623.9	16.68 \pm .09	16.86 \pm .09	21.94 \pm .10

Table 2.4: Photometry of Red PG Candidates

In addition to the two objects which are separated from the normal galaxies in the color-magnitude diagram, there are also several objects which are not detected at R. These objects are all near $K = 18$ and thus have $R - K$ colors greater than 5 from the original R images. These may either be passively evolving elliptical galaxies at $z > 1$ or they could be further members of the class of red objects which are separate from the known galaxies.

To test if these objects are viable candidates to be PGs we can compare the observed properties to those expected for PGs. We observe a number density of about 1000 deg^{-2} which is uncertain by at least a factor of 2-3 (equation 2.4). This would be consistent with $z=6$ ($h=.5$, $q_o=.5$) which would be consistent with having the Lyman limit between the R and K bands. For $K=17$ the luminosity of a PG at ($z=7$, $h=.5$, $q_o=0$) would be $10^{32} \text{ erg sec}^{-1} \text{ Hz}^{-1}$. For a short bright phase PG ($\tau < 5 \times 10^7 \text{ years}$) these luminosities can be achieved (equation 2.6) but it implies a very large star-formation rate of $10^4 M_{\odot} \text{ year}^{-1}$. A bimodal initial mass function as proposed by Larson (1986) could reduce this mass requirement greatly. Lastly, these objects have a sky brightness of $10^{-24} \text{ ergs cm}^{-2} \text{ Hz}^{-1} \text{ deg}^{-2}$ with an uncertainty of at least a factor of 2-3. Within these uncertainties it seems these objects are consistent with them being PGs.

Band	130526.6+294646 Sa3-4	130528.0+294624 Sa3-6	$z=.77$ E Galaxy
K	$17.01 \pm .07$	$16.86 \pm .07$	
H-K	$1.03 \pm .14$	$1.31 \pm .19$.80
J-K	$1.88 \pm .12$	$1.74 \pm .14$	1.85
R-I	$1.54 \pm .25$	$1.36 \pm .22$	1.38
R-K	$4.80 \pm .17$	$5.08 \pm .15$	4.94
V-R	$1.44 \pm .21$	$0.92 \pm .18$	1.74
B-V	$1.36 \pm .20$	$0.84 \pm .22$	2.11

Table 2.5: Photometry of Luminous Red Galaxies

2.7 Follow Up Observations of Red PG Candidates

Since the SED of a PG should be very distinctive, we obtained *BVRIJHK* SEDs for these objects using the IR photometer on the MMT and the TI CCD on the 90" as described in the observations section of this chapter. Table 2.5 gives the photometry of the two red PG candidates.

While there is no indication that PGs should have strong UV emission lines for an extended period of time (Hartman et al. 1988) we obtained optical spectra since such observations could provide the best proof of a lower redshift object. Long slit spectra were obtained using a 1.5" slit on the MMT during two observing runs. The spectra were obtained in the red (5000Å to 8000Å) since such spectra would give the best chance of finding a 4000Å break at $z=1$ which would be consistent with the R-K colors. Two one hour exposures were taken using the FOGS spectrometer with

a 150 l mm^{-1} grism, which gave 10\AA resolution from 4500\AA to 8500\AA . Additionally, 3 one hour spectra were taken using the Red Channel spectrometer with a 300 l mm^{-1} grating which gave 7\AA resolution from 5000\AA to 8000\AA . Flux calibration was applied using standard stars from Stone (1977). The FOGS spectra and the Red Channel spectra were compared and found to be consistent. The five hours of optical spectra for each object were combined and are presented in figures 2.9. To study how the optical was connected to the near IR, two one hour spectra were taken from 7000\AA to 10000\AA using the 300 l mm^{-1} grating with the Red Channel spectrometer, but these data were only useful below 9500\AA , due to atmospheric emission and absorption.

The spectral energy distributions of the sources are presented in figures 2.10. From the SEDs it does not appear that these sources are PGs. The near IR is rather flat in both sources, rising very slowly from J to K , and the optical from B to R is also rather flat but the rise from the optical to the near IR is not as sharp an edge as would be expected in a PG (Partridge and Peebles 1967, Meier 1976). Since the Lyman limit edge in a PG could be softened by Lyman α forest absorption between the PGs Lyman α and the Lyman limit, the comparison to model PG SEDs is not certain but in this section we will show that the optical spectra and SED are consistent with $z=.8$ galaxies.

The optical spectra in figure 2.9, while being of rather low signal to noise, do indicate a spectral break. In 130526.6+294646 the break occurs at $7072 \pm 10\text{\AA}$. The break

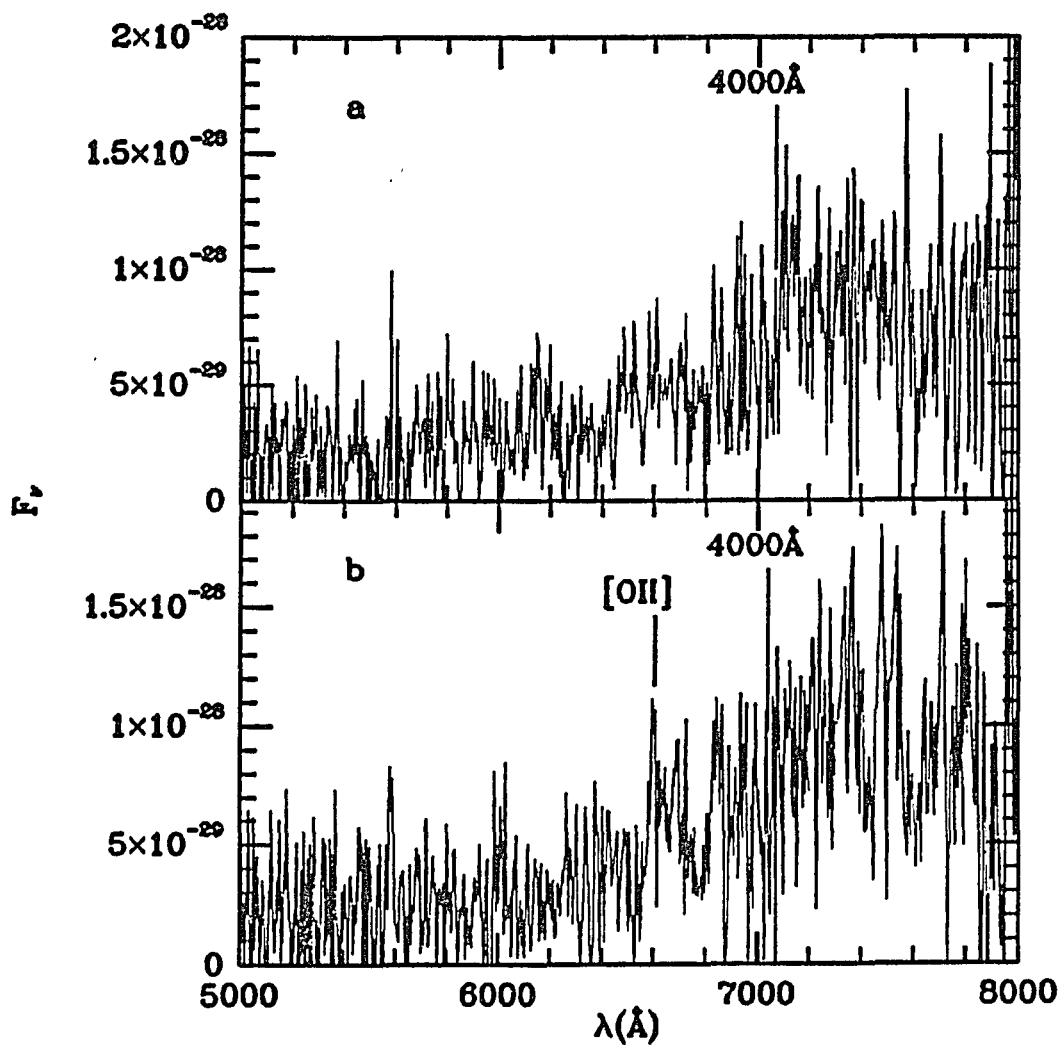


Figure 2.9: Optical spectra (5 hours with MMT) of luminous red galaxies found above the locus of galaxies during the 2 micron survey. While noisy they both appear to have a spectral break near 7000 \AA which we indicate. If this is the 4000 \AA break these galaxies have $z=.8$.

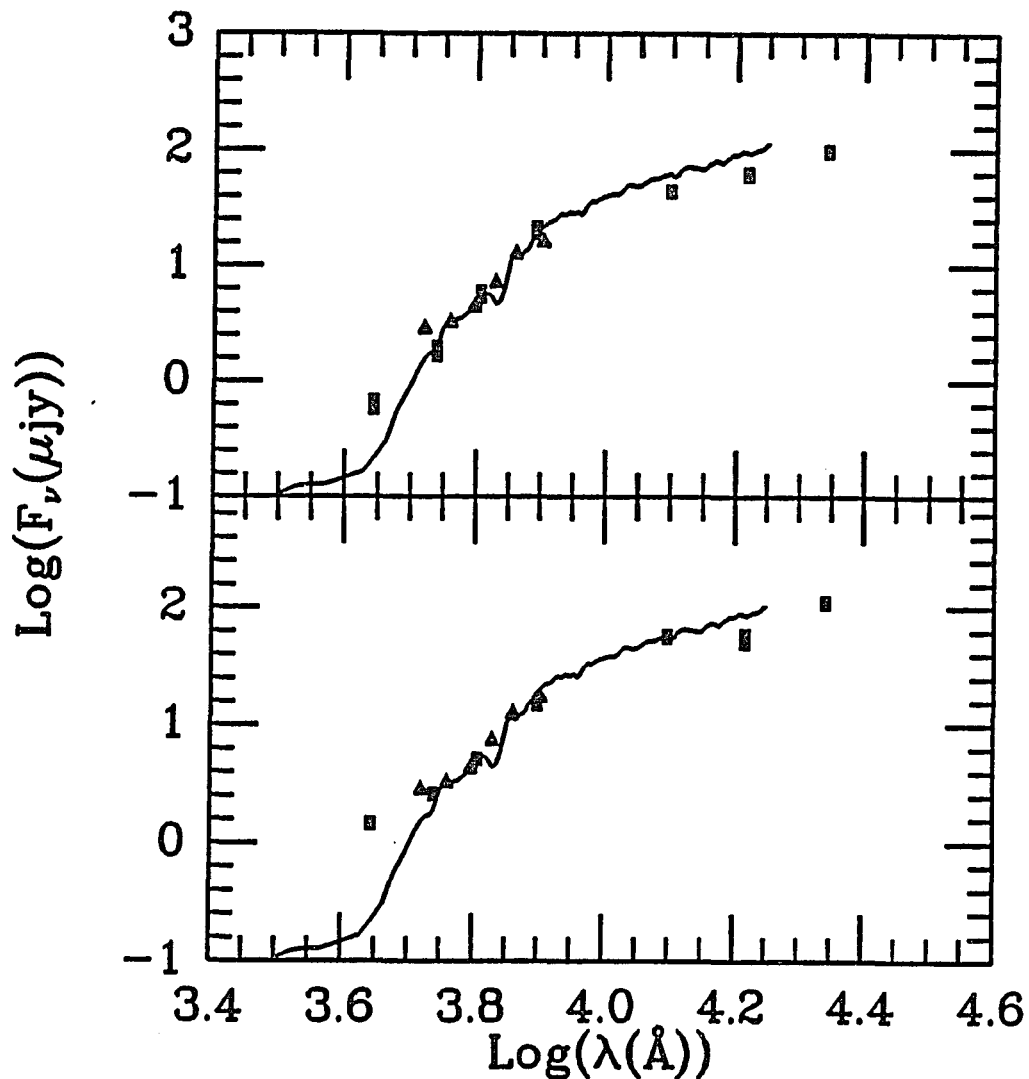


Figure 2.10: Spectral energy distributions from B to K for the luminous red galaxies found above the locus of galaxies during the 2 micron survey. Boxes are photometric points in the $BVR IJHK$ bands. The triangles are the spectra binned into 500\AA regions. The solid lines are an elliptical galaxy shifted to $z=0.8$ taken from Coleman, Wu and Weedman (1980). These SEDs seem to confirm the spectroscopic redshifts shown in figure 2.9. It also shows that these galaxies are similar to current day ellipticals with only a slight bluing of the SED beyond R .

amplitude is $1.71 \pm .10$ as defined by Hamilton (1985). 130528.0+294624 has a break near $7090 \pm 20 \text{ \AA}$ with an amplitude of $1.56 \pm .10$. If we assume that this is the 4000 \AA break then redshifts of $.768 \pm .003$ and $.773 \pm .005$ are found for 130526.6+294646 and 130528.0+294624 respectively. We also looked for additional features in the spectra and found none in 130526.6+294646. In 130528.0+294624 we found an emission line at $6608 \pm 3 \text{ \AA}$ which could be [OII]3727 \AA at $Z=.773 \pm .001$. Thus the redshift of 130528.0+294624 looks rather secure at .773 but 130526.6+294646 is uncertain since there is only one feature and we do not know with certainty that it is the 4000 \AA break.

In figure 2.10 we have also plotted the spectrum of an elliptical galaxy taken from Coleman, Wu and Weedman (1980) shifted to the redshift given by the spectral break. As can be seen the agreement from the R band to K is rather good. This can be used as further confirmation that the observed break is at 4000 \AA . The near IR colors are dominated by giants, whose properties are rather insensitive to the main sequence turn-off mass, and are thus reasonable redshift indicators. Table 2.5 gives the expected colors of a current day elliptical galaxy at $z=.77$ which should be accurate to about .1 mag. 130526.6+294646 has IR colors very similar to those of a $Z=.8$ galaxy. The $J - K$ colors of 130528.0+294624 are near those of a $Z=.8$ galaxy, but the H flux is 2σ below the expected color. While the red portion of the SED agrees well with a current day elliptical the blue portion of the SED and the break amplitudes are different.

Typical break amplitudes in current epoch E galaxies are about 2 (Hamilton 1985). A break amplitude of 1.6 implies a younger component in the stellar population than is found in current day E galaxies. Similarly, the $B - V$ and $V - R$ colors are very blue compared to a current day elliptical indicating more recent star formation. 130528.0+294624 has UV colors similar to those of a blue spiral galaxy at $z=.8$ (Coleman, Wu and Weedman 1980) and an [OII] 3727 with an equivalent width of $10 \pm 5 \text{\AA}$. 130526.6+294646 has redder colors and a larger break amplitude like those of a red spiral galaxy. Thus, these objects have composite spectra: they are dominated by a population like an old E galaxy in the red and by a young stellar population in the blue.

By comparing the observed SEDs with model galaxy SEDs by Bruzual (1983) it appears that a 14Gyr 'c' model reproduces the bulk of the observed SED, from the the R band to K. A problem arises because the 4000\AA break amplitude and the blue optical colors do not match the model well and suggest a main sequence turn off near early G type to middle F (Bruzual 1981). Since published model SEDs become both bluer in their optical-IR colors and UV- optical colors simultaneously (Struck-Marcell and Tinsley 1978, Bruzual 1983), it appears that no conventional galaxy model with a nonevolving giant branch can match the observed SEDs of these objects. Color evolution similar to that observed here is noted in a sample of red cluster galaxies by Lilly (1987) and he models the continued redness of the optical-IR colors as being due to an enhanced AGB population. Without model SEDs which

include evolution of the giant branch population it is difficult to predict the actual age of the stellar population, but a main sequence turnoff slightly above $1M_{\odot}$ would match both the break amplitude, blue colors and the appearance of a red AGB (Iben and Renzini, 1983). Such a main sequence turnoff would imply a formation epoch about 4Gyr before $z=.8$ ($z_{form} = 2$ for $h=.5$ $q_o=.1$, $z_{form} = 10$ for $h=1$ $q_o=.1$).

We combined the optical CCD images to form an image with a 3σ R detection limit of about 27mag $arcsec^2$ (figure 2.11). As can be seen in this image these objects are clearly extended. The GASP surface photometry program was used to measure the surface brightness profiles of these objects as in Cornell et al. (1986). The profiles are shown in figure 3a and 3b and are fit by an $R^{1/4}$ law and an exponential disk outside of the seeing dominated region. The fit parameters for an exponential disk seem plausible with a rest frame B central surface brightness of 20.5 and a scale length of 2.5Kpc (Freeman, 1970). The $R^{1/4}$ law fit yields a half light radius (r_e) of 10 Kpc and a very bright half light B surface brightness (B_e) of 19.7 (Kormendy 1977). With several magnitudes of luminosity evolution, to reduce the surface brightness further, either fit could agree with current epoch disks or spheroids. All we can conclude is that the profiles are consistent with an $R^{1/4}$ law or an exponential disk but given the data we can not tell which. An examination of the region surrounding these galaxies does not reveal any concentration of fainter galaxies near them. Since the composite image (Figure 2.12) reaches at least 3 magnitudes fainter than these galaxies we can conclude that there is no rich cluster associated with either of them.

Finally, it is worth considering why these objects would be found in our survey of only 15 arcmin^2 . Their K magnitudes of 16.8 compare closely with the average found for bright radio galaxies at the same redshift, $K = 16.4$ (Lilly, Longair and Allington-Smith 1985; Lebofsky and Eisenhardt 1986). Since these radio galaxies are of similar luminosity to brightest cluster galaxies (BCGs) (Spinrad, 1986) we can assume that the two new objects have luminosities similar to BCGs. This conclusion results in an interesting interpretation of our $R - K$, K diagram if we associate the $R - K$ color with galaxy redshift. In this case the red envelope of normal galaxies with $R - K$ of about 5 lies 1.5 magnitudes fainter than the two luminous galaxies, indicating that the brightest galaxies at the same redshift have luminosities close to L_* . From the luminosity function of Davis and Huchra (1982), one would expect about 1000 L_* galaxies per square degree between $z=.5$ and 1.0, and in fact we observe this density of galaxies along the red envelope for $4 < R - K < 5$. However, the luminosity function of Davis and Huchra (1982) predicts only 3 to 4 galaxies per square degree for $0 < z < 1.5$ ($q_0=.5$) and with luminosities 1.5 magnitudes brighter than L_* . Thus, the probability of our finding two such galaxies is about 1 part in 10^4 .

Given that our two galaxies are near each other on the sky and appear to be at similar redshifts, one could argue that they are correlated and that the probability of finding them should be the probability of finding a poor cluster with two BCGs.

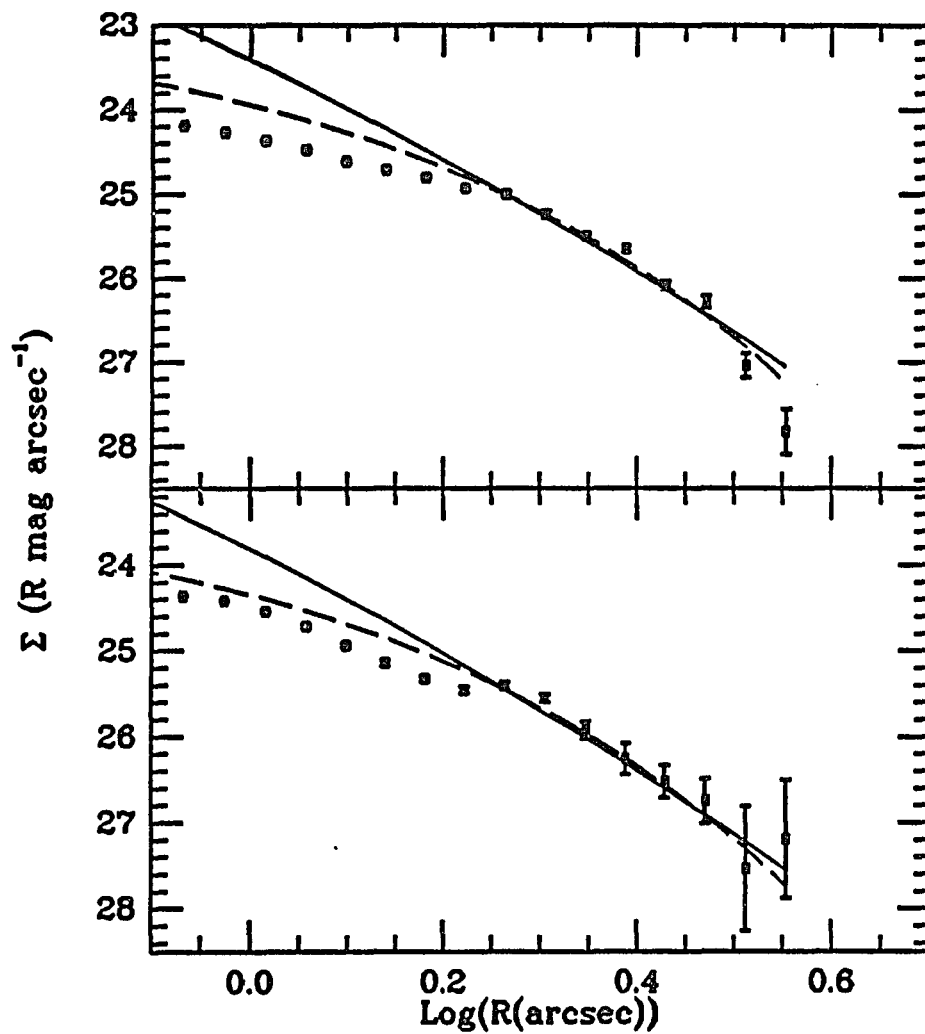


Figure 2.11: Surface photometry for the luminous red galaxies. The solid lines are $R^{1/4}$ fits to the data outside the seeing ($\sigma = .66''$) while the dashed lines are exponential fits. Note that the objects are nearly $10''$ across.

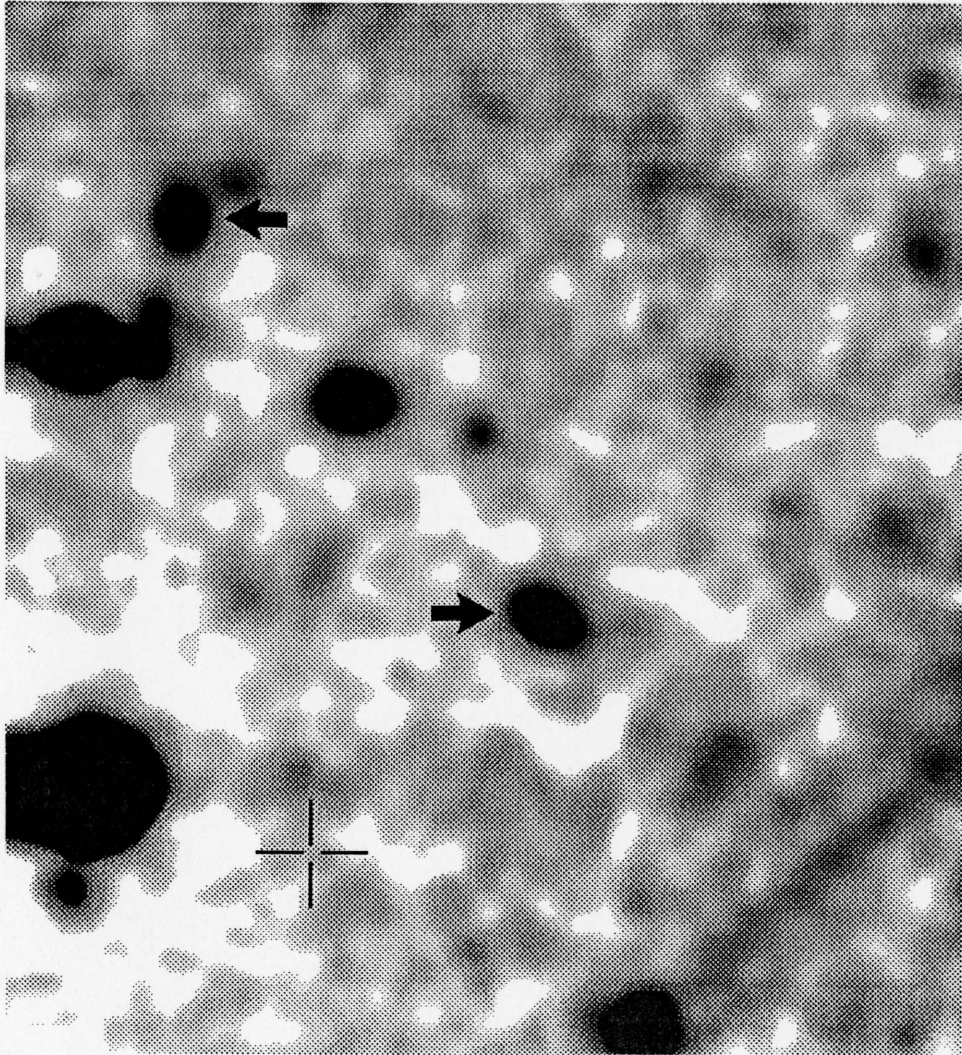


Figure 2.12: Optical image of the red luminous galaxies and the blue PG candidate 130527+294636. The red galaxies are indicated by the arrows and the blue object is between them. The image is a composite of BVRI frames and reaches a 3σ detection limit of about 27mag sec^2 in R and is one arcmin on a side. Even though this image reaches 3 magnitudes below the objects we see no concentration of galaxies near them indicating they are in a poor environment.

At redshifts up to $z=1$ ($q_o=.5$) about 45 clusters are expected per square degree (Gunn, Hoessel and Oke 1986), of which about 20% will contain giant ellipticals (Bahcall 1977). From this alternative statistic we would expect about 9 BCGs per square degree to $z=1$ and 1 chance in 40 of finding one such galaxy in our survey. However, Van den Bergh (1975) estimates that 93% of giant ellipticals lie in rich clusters, whereas we know that the two objects under discussion must be in poor ones. The probability of a giant elliptical in a poor cluster is small, probably $< 8\%$ (Bhavsar and Barrow 1985). Thus, there is about 1 chance in 400 that we would have found one such galaxy in our survey. Bhavsar and Barrow (1985) argue that the incidence of giant ellipticals in groups is consistent with random statistics of the galaxy luminosity function. In this case, the probability of two such galaxies in a single group or poor cluster is the square of the probability of one, and the likelihood of our finding two giant ellipticals in our survey is 1 part in 10^4 , whether they are in a single group or cluster or in separate ones.

Both galaxies lie very close to the expected R-K color for a non-evolving galaxy at $z=.8$. In contrast, most galaxies known near this redshift show evidence for significant evolution in this color and are bluer than the two galaxies under discussion (Lilly and Longair 1984; Lilly, Longair and Allington-Smith 1985, Eisenhardt and Lebofsky 1987). Since most other $z=.8$ galaxies were discovered through their strong radio emission or because they lie in rich clusters which requires strong evolution of the UV luminosities to have been detected (Couch et al. 1984), their blue colors

may result from their environments and selection. Thus, the two galaxies under discussion may not be as exceptional in this regard as the existing data would imply.

The newly discovered galaxies appear to be similar to ones discovered by Hamilton (1985) in a survey that selected galaxies by red color in the optical and near infrared. He used photographic plates to image approximately 5 square degrees, and obtained spectrophotometry of red, extended objects that did not lie in rich clusters. In common with our two galaxies, the galaxies so discovered are distinguished by H and K breaks that are nearly as strong as those for non-evolving galaxies. Curiously, the two highest redshift objects in his survey, SA 68:2 7024.0 and 6947.0, are both at redshift .78 and lie within 13 arcsec of each other on the sky. This pair of galaxies is incredibly similar to the pair we have discovered, which are at $z=.77$ and lie within 29 arcsec.

Either we were exceptionally lucky in finding the two galaxies, or the density of such objects on the sky is not predicted accurately by our present understanding, or a combination of both. The first possibility will be addressed by surveying a larger area of the sky; fortunately, the development of larger format infrared arrays will facilitate this work. The second possibility might result if there is a change in the luminosity function at $z > .5$, i.e., there is an increase in the percentage of very high luminosity galaxies. Such evolution of the near IR luminosity is not easily understood since the IR luminosity depends most strongly on the number of

giants, (Tinsley 1980) which is determined by the rate at which stars leave the main sequence. Large variations in the luminosity evolution of galaxies would imply large variations in the initial mass function (IMF) from object to object. In particular one needs a large high mass bump in the IMF to make a galaxy over-luminous in the past.

The fact that the high redshift, luminous, red, non-cluster galaxies found so far seem to come in pairs at projected separations of $< 100 Kpc$ suggests a means of getting a bump in the IMF: they could be post-interactive systems. If so, the high luminosities could result from stars created in interaction-triggered starbursts; since the colors and depth of the H and K break imply an old population, the starburst would have been initiated at very large redshift, $z > 3$. So that the galaxies luminosities would decay relatively rapidly from $z=.8$ to the present epoch the IMF of the interaction-triggered starburst would need to contain a large proportion of massive stars.

Now that these objects appear to be eliminated as PG candidates, we can place limits on models for high redshift PGs. In section 4 we related the luminosity of a PG to the duration of the initial burst. From the lack of PGs with K magnitudes brighter than 18 in $15 arcmin^2$, we can place limits on the initial burst duration for large elliptical galaxies. From our models, it would appear that PGs with an initial burst of less than 10^8 years are not common at $5 < z < 20$ ($q_0=.5$ and $h=1$). However, given the uncertainty in the models it is probably safer to conclude that

PGs with starformation rates greater than a few $10^3 M_{\odot} \text{year}^{-1}$ are not common at $z > 5$. For an alternative set of PG model constraints which these data can be applied to, see Boughn, Saulson and Uson (1986).

Additionally, there are the objects from the tip of the galaxy locus, which are of interest. One object (130527.06+294354.9) has been confirmed in the near IR with the MMT. It has $K = 17.95 \pm .20$ with an R-K color of $5.9 \pm .4$. At these faint levels we can not tell if this source is stellar or extended but we believe it is not an extreme halo dwarf since it has a $V - R$ color of $1.46 \pm .5$. With $K=18$ and R-K of 6 this object is about as far above the red envelope as the sources considered here. This object is probably be a further example of the type of galaxy described in this paper but at $z=1.2 \pm .2$. Alternatively, it is very near the most extreme R-K color which can be achieved by a galaxy at any redshift and could be a PG. There are also 2 sources which are not detected at $R = 25$: these must have $R - K$ colors in excess of 6 making them candidates to be lower luminosity PGs at $z > 6$. We have not yet been able to make confirming observations of these sources but s2-4 appears very extended with low surface brightness and is thus very similar to the false sources found in L1 and therefore seems likely to be an artifact.

2.8 Blue PG Candidates

A large population of galaxies with blue optical colors is known to exist at faint levels (Tyson 1988 and references there in). It is also well known that blue galaxy colors are indicative of active star formation (Struck-Marcell and Tinsley 1978, Bruzual 1983). Stellar population models with constant star formation rates and an evolving giant and AGB population maintains their blue colors for less than 10^8 years (Wyse 1985, Chokshi and Wright 1987). Thus, we shall consider a population formed during the last 10^8 years to be a young population since it will produce a flat SED. Any population older than a few times 10^9 years will be considered an old population because its red SED should be easily distinguished from that of a young population.

The major difficulty with understanding the blue objects is that the UV to optical portion of the SED can be completely dominated by a small young stellar population even if there is a much larger old population ($M_{young} \ll 1\% M_{old}$). As a result, UV and optical measures cannot determine whether the blue colors represent a major star forming phase. Since the SED of an old population peaks in the near IR the addition of K photometry can place a more significant lower limit on the relative mass of the young population. From combining Bruzual SEDs with ages of 5×10^7 years and 4×10^9 years it seems that an $R - K$ color less than 2 at rest or 3 for objects with $1 < z < 4$, places a firm lower limit on the relative mass of a young stellar population, requiring it to be more than a percent of the old stellar

mass. This is a fairly general conclusion for a large range of stellar population ages and suggests that reasonable limits can be placed on a young population by K photometry.

Depending on its redshift the observed SED of a star forming galaxy will appear rather different. Basically, the SED of a star forming galaxy is flat except for the prominent spectral breaks at the Balmer edge and the Lyman limit (Bruzual 1983). From $z=0$ to $z=1$ the Balmer edge will fall in the optical producing a flux decrement of about a factor of 1.5 or less. From $z=1$ to $z=3.5$ the optical portion of the SED will be smooth since no major flux decrement lies in the optical. Finally, from $z=3.5$ to 7 the optical SED will have a large spectral break due to the Lyman edge. Since we have 6 band photometry we can use the break features to try and constrain the redshifts of the objects.

To investigate the blue population we used the $BVR IK$ images of 6 arcmin^2 of sky obtained during these follow up observations. We selected all sources brighter than 22 at R but which were not detected or were weakly detected at K ($K > 18.5$ 3σ for galaxies). In such a source the K flux is constrained to be less than about 5 times the R flux. This yielded 7 extended sources, of which 1 was not detected at K because of source overlap in the object and offset frame in the K image. Photometry of the blue galaxies is presented in table 2.6. U photometry has been kindly supplied by D. Koo from his 4m photographic plates.

The sources all have blue SEDS from V to K but seem to fit into two groups

RA(1950)	DEC(1950)	U*-B	B-V	V-R	R	R-I	R-K
130530.55	+294608.1	-1.03±.25	1.01±.13	.27±.14	21.02±.13	.51±.16	2.96±.34
130527.09	+294633.5	-1.35±.35	1.40±.17	.18±.18	21.73±.16	.59±.18	2.63±.8 (<3.2)
130525.55	+294453.9		.53±.16	.31±.18	21.96±.16		<3.5
130528.46	+294501.3		.39±.16	.27±.18	22.00±.16		<3.5
130518.45	+294633.4		.74±.28	.90±.28	21.82±.18		<3.3
130519.34	+294622.1		.03±.25	.66±.31	21.82±.23		<3.3

• U photometry is from Koo(1988)

Table 2.6: Photometry of Blue IR Selected Objects

depending on the $B - V$ color. The first group has very red $B - V$ colors ($B - V > 1$) and consists of 130530.5+294608 and 130527.1+294634. The second group has bluer $B - V$ colors and consists of 130525.6+294454, 130528.5+294501 and 130519+294622. 130518.5+294633 seems to be redder across its entire optical SED, although the photometric errors make it difficult to classify, it is probably a spiral galaxy. We shall consider the sources with the prominent spectral break between B and V first.

2.8.1 Candidate Star Forming Galaxies at $z=4$

In this section we will discuss two objects which based upon extensive photometry but limited spectroscopy appear to be good candidates to be luminous star forming galaxies at a redshift of about 4. Final confirmation of their nature will have to await a moderate signal to noise spectrum extending into the blue. We present them now since they appear to have SEDs which are not consistent with known galaxies and

should be of interest even if they are not at a redshift of 4. Additionally, we present them to illustrate that the simple notion of what the SED of a PG should look like (Partridge and Peebles 1967, Meier 1976) may be in error since these objects possess neither a strong Lyman α line or a very large flux decrement at the Lyman limit.

From the photometry 130530.5+294608 and 130527.1+2934. seem to have very flat SEDs from V to K indicating they are dominated by star formation, however they have a strong spectral break between B and V (Figure 2.13). 130527.2+294636 is of particular interest since we have obtained an optical spectra of it. The spectrum is flat and featureless from 5000Å-8000Å (Figure 2.14). From the absence of emission lines but the presence of a very blue SED we can probably rule out redshifts below 1.2, since H alpha, O[III]5007 and O[II]3727 with equivalent widths greater than 40Å are commonly present in galaxies with optical to IR colors this blue and should have been detected. This suggests that the spectral break cannot be the Balmer edge but must rather be the Lyman Limit at $z=4$.

We can also use the SED alone to consider what redshifts these star forming galaxies could have. In figure 2.13 we compare the SEDs to that of a star-forming Im galaxy from Coleman, Wu and Weedman (1980). These objects are as blue from V to K than an Im galaxy at any redshift (Coleman, Wu and Weedman 1980) but the $B - V$ colors of 1 and 1.4 are redder than an Im galaxy at any $z < 3$. This implies that the spectral break between B and V is stronger than the Balmer decrement found in Im galaxies. While it is possible to make the Balmer edge of a

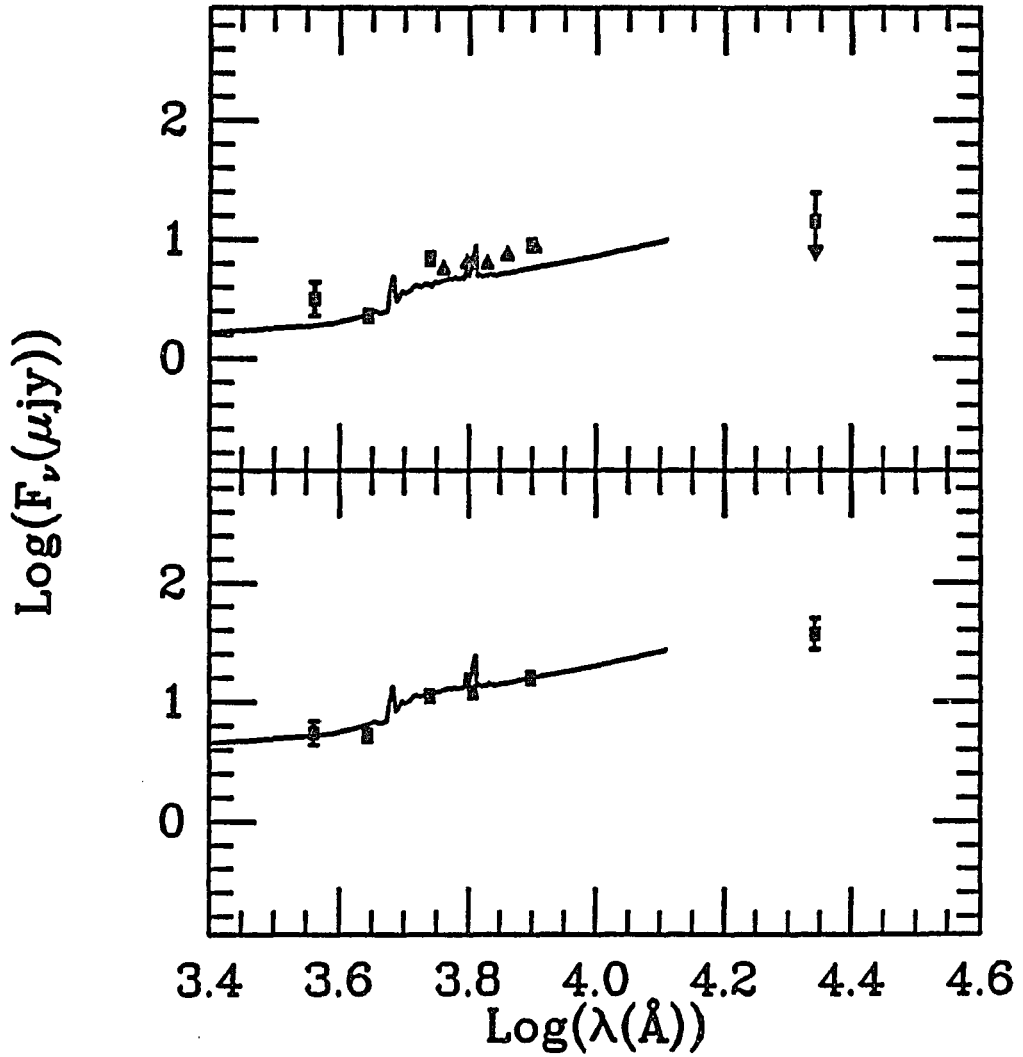


Figure 2.13: Spectral energy distributions of 130527.1+294634 (top) and 130530.6+294608 (bottom). Square points are *UBVRIR* photometry while triangles are points derived from the optical spectra. U photometry has been supplied by Koo (1988). The solid line is an Im galaxy taken from Coleman, Wu and Weedman (1980). 130530.6+294608 can be fit approximately by an Im galaxy with $z=.2$ but the photometry indicates that the break between *B* and *V* has slightly too large an amplitude to be the Balmer limits. 130527.1+294634 clearly has too large a break to be the Balmer limit and we suggest that this is the Lyman limit.

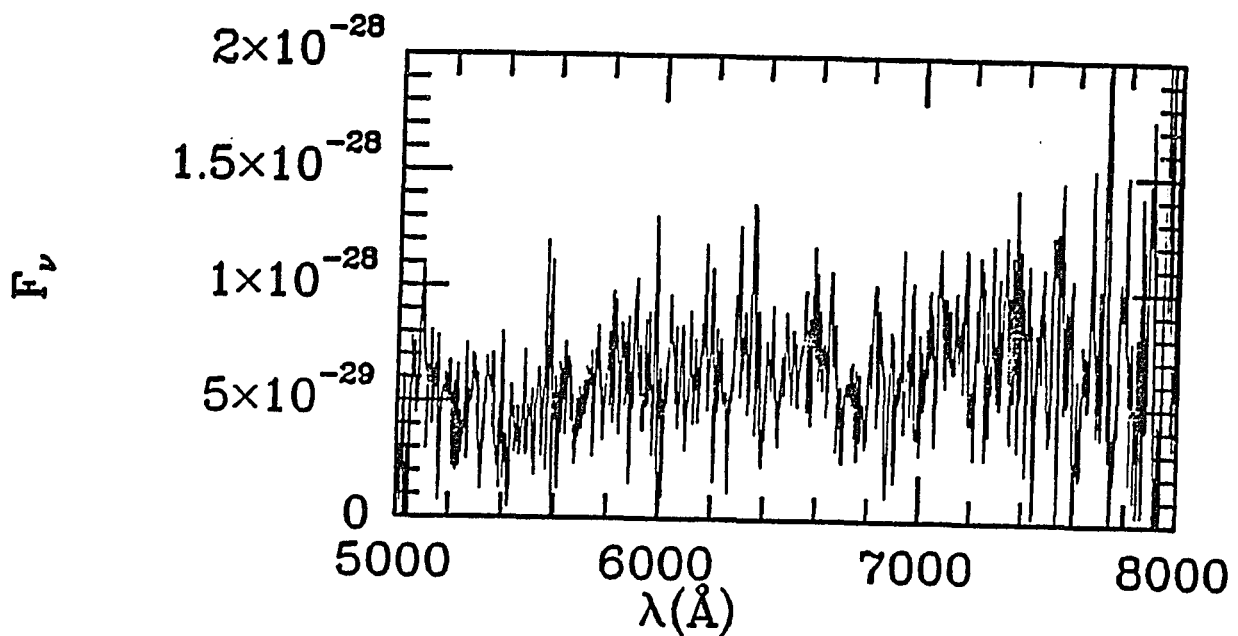


Figure 2.14: The optical spectra of 130527.1+294634 obtained in 5 hours of integration with the MMT. The spectrum possesses only a blue continuum. From the absence of emission lines it appears that the redshift must be greater than one to exclude the O[II]3727 line which is usually present in objects this blue. The only other feature is a slight decrease in flux at 5800Å which appears in both the FOGS and MMT red channel spectrum. This break is consistent with Lyman α forest absorption at $z=3.8$ while the photometric break between B and V would be the Lyman limit.

galaxy vanishingly small by adding hot stars (OB types) one can only make the edge stronger by adding very cool stars (types latter than G). In 130530.5+294608 the drop in flux by a factor of 1.7 is rather too large to be consistent with the Balmer decrement in stars hotter than G (Bruzual 1981). 130527.2+294636 seems to have a flux decrement of 3. If this were the Balmer edge it would require stars of type K or later to dominate the spectrum. But let us reemphasize that these objects have a nearly flat spectrum from V to K making a SED dominated by such late spectral types impossible. Once again this argues against the spectral break bring the Balmer edge and for the other possibility that the break is the Lyman limit.

An additional source of uncertainty is Lyman α forest absorption which could produce a flux decrement at Lyman α , producing an additional spectral break. From examination of the spectra of $z=4$ quasars we find that the flux decrement due to the Lyman α forest is about a factor of 2 (Warren et al. 1987a, Warren et al. 1987b) and the density of Lyman α forest absorbers scales as $(1+z)^{2.3\pm.3}$ (Tytler 1987). If we are observing Lyman alpha forest absorption between B and V this would correspond to a redshift of 3. Thus, we would expect a Lyman α forest amplitude of 1.2 which is less than is observed. Also, if this were the case we would expect to see a flux decrement further into the blue (3700Å) which is due to the Lyman limit, but this is not observed in the U band. The optical spectrum of 130527.2+294636 appears to have a flux decrement of a factor of $1.3 \pm .1$ at 5800Å. This drop is seen in both the FOGS and MMT spectrograph observations and could be due to

Lyman α forest absorption ($z=3.8$) while the larger flux decrement between B and V might be due to the Lyman limit (4400\AA). But the significance of this break is questionable and it should be observed at higher signal to noise.

We should also comment on the fact that these objects have breaks which are weaker than predicted in traditional PG models (Partridge and Peebles 1962 and Meier 1976). Model atmospheres for hot stars (Kurucz 1979) indicate that for $T > 30000$ the Lyman Limit becomes very weak nearly vanishing at $T > 45000$. By adding hot stars the strength of the Lyman limit can be greatly reduced. In particular Meier's (1976) model had an upper mass cut off of only $30M_{\odot}$ producing a Lyman limit amplitude of about 10. An upper mass cut off of $100M_{\odot}$ produces a flux decrement between 2 and 4 at the Lyman Limit for a constant star formation rate with a Salpeter IMF and solar metallicities (Kennicutt 1988). Lower metallicities, flatter IMFs and higher upper mass cut off all make the break amplitude weaker. The break between B and V in 130527.1+294633 lies nicely in this range but 130530.56+294608 would require a model biased toward hotter stars to accommodate its break amplitude comfortably. Clearly, if an extensive hydrogen nebulae was present the break amplitudes could increase significantly. A very large ionizing flux, an interstellar medium with a covering factor less than 1 and disk like geometry would all make escape of a large fraction of the Lyman continuum radiation possible, suggesting that the Lyman limit need not be large.

Our optical spectrum does not reveal the presence of a Lyman α emission line

even though it would be expected in our spectrum from 5000-8000Å if the B to V flux decrement is due to the Lyman limit. The lack of a Lyman α line with an equivalent width greater than 40Å is not unexpected in view of the observations of local star formation regions in galaxies by Hartman et al. (1988). Particularly, if the star formation has continued for more than a few times 10^7 years, the galaxy would already be polluted by metals from massive stars. Since metallicity seems to correlate with weaker Lyman α emission such galaxies would have weak or nonexistent Lyman α emission (Meier and Terlevich, 1981). Also, Lyman α forest absorption could completely remove a Lyman α emission line as seen in the blue wings of Lyman α in some high redshift QSOs.

We can also apply the tests outlined in section IV to see if these objects are viable PG candidates. The highly uncertain number density of these objects is 1000 deg^{-2} , consistent with PGs having bright phases lasting a few times 10^8 years at $z=4$. The brightness of these sources is also consistent with the luminosity of a PG at $z=4$ with a bright phase of 10^8 years. The luminosity of $2 \times 10^{30} h^{-2} \text{ erg sec}^{-1} \text{ Hz}^{-1}$ ($q_0=0$, $h=.5$, $z=4$) would imply a star formation rate of $400 M_\odot \text{ yr}^{-1}$. Making the cosmology small ($q_0=.5$ and $h=.8$) would reduce the star formation rate by nearly a factor of 10. Finally, we have a sky brightness of $10^{-25} \text{ ergs cm}^{-2} \text{ sec}^{-1} \text{ Hz}^{-1}$ which is consistent with the sky brightness required to produce the fraction of the metals in current day spheroids or disks.

The optical SED of these objects are similar to objects described by Cowie

(1987). He reports that he and Lilly have found objects which have flat spectra between V and I but are faint at B . However, their sources are fainter than I of 24. Since these objects have a spectral break in the optical we can look for similar objects in the deep CCD photometry of Tyson (1988). We defined a sample of objects bluer than $R - I < .5$ and steeper than $B - R > 1$. We find a large number of objects in Tyson's data that fit this requirement (7, 21, 46 and 28 in bins centered at $R = 21, 22.5, 23.5, 24.5$). At magnitudes fainter than $R = 24$ Tyson's counts will become incomplete at I for objects this blue. From these we can compute a more statistically significant sky brightness of $4 \pm 1 \times 10^{-26} \text{ ergs cm}^{-2} \text{ sec}^{-1} \text{ Hz}^{-1}$. This is about 1/10 that expected from spheroids or disks as defined by Cowie (1987). Thus, it does not seem that these objects could be the dominant star forming phase of spheroids or disks. These could be only the highest redshift members of one of these classes with most of the objects being at lower z and having no strong spectral break in the optical. If these were young disks for example, this would be expected since disk formation has continued until the current epoch.

We conclude that we have found objects which seem to satisfy all the requirements to be rapidly star forming galaxies at $z=4$. For 130527.1+294634 we have argued that the flux decrement between B and V is the Lyman limit on the basis of both the optical spectra and the amplitude of the flux decrement. The case for 130530.6+294608 is not as strong since we have no optical spectrum for this source and the break amplitude is only slightly too large to be the Balmer decrement

in a galaxy with such a flat SED from V to K . The final evidence to verify that these are PGs is a reliable spectroscopic redshift. As can be seen in figure 2.14 this may not be easy to achieve since local star forming galaxies have either very weak or nonexistent emission lines in the UV. A blue spectrum should show the Lyman limit and higher signal to noise may yet reveal a weak Lyman α emission line and clear break due to the Lyman α forest. Also, using new IR spectrometers it may be possible to observe OII[3727], $H\beta$ and OIII[5007] emission in the near IR windows. These are clearly the crucial tests of these objects as PG candidates.

2.8.2 Star Forming Galaxies at $z < 3$

The remaining blue objects have no large flux decrements in the observed spectral region. Objects similar to these are discussed by Cowie et al. (1988) and are presumably star forming galaxies at $z < 3$ so that the Lyman limit does not pass into the optical. With no spectral breaks and without optical spectra all we can conclude is that these objects have optical SEDs dominated by star formation and that they have redshifts less than 3. The $B - V$ colors of .4 are nondescript and are compatible with spiral galaxies with redshifts between 0 and 1.5 (Coleman, Wu and Weedman 1980). The addition of I photometry in Cowie et al. (1988) does point out the odd nature of these sources. The typical $V - R$ color of our blue source is .3. To compare with the galaxies of Coleman, Wu and Weedman (1980) our Kron-Cousins R must be converted to Johnson R a correction of about .2 magnitudes

($R_J = R_{KC} - .2$). Our $V - R$ color becomes a rather nondescript .5 which is compatible with spiral galaxies over a large range of redshifts.

Without redshift information we cannot place very tight limits on the mass contribution of the young population since the objects could be at low redshift. Red galaxies (E,S0 and Sb) typically have $V - K$ colors of 3.2 at zero redshift. The typical limits we and Cowie et al. (1988) have are of this order. Without redshift information one needs $V - K$ colors less than 2.2 to conclude that a significant ($M_{young} > 1\%M_{old}$) young population exists. Even if star formation in the past $10^8 years$ provided a percent of the stellar mass, it is not incompatible with these objects having constant star formation rates for nearly the Hubble time.

We can also apply the sky brightness test of Cowie (1987) to these sources and we confirm the result of Cowie et al. (1988) that they have a sufficient brightness to produce a large fraction of the metals in either disks or spheroids. This type of argument is uncertain by about a factor of 10 because of small number statistics, uncertainty in what fraction of the metal density of the universe is retained in stars, uncertainty in the Hubble constant and the assumption of a perfectly flat SED so that there is no K correction. It should be very interesting to obtain redshifts so that star formation rates can be determined.

2.9 Galaxy counts in the Near IR

The number magnitude counts of objects can also be used to locate primeval galaxy candidates if they are the dominant population at a given magnitudes. While not directly related to the search for primeval galaxies galaxy counts in the near IR are of interest for studies of galaxy evolution and cosmology. Optical counts of galaxies have been a major industry for the past 10 years or so (Kron 1980, Shanks et al. 1984, Koo 1986b). Since Hubble and Tolman (1935), it has been hoped that galaxy counts may be a viable test for differentiating world models. But in the optical band the counts are dominated by evolution effects which mask the cosmology dependence (Brown and Tinsley 1974). Thus, while optical counts do yield interesting but controversial information on the evolution of the SEDs of galaxies they have produced only very model dependent results for q_0 . In this section we shall show that IR counts hold the promise of being able to measure q_0 . Unfortunately, the present counts are not extensive enough to provide this answer but they are well predicted by the simple model described here.

Several model dependent problems presented by optical counts can be largely overcome by making galaxy counts in the near IR. First the counts depend critically on the luminosity evolution of the galaxies. From Bruzual(1983) we can see that in the B band at $z=1$ this can amount to from 1 to several magnitudes depending on the model adopted. Also, the K corrections in the optical are very large. From

Coleman, Wu and Weedman (1980) the K corrections for the B band vary from 4 to .2 magnitudes at $z=1$ depending on the galaxy type. From the size of these corrections it is clear why the results of galaxy count studies are so uncertain, they depend critically on the choice of these uncertain parameters.

In the near IR both of these problems are greatly simplified. Since the near IR light of galaxies is dominated by giants, almost all types of galaxies have similar near IR colors and K corrections. Figure 2.15 shows the K corrections for the K band for various redshifts. These were computed by convolving the K filter with the observed near IR spectrum of E galaxies and spiral bulges. This spectrum was kindly provided by M. Rieke and seems to produce the rest colors of E galaxies very well. The uncertainty in these K corrections is probably less than .2 mag until the optical is shifted into the near IR ($z > 2$). At higher redshifts the K corrections will begin to depend on galaxy type once again but this matters very little since at such high redshifts galaxies will not be present in IR surveys with present techniques (K limits near 21).

Tinsley (1980) pointed out that since the near IR luminosity is dominated by giants the luminosity evolution is simply governed by the rate at which stars turn off the main sequence. For the simple luminosity evolution model we shall adopt here, we will assume that the bulk of the stars were formed at very early times. Thus, the past luminosity evolution depends only on the IMF. Tinsley (1980) gives

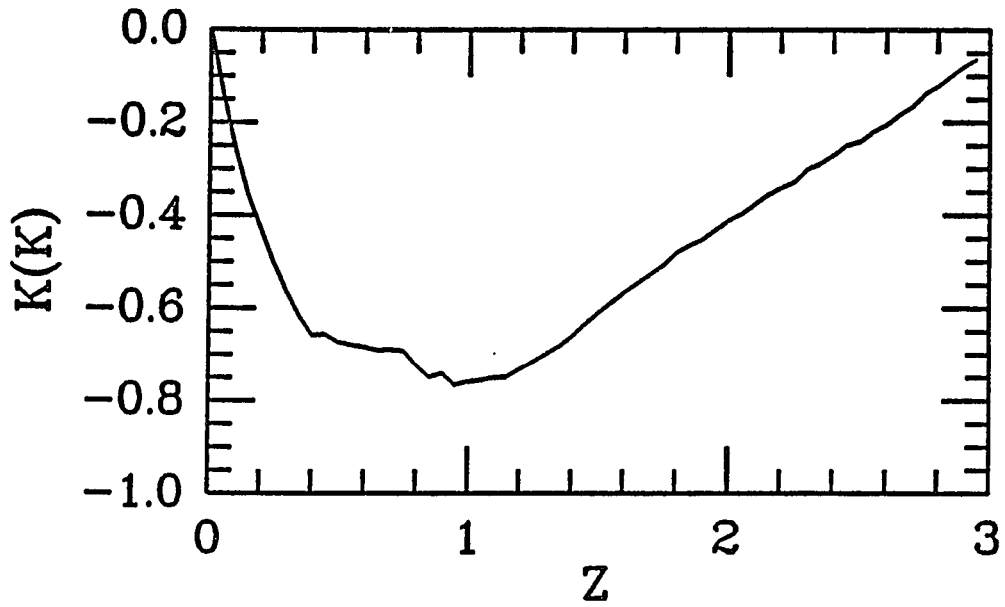


Figure 2.15: The K corrections for an elliptical galaxy with redshifts between 0 and 2. These K corrections were derived from an observational SED of an elliptical galaxy provided by M. Rieke. We note that these K corrections are small and should be very similar for all galaxy types until $z=2$ at which time the optical begins to be redshifted into the K band.

the change in luminosity as:

$$\frac{dM}{d\ln(t)} = (1.2 - .25X) \quad (2.7)$$

where X is the slope of the IMF. She originally derived this evolution prediction for the V band but since her models predict very little color evolution it is probably appropriate here. The uncertainty in the IMF is the major unknown in this calculation but as we shall show the effects of evolution on the counts are small. For our simple calculation here we shall adopt the Salpeter (1955) slope of $X = 1.35$.

Additionally, we need to adopt a luminosity function. We shall use a luminosity function of the type parameterized by Schechter (1980).

$$\Phi(M) dM = \frac{\Phi^*}{1.09} \exp(-\exp(-.92(M - M^*)) - .92(M - M^*)(\alpha + 1)) dM \quad (2.8)$$

We shall adopt the luminosity function parameters given by Efstathiou, Ellis and Peterson (1988) ($\alpha = -1.07$, $\Phi^* = 1.56 \times 10^{-2} Mpc^{-3}$ and $M^*(K) = -23.9$ for $h=1$).

Then we simply integrate the equation:

$$N(m) = \int_0^{z_{form}} \Phi(M(m, z)) \frac{dV}{dz} dz \quad (2.9)$$

where $M(m, z)$ is the absolute magnitude of a galaxy with observed magnitude m and redshift z . This is given by:

$$M = m - K(z) - E(z) - \Delta m(z) \quad (2.10)$$

where the K correction and evolution corrections are given above.

We have produced 4 sets of models to illustrate how IR counts can be applied. The models are for $q_o=.1$, $q_o=.5$, with evolution and without evolution to illustrate the sensitivity to both. The models along with the IR counts from this survey are given in figure 2.16. In computing our IR counts we included all objects detected in both R and K . We applied a correction for the gradual covering of the sky by objects in the frame and the reference field by assuming that no source could be found within $3''$ of a brighter source. We also limit our counts to $K = 18$ since all fields should be complete to this level. The observed counts and the simple model with evolution seem to agree within the large errors. The observed counts seem a bit higher than the model in the $K = 17$ bin but this can be attributed to the inclusion of the very luminous red galaxies discussed in section 5, since such objects would not be predicted by the simple evolution model. At the 2σ level the counts do seem to prefer the model with evolution over the no evolution model.

The most important result of this section is that the count models in figure 2.16 are sensitive to cosmology and rather insensitive to the evolution. With counts to $K = 20$ or 21 the $q_o=.1$ and $q_o=.5$ models separate by a factor of about 1.6. Also, since evolution shifts the curve without changing its shape significantly, it seems possible to untangle evolution from q_o . Since it is now feasible to pursue IR counts to this level this looks like a very promising means to measure q_o .

An alternative approach to measuring q_o from counts alone is to look at the redshift distribution of galaxies at a given magnitude. To model this, one integrates

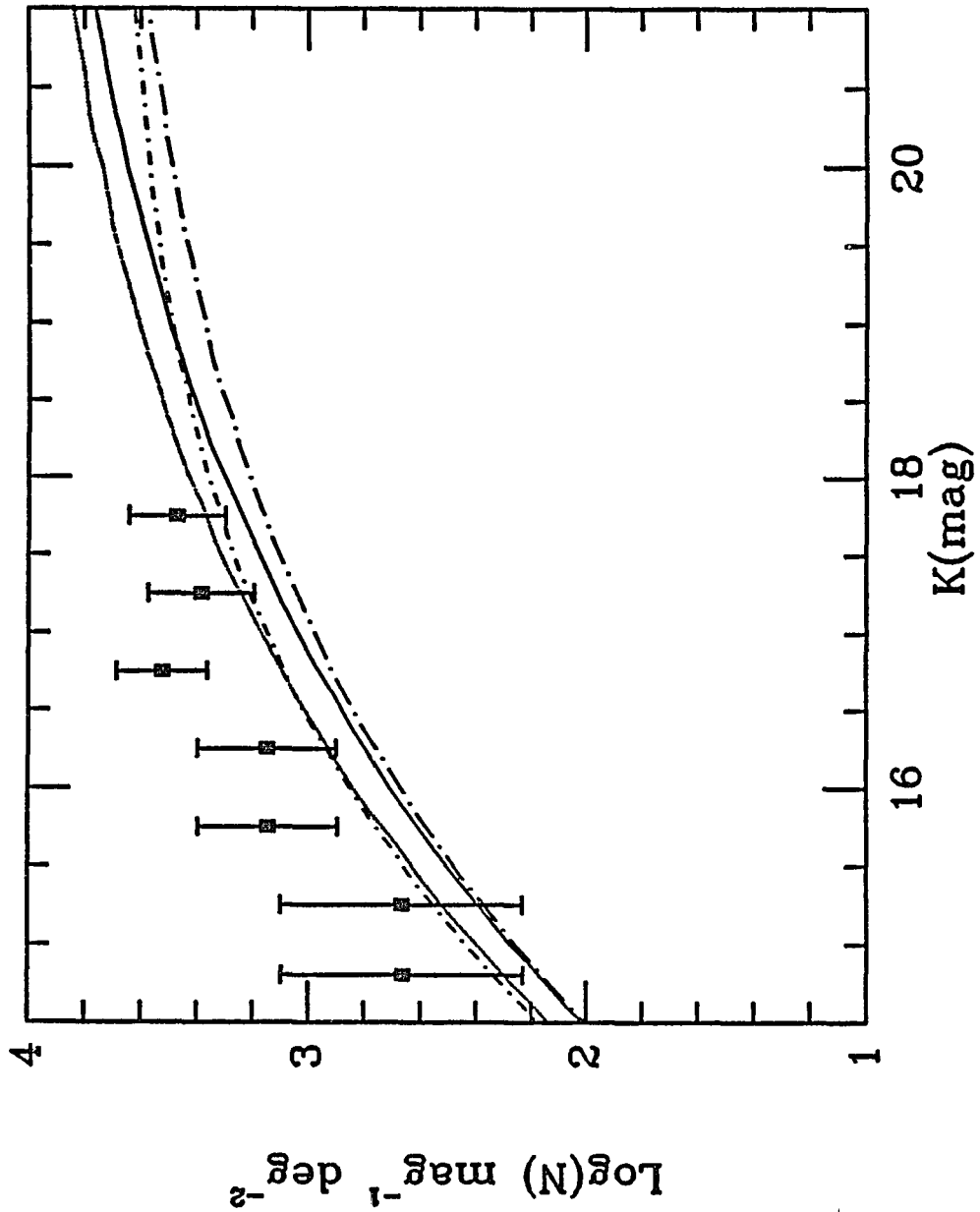


Figure 2.16: Counts of nonstellar objects detected both in the near IR and optically in 15 min^2 of sky. The dotted line and the short dash-dotted line are model counts with luminosity evolution for $q_o=.1$ and $.5$ respectively. The solid line and the long dash-dot line are with no evolution and $q_o=.1$ and $.5$ respectively. We note that the observed counts seem to fit the evolving model better at the 2σ level. Also, at $K = 20$ or 21 the $q_o=.1$ model should have 60% more galaxies than the $q_o=.5$ model independent of evolution.

equation 2.9 over a small range of magnitude while holding z constant. Figure 2.17 shows the z distributions for magnitudes ranging from $14 < K < 21$. Even at K of 17 or 18 one can differentiate $q_0=.1$ from $q_0=.5$ by the redshift distribution. This would require the measurements of some redshifts at $R = 23$ which, while difficult, can be done. With multiple slit spectrographs obtaining the 200 or 300 redshifts mostly at $R < 22$ will be possible. Such a survey coupled with counts would provide tests of both cosmology and the simple galaxy luminosity evolution model used here.

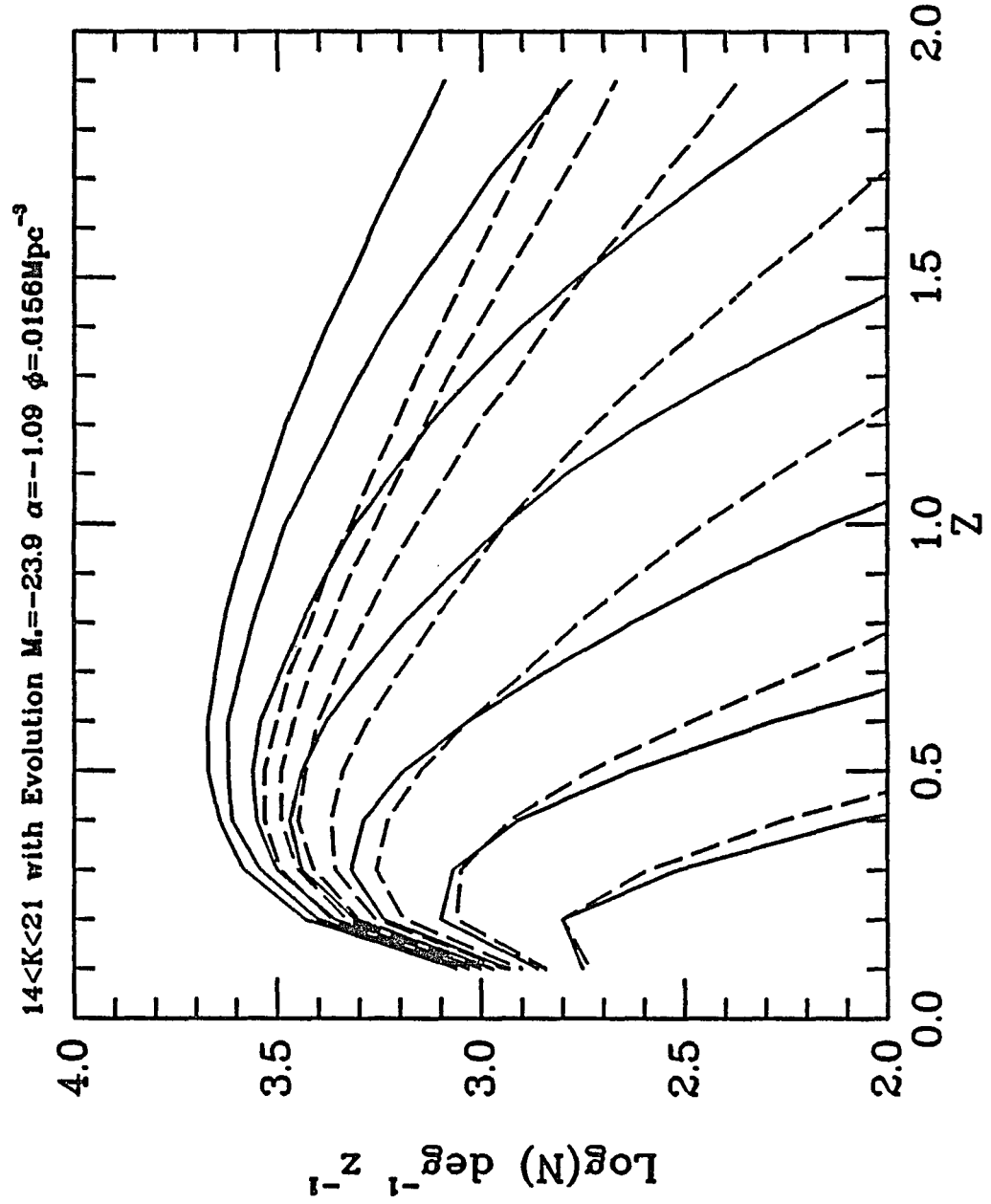


Figure 2.17: The number redshift relation for galaxies in the K band. Solid lines are for $q_0=0.1$ and dashed lines are for $q_0=0.5$. The models are for 1 magnitude bins spaced between $14 < K < 21$. By $K = 18$ or $K = 19$ the two cosmologies separate by a factor of 2 in counts near the peak and the curvature can be easily measured.

Chapter 3

Lyman Alpha Imaging Of $Z=3$ Quasar Environments

3.1 Introduction

At redshifts greater than 3 the number of quasars decreases rapidly with increasing redshift (Schmidt et al. 1986, Hazard et al., 1987). Could this turn-on of the quasars correspond to the epoch of formation for structure of the size of galaxies? At redshifts of 3 we lose the Lyman break into the UV, where until recently CCD detectors had very poor response (Leach and Lesser, 1987). Thus, we are forced to use some other signature for locating PGs. Given that the number of PGs with Lyman α emission is probably a small fraction of all PGs (due to Lyman α forest absorption and trapping within the object), and that the Lyman α line is probably no stronger than a few hundred Angstroms equivalent width, the task of finding such objects in the field is formidable. It requires both large sky coverage and good sensitivity to a single spectral line. While a specially designed spectrograph with a

very long slit and or a fiber feed could survey as much as one min^2 at a time no such device now exists and current spectrographs only cover about $.1 \text{ min}^2$. As an alternative approach one could use narrow band imaging if one knows the redshifts of PGs beforehand. In this chapter we shall discuss a survey for Lyman α emitting objects near QSOs at $z=3$ to search for PGs and to study the environments of high redshift quasars.

Why should one look near QSOs to find galaxies? The most fundamental reason comes from the galaxy correlation function (Groth and Peebles, 1977). Simply put, the best place to find a galaxy is next to another galaxy. Thus, if quasars are living in host galaxies at high redshifts the best place to find a PG may be near a quasar. Also, studies of nearby quasars (Yee and Green, 1984) suggest that quasars are in regions of higher than normal galaxy density and at $z > .5$ radio bright quasars are often found in very rich environments (Yee and Green 1987). While none of these observations of lower redshift quasars may be applicable to high redshift quasars, the absorption lines found in distant quasars may give us a direct indication of their environments. The CIV absorption lines seen in quasars seem to have clustering properties and number densities similar to galaxies (Sargent et al. 1980, Young et al. 1982) and may be intervening galaxies. Weymann et al. (1979) and Foltz et al. (1986) found that radio loud quasars often have a large concentration of CIV absorbers near the redshift of the quasar. These could be due to galaxies in clusters associated with the QSO. Thus, there seems to be good reason to hope that quasars

may indeed have a higher than normal density of galaxies associated with them.

Before this survey the only publicized (but unpublished) survey of the environments of quasars at high redshift was by Mackay (1985). He used photographic plates and narrow band imaging. Using modern CCDs we felt it possible to make significant improvements over this work. Also, during our survey Djorgovski et al. (1985) announced the discovery of a Lyman α bright companion to the quasar PKS1614+051 at $z=3.2$, found using a narrow band imaging technique. While this object has a very strong Lyman α with an equivalent width in excess of 2000\AA , making it rather too extreme to be a star forming galaxy, it did give hope that high redshift quasars may be in rich environments. Also, Schneider et al. (1987) found Lyman α companions to the lensed quasar 2016+112. All this gave great hope that such objects would be very common. But extended searches by Hu and Cowie (1987) and Spinrad (1987) have yielded no new candidates.

Additional motivation for such a survey is provided by the interest in the environments of quasars. Even if not in the form of galaxies, gas near quasars may be visible due to the ionizing photons emitted by the quasar. Such gas could be secondary infall into the quasar from the intergalactic medium or in the form of dissipatively merging gas clouds (Baron and White 1987), providing the fuel to the AGN. Stockton and McWeathy (1987) have found extensive regions of ionized gas (observed in O[III] 5007 emission) associated with low redshift quasars.

In the next section we shall discuss the expected Lyman α emission from PG

companions to quasars. In section 3 we shall discuss the observations made during our survey and in the final section we shall compare the properties of the objects found to those of PGs at $z=3$.

3.2 The Expectation for Lyman α emission from PGs.

To evaluate whether star forming galaxies at $z=3$ can be detected, we must consider both the luminosity of such objects and the strength of the Lyman α line. Let us first look at the continuum luminosity of such objects. In equation 2.6 we gave a rough relation between star formation rates and the continuum luminosity derived from the PG model of Meier (1976). If we place such an object at $z=3$ we can parameterize its V magnitude as ($q_o=0, h=.5$):

$$V = 24.1 - 2.5 \text{Log} (M_{100}) \quad (3.1)$$

Where M_{100} is the star formation rate in $100M_{\odot} \text{year}^{-1}$. Even in this very large cosmology a galaxy with large but not implausible star formation rate will be easily detected at V if it is compact. Such star formation rates could even be appropriate for young galaxy disks where one forms $10^{11}M_{\odot}$ of stars in 10^{10}years with a slowly declining star formation rate (Twarog 1980).

To begin our evaluation of the strength of Lyman α emission from a PG let

us consider simple case B recombination (Osterbrock 1974). Almost all Lyman continuum photons absorbed by a hydrogen atom cause the emission of a Lyman α photon. The only substantial sink of Lyman α photons is from e^- which fall into the 2S state which is a forbidden transition to the 1S ground state. If the density is low ($n < 10^4 \text{ cm}^{-3}$) these electrons move to the ground state by way of 2 photon emission. At high density, collisions will tend to depopulate the 2S state because of its long lifetime. Thus under case B recombination $I(\text{Ly}\alpha)/I(H\beta) = 23$ or 34 for the low and high density regimes respectively. For almost all star formation regions we will be dealing with the low density regime and the conversion of Lyman continuum photons to Lyman α photons can be given by equation 3.2.

$$I(\text{Ly}\alpha) = 10^{-11} N_{\text{Lyc}} \text{ ergs} \quad (3.2)$$

Here N_{Lyc} is the rate of emission of Lyman continuum photons and $I(\text{Ly}\alpha)$ is the intensity of the Lyman α emission line. To compute the Lyman α equivalent width (EW) we have integrated the single burst models of Lequex et al. (1981) for a constant star formation rate. These models used an upper mass cut-off of $100M_{\odot}$ and a power law IMF. Solar metallicity stellar evolution tracks with mass loss and stellar atmospheres from Kurucz(1979) were used. We then use equation 3.2 to convert the Lyman continuum flux into a Lyman α flux. Figure 3.1 shows the Lyman α EW versus time for continuous star formation for three slopes of the IMF. The EW is very sensitive to the IMF. Melnick (1986) has studied the IMF of violent

star forming regions and finds a slope of $1 \pm .3$ ($dN/d\ln(M) = N^{-\alpha}$) for $M > 4M_{\odot}$ to be appropriate; this is very near the Salpeter IMF value of 1.3. A value between the curves with IMF slopes of 1 and 1.5 seems appropriate. In no case does the EW become greater than 1000\AA , making it very unlikely that star formation is the cause of excitation in the object found by Djorgovski et al. (1987a) near PKS1614+051. By using solar metallicity one underestimates the effective temperatures of the stars and over estimates UV line blanketing in the stellar atmosphere. Therefore these EW are possibly slightly underestimated. In any case an EW of 100\AA to 150\AA seems plausible for star formation and if we restrict ourselves to only the first 10^7 years of a burst then EWs up to several hundred are possible. At a redshift of 3 the observed EW of Lyman α would be 4 times greater than in the rest frame.

Using the narrow band imaging technique we measure a differential magnitude between the narrow band filter and a broader continuum filter. If the continuum filter and narrow band filter are very close or overlap we can consider the continuum flux equal in both filters. Thus, we can write the differential magnitude as :

$$\Delta mag = -2.5 \left(\text{Log} \left(\frac{EW + W_{wide}}{EW + W_{narrow}} \right) - \text{Log} \left(\frac{W_{wide}}{W_{narrow}} \right) \right) \quad (3.3)$$

$$\Delta mag = -2.5 \left(\text{Log} \left(\frac{W_{wide}}{EW + W_{narrow}} \right) - \text{Log} \left(\frac{W_{wide}}{W_{narrow}} \right) \right) \quad (3.4)$$

Where 3.3 is for the case when the continuum filter and the narrow filter both contain the emission line and 3.4 is for the case when only the narrow band filter contains the line. For our observations we used a narrow band $H\beta$ filter with a

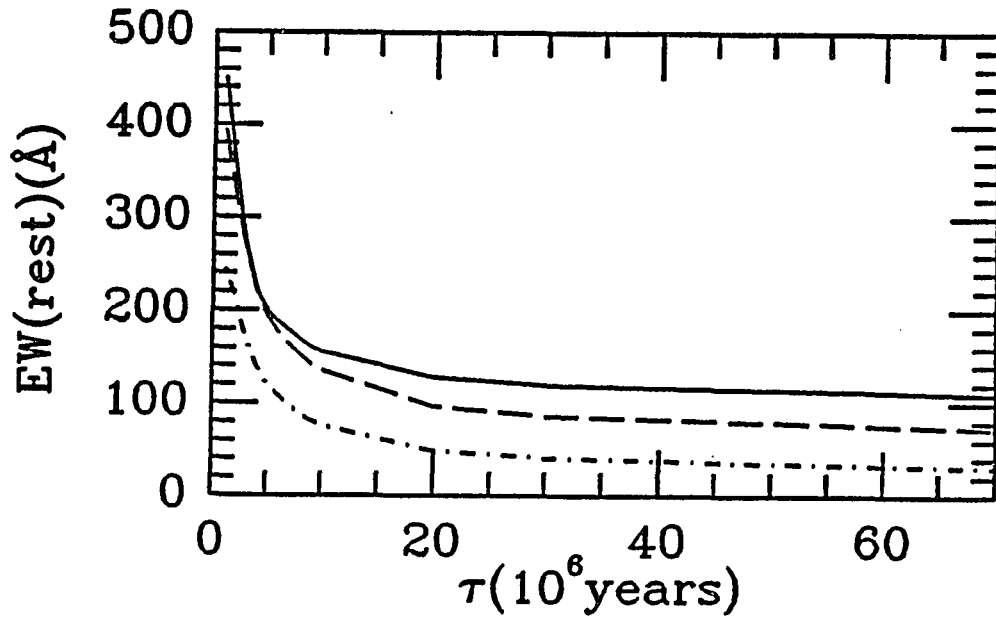


Figure 3.1: The equivalent width of Lyman α as a function of time for a constant star formation rate assuming case B recombination. The solid, dashed and dot-dashed line are for initial mass function with slopes of -1, -1.5 and -2 respectively ($\frac{dN}{d\ln(M)} = M^{-\alpha}$). A star formation episode lasting more than 10 million years will have a relatively constant EW of Lyman α with a value less than 150 Å.

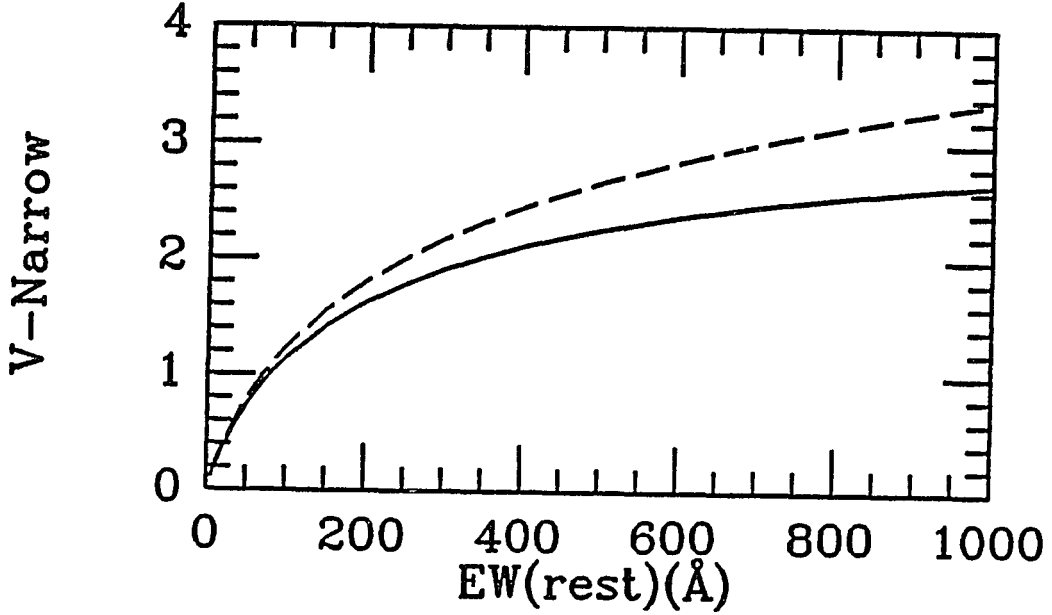


Figure 3.2: The change in $V - N$ color as a function of the rest frame equivalent width for Lyman α at $z=3$. The dashed line is for the case that only the narrow band filter contains the Lyman α line while the solid line is for the case that both the narrow band filter and the V filter contain the Lyman α line. These are computed for the filter widths used in this study.

width of 188\AA and a broad band V filter with a width of 1122\AA . In figure 3.2 we plot the Δmag as a function of the rest frame EW for these filters. To measure line excesses for Lyman α of a hundred angstroms requires measuring differential magnitudes to about .2 mag. At $V = 24$ and brighter this can be done.

An additional complication in calculating the Lyman α emission intensity is extinction. From observations of nearly star forming galaxies with the IUE telescope, Hartman et al. (1988), Deharveng et al. (1986), and Meier and Terlevich, 1981) have noted that the ratio of Lyman α to $H\beta$ is usually much lower than given by recombination theory. It is also found that the $L\alpha/H\beta$ does not correlate with the

Balmer decrement ($H\alpha/H\beta$). This is probably due to the large optical depth of the Lyman α line resulting from multiple scatterings. Thus, the path length for Lyman α absorption by dust and destruction of Lyman α by two photon emission will be primarily determined by the number of scatterings needed for the Lyman α photon to escape. The number of scatterings is probably not large enough for 2 photon conversion but could significantly enhance the path length for dust absorption (Ferland and Netzer 1979). As a result, details of the star formation region such as the velocity gradient (allowing Lyman α escape by Doppler shifts into the line wings) and geometry are likely to be very important in determining the Lyman α intensity, washing out any simple relation to the Balmer decrement.

An empirical trend of $L\alpha/H\beta$ with metallicity is observed (Hartman et al. 1988, Deharveng et al. 1986, Meier and Terlevich, 1981). In particular for O/H less than 1/10 solar the value of $L\alpha/H\beta$ becomes close to the recombination value. At higher metallicity the Lyman α line almost completely disappears. Lequex et al. (1981) derive the rate at which metals are released by a single age stellar population. Most of the metals are released after a few times 10^6 years. This time is short compared to the burst duration so that this metallicity will be achieved after about 1/10 of the gas is converted into stars. Thus, the Lyman α bright phase could be about 1/10 of the continuum bright phase. This could be much shorter if the metals are not well mixed throughout the PG but are localized to the star formation regions. Such lack of mixing is suggested by the lack of very low metallicity dwarf galaxy

star formation regions (Kunth and Sargent 1986).

The main conclusion of this section is that star forming galaxies will probably have Lyman α emission with an EW of about one hundred angstroms for at least a small part of the bright phase. At a redshift of 3 these objects will have V magnitudes brighter than 24 and will need differential narrow band/broad band photometry good to a few tenths of a magnitude to be detected.

3.3 Observations

The observations for Lyman α emission near quasars were carried out using two TI CCDs at the SO 2.25m telescope at Kitt Peak. As in chapter 2 the CCD was binned before read out into an array of 400 pixels each .3" square. The observations consisted of 10min V band observations and 40min exposures in the narrow band filter (N). Typically, 2 or 3 pairs of images were taken for each quasar. The data were reduced as in chapter 2. Observing for this program began in the fall of 1985 and continued until the spring of 1987 with 2 or 3 nights being allocated each fall and spring. Table 3.1 list the log of observations. Data were taken under conditions which were not photometric since we were concerned with differential magnitudes for which the zero points could be determined from objects on the frame.

The V filter is of the "nearly Mould" type with a center wavelength of 5465Å, a full width at half maximum of 1122Å, and the 1% transmission points at 4725Å

Name	RA(1950)	DEC(1950)	Z	Radio	V image	N image
UM141	014644.0	+014230	2.91	no	9/6/86	9/6/86
UM148	015359.7	+043058	2.99	no	1/10/86	1/10/86
0731+65	073134.3	+651950	3.04	95mjy	1/10/86	1/10/86
0830+115	083029.9	+113353	2.98	220mjy	1/9,10/86	1/9,10/86
WEE43	111330.1	+141424	3.06	no	4/14/86	4/14/86
Coma	125726.6	+284339	2.99	150mjy ^{1*}	4/15/86	4/15/86
WEE94	130248.9	+364000	3.00	no	4/13,14/86	4/13,14/86
BG5711	130446.3	+292208	3.05	no	1/9,10/86	1/9,10/86
h1504+106	150401.5	+104107	3.07	?100mjy? ¹	1/10/86 4/14/86	1/10/86 4/14,15/86
1602.8+1753	160246.4	+175322	3.02	700mjy ^{1*}	4/13/86	4/13,15/86
1615.1+1713	161503.0	+171249	3.00	no	4/13,14/86	4/13,14/86
1623.5+15.5	162331.3	+153353	3.07	no	9/6/86	9/6/86
UM184	234824.0	-010851	3.01	200mjy ¹	9/6/86	9/6/86
BGKPN13	235953.2	+010007	2.99	no	9/6/86	9/6/86
					Date	Weather
					1/9/86	Phot
					1/10/86	Phot
					4/13/86	Broken Clouds
					4/14/86	Cirrus
					4/15/86	Mostly Phot
					9/6/86	Phot

¹ Values are estimated from the Sky flux map of Condon and Broderic (1987) which has a detection limit of 150mjy at 6cm.

* Radio ID may not be the quasar. Could be low redshift galaxies in clusters near the quasars (coma and hercules)

Table 3.1: Quasars Observed at Lyman α

and 6350Å. The narrow band filter was borrowed from NOAO and was the $H\beta$ filter 1335F. It has a center wavelength of 4872Å with a FWHM of 188Å. This filter was chosen because of its high transmission (77%) and because its bandpass was wide enough to permit many quasars to be observed. The quasars were selected from the Veron-Cetty and Veron (1984) catalog. We observed those objects which had the most reliable redshifts between 2.95 and 3.05.

In all 17 sources were observed. Two of these (Coma and 0731+65) had large amounts of scattered light in the V frames which prevented accurate V photometry. 3 of the sources were observed during the spring of 1987 with a badly damaged TI CCD which had nonlinear behavior due to serious trapping which also made the data impossible to flat field. This leaves 12 sources with reliable narrow band and V frames.

All sources in the field of the quasar were measure using IRAF APPHOT. To maximize the signal to noise for differential photometry an aperture of 3'' was used whenever possible. In some cases a 2'' aperture was used if there was difficulty with the sky determination or a nearby source. The zero point for the differential magnitudes was determined for each pair of images by setting the $V - N$ magnitude of bright sources to zero. The reliability of sources was checked in several ways. First, the centroid of the object had to be within 1'' of the same position on both frames. Also, the curve of growth was checked to verify the object had normal extent. Finally, the sources were carefully inspected on both frames to make sure there was

no contamination by bad columns or hot pixels. Any questionable sources were excluded. Figure 3.3 gives the differential photometry versus V magnitude color magnitude diagrams for objects in the fields of the quasars. Those objects several σ above the zero color line are considered to be candidate Lyman α emission objects. Table 3.2 gives the photometry of the narrow band excess sources found in the fields of 12 quasars.

The data were roughly photometrically calibrated by observing M67 stars given by Schild (1983). Also, the narrow band flux was calibrated by observing stars from Oke (1974) and Stone (1977). The rough transforms are (for a 1 sec exposure with $M_o = 25$):

$$V = v(1sec) - 1.1$$

$$AB = N(1sec) - 2.9$$

Where AB is the AB magnitude of the star on the scale of Oke (1974). Once again we should stress that some of the data were taken under conditions which were not photometric and the magnitudes only give a rough measure of the source brightness (probably good to .5mag in the worst cases).

An additional sources of uncertainty is the effect that object color will have on the differential photometry. To assess this we measured the differential colors of 10 stars with known $B - V$ colors. We found a weak correlation between the $B - V$ color and the differential color ($V - N = .2 \pm .1(B - V)$). The distribution of

Object	Number	X	Y	V	$\sigma(V)$	V-N	$\sigma(V-N)$	Comment
UM141	QSO(4)	126.4	199.7	18.025	0.01	0.84	0.0141	
BGKPN13	QSO(5)	125	200	19.405	0.01	1.07	0.0141	
	15	208	64.7	23.635	0.28	1.34	0.3008	
	16	202.4	26.3	23.015	0.17	0.76	0.2024	
	18	228.8	27	23.465	0.16	0.99	0.1835	
	23	203	247.7	22.855	0.14	0.68	0.1720	
UM148	QSO(1)	167.7	175.8	17.915	0.01	0.81	0.0141	
	5	235.1	121.3	22.625	0.1	0.55	0.1166	
	10	271.1	277.3	22.905	0.13	1.1	0.1392	
0830+115	QSO(23)	145.9	178.2	18.815	0.01	1.38	0.0141	
	2	114.7	286.1	23.095	0.13	0.61	0.1581	
	7	11.7	191.3	23.925	0.19	1.43	0.2024	
	11	16.8	71.8	23.795	0.27	1.59	0.2816	
	12	29.4	72.4	23.805	0.25	1.62	0.2624	
	13	28.9	52.1	24.815	0.41	1.98	0.4197	
	17	102.5	89.1	23.695	0.22	0.72	0.2555	
	18	145.2	20.3	22.365	0.06	0.86	0.0721	
	31	265.1	201.3	24.045	0.29	0.89	0.3204	
WEE94	4	93.4	66	23.895	0.27	0.81	0.2915	no quasar
1615.1+1713	QSO(5)	109.8	89.6	19.915	0.01	1.3	0.0141	
	1	133.7	240.7	23.085	0.13	0.64	0.1476	
	16	287.6	46.5	23.665	0.21	0.56	0.2418	
1623.5+15.5	QSO(4)	75.4	185.2	19.425	0.01	1.05	0.0141	
UM184	QSO(38)	129	203	18.795	0.01	0.79	0.0141	
	7	48.1	214	24.515	0.38	0.87	0.4204	
	11	36.9	161	24.595	0.64	1.81	0.6511	
	25	125.5	113	24.505	0.604	1.22	0.6362	
	39	153.3	201.8	23.525	0.24	0.76	0.2729	
h1504+106	QSO(8)	114.7	91.7	19.365	0.01	-0.62	0.0141	BAL quasar
	3	42.6	189.7	24.165	0.46	0.98	0.4808	
	19	198.2	271.4	24.515	0.43	1.2	0.4464	
1602.8+1753	QSO(4)	115.1	83.9	19.735	0.01	0.99	0.0141	
	11*	174.8	200.3	22.135	0.1	0.5	0.1118	near star
WEE43	QSO(7)	156.9	9.5	20.525	0.01	0.74	0.0141	
BG5711	QSO(1)	81.7	252.2	20.565	0.02	0.56	0.0282	
	2	93.3	243.3	23.125	0.15	1.08	0.1802	
	6	140.1	204.3	23.135	0.17	0.95	0.2140	
	8	133.1	118.4	23.635	0.25	1.4	0.2773	
	9	160.7	115.9	22.295	0.07	0.22	0.1220	
	14	67.3	87.2	22.815	0.12	0.73	0.1697	
	17	202.9	60.2	23.415	0.21	0.64	0.29	
	18	241.6	85.4	22.965	0.13	0.84	0.1702	

Table 3.2: Photometry of Narrow Band Excess Objects

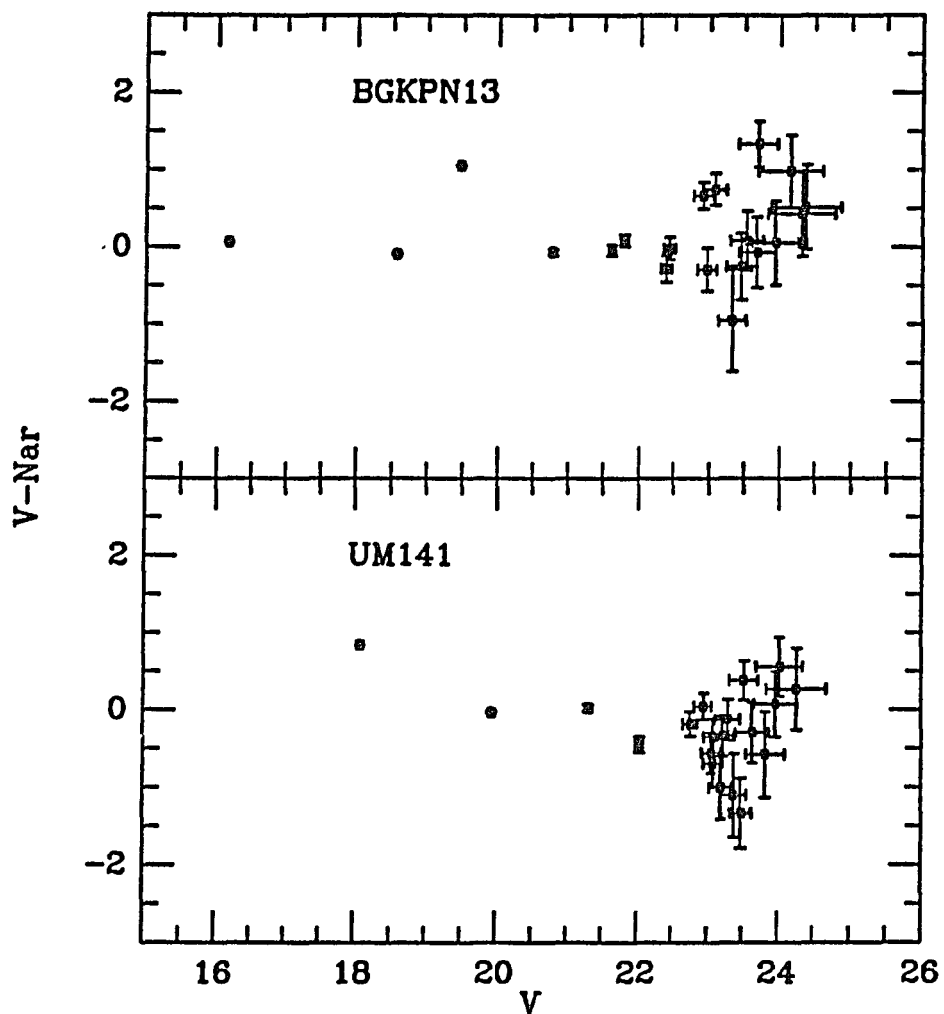


Figure 3.3: The observed color-magnitude diagrams for the 12 quasars observed. The $V - N$ zero point has been shifted so that $V - N = 0$ is an object with no narrow band excess.

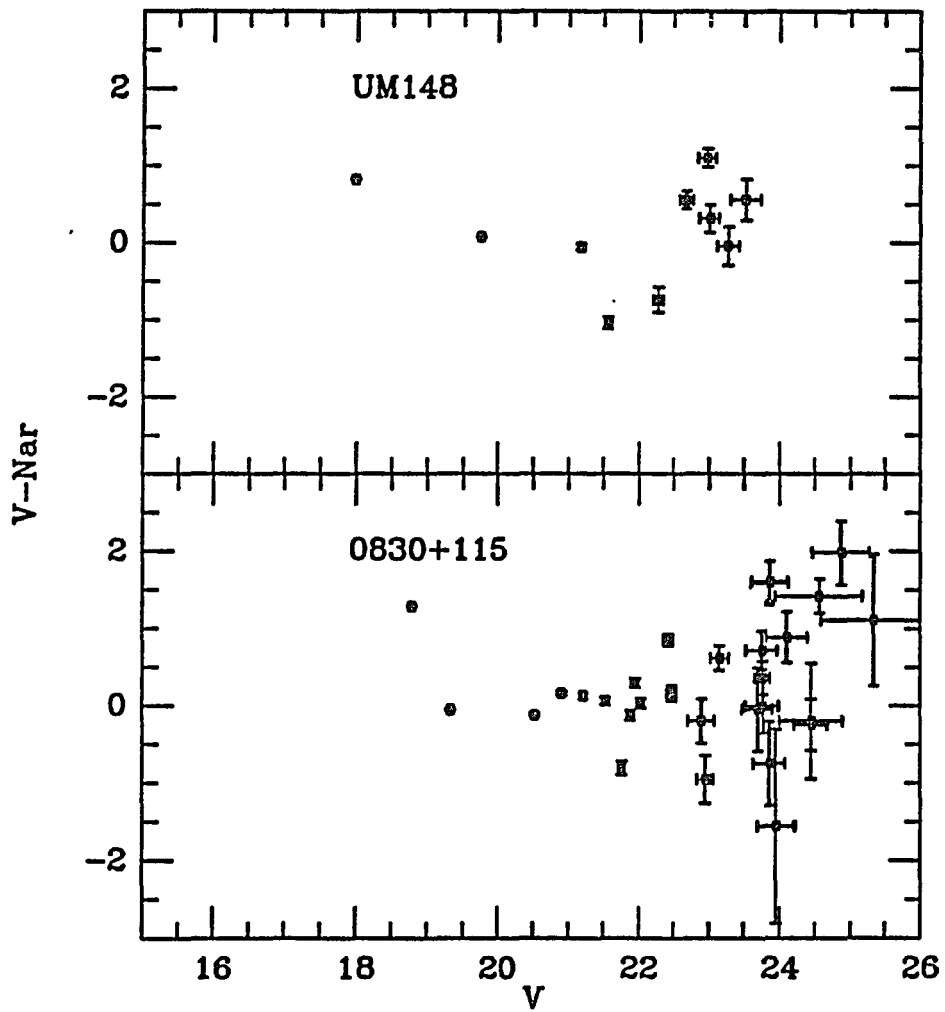


Figure 3.3: The observed color-magnitude diagrams for the 12 quasars observed. The $V - N$ zero point has been shifted so that $V - N = 0$ is an object with no narrow band excess.

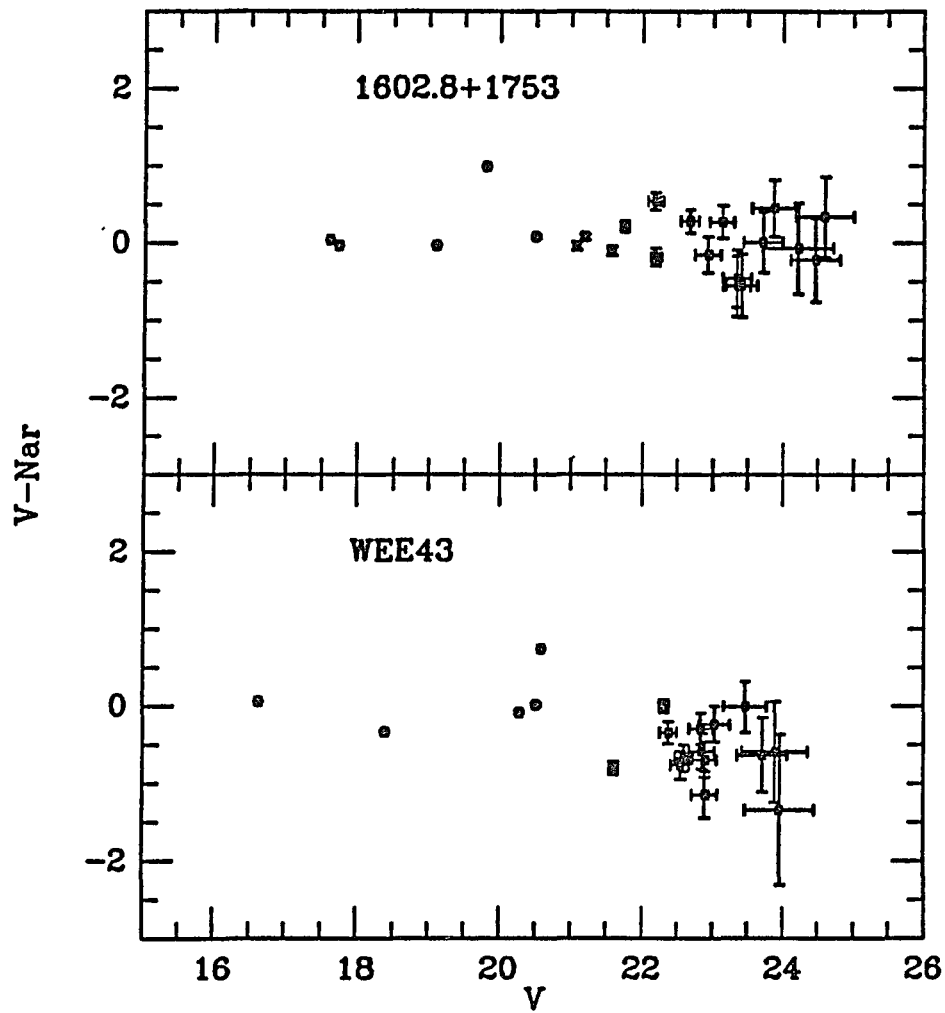


Figure 3.3: The observed color-magnitude diagrams for the 12 quasars observed. The $V - N$ zero point has been shifted so that $V - N = 0$ is an object with no narrow band excess.

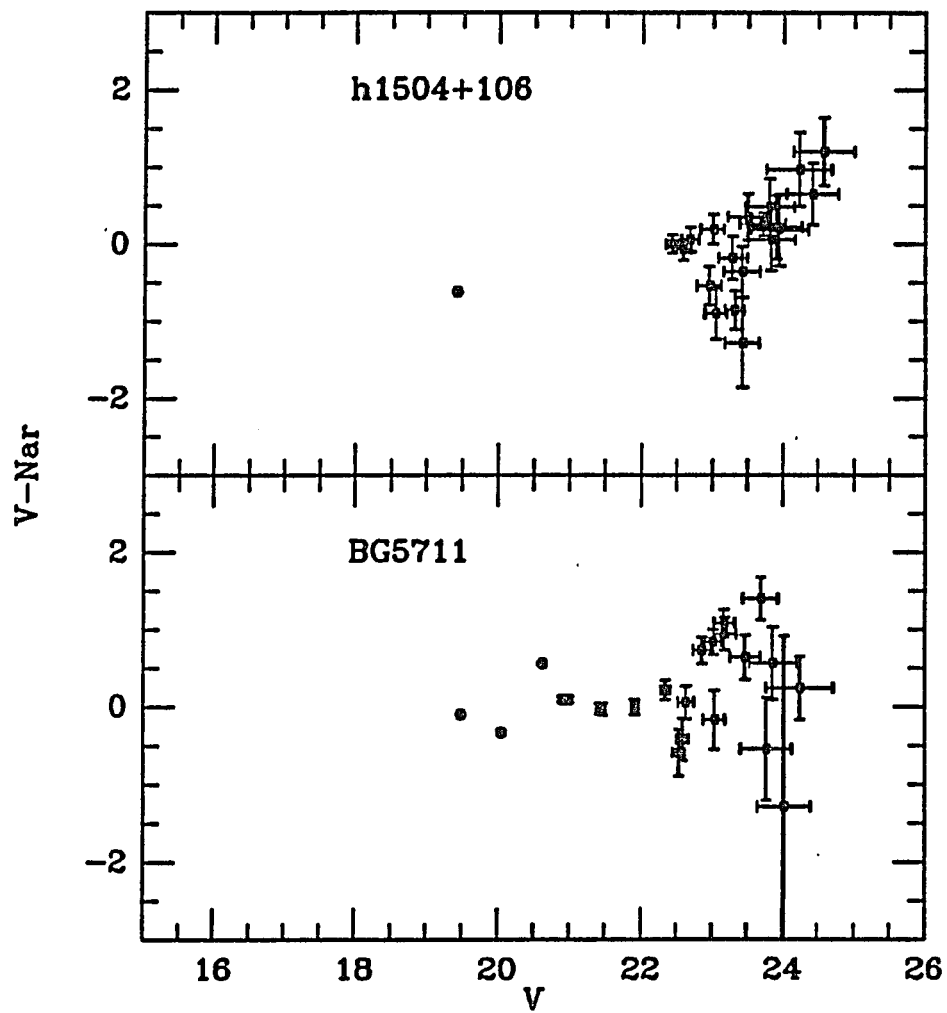


Figure 3.3: The observed color-magnitude diagrams for the 12 quasars observed. The $V - N$ zero point has been shifted so that $V - N = 0$ is an object with no narrow band excess.

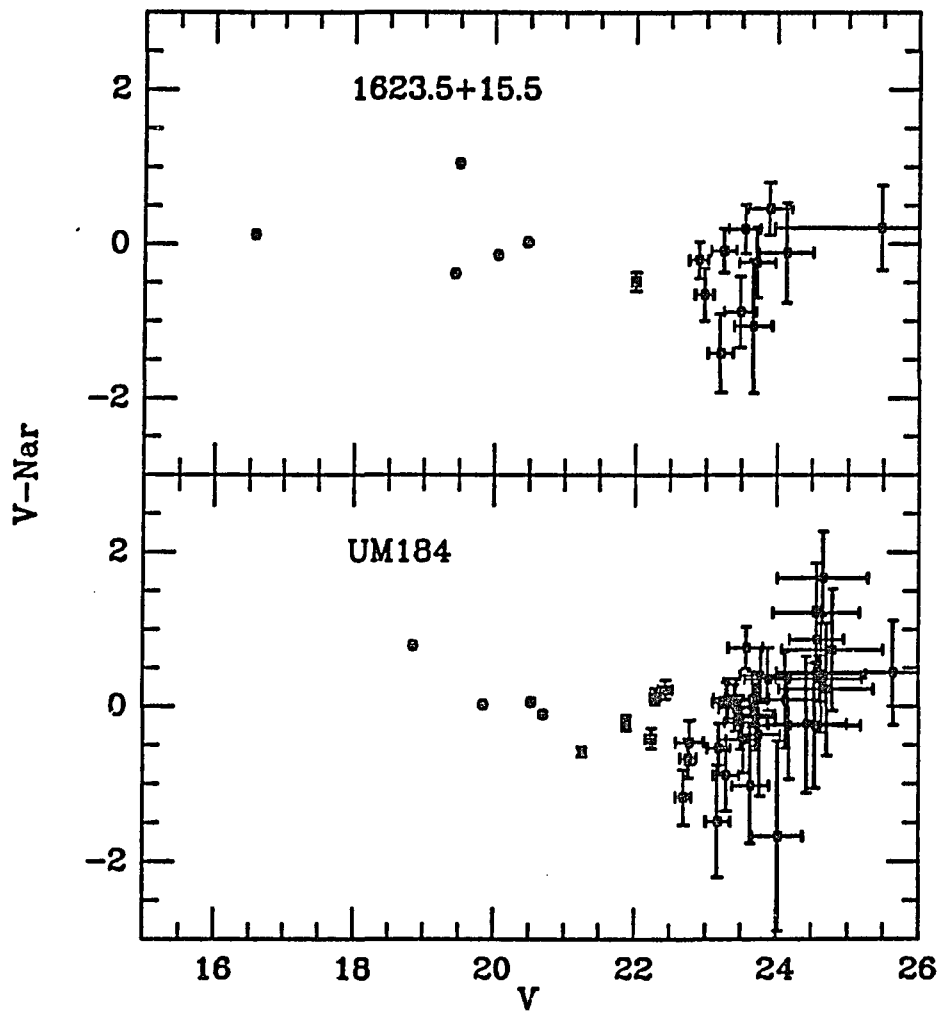


Figure 3.3: The observed color-magnitude diagrams for the 12 quasars observed. The $V - N$ zero point has been shifted so that $V - N = 0$ is an object with no narrow band excess.

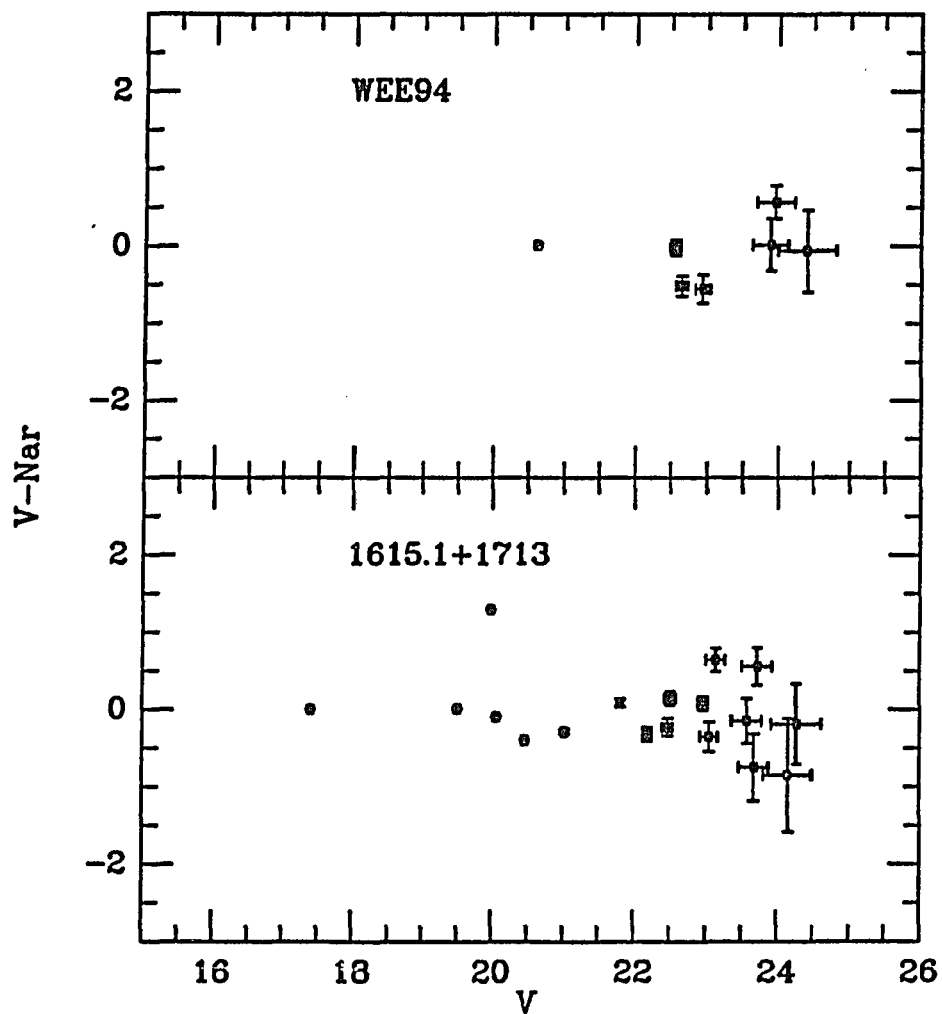


Figure 3.3: The observed color-magnitude diagrams for the 12 quasars observed. The $V - N$ zero point has been shifted so that $V - N = 0$ is an object with no narrow band excess.

faint objects in $B - V$ colors can be used to investigate the scatter in differential magnitudes due to the color correlation. Most faint galaxies have $B - V$ colors near .8 for $B \leq 24$. There is fairly little blueward scatter extending to $B - V$ of .2 while there is a large amount of red scatter extending to $B - V = 2$. Thus, we would expect little scatter toward large line excess, certainly less than .1 magnitude. The scatter toward smaller differential magnitudes will be larger approaching .3 mag for very red objects. Little scatter toward large excess is expected since normal sources get no bluer than a flat SED while there will be large red scatter since objects can become arbitrarily red. This seems to be the observed trend. There appears to be a well defined upper limit to the differential color with greater scatter toward redder colors. As a result of galaxies not getting bluer than $B - V$ of a few tenths, the objects found with narrow band excess cannot be explained by color effects alone.

Let us comment on some of the sources observed:

UM141. The only excess object in this field is the BAL quasar itself.

This object nicely shows how objects without significant excess in the narrow band filter are distributed.

UM148. Observations of this object were made under very poor seeing ($3''$) and should be observed again to achieve greater depth.

WEE94. We can find no excess emission from the quasar. In this field, the only marginally detected excess source is far too faint to be the

quasar. This could be due to an incorrect ID of the quasar from the very poor finder of Weedman (1980) or an incorrect redshift.

0830+115. This object has many excess sources associated with it and seems to be a good candidate for a $z=3$ cluster. Objects 11,12 and 13 form a very compact group.

h1504+106. The quasar in this field possesses a narrow band deficit since it is a broad absorption line quasar.

1602.8+1753. This quasar is in a very crowded field in a cluster of galaxies. The only excess source other than the quasar (object 11) is probably not reliable since it is near a very bright star.

BG5711. This quasar possesses a number of excess sources and may be another $z=3$ cluster.

Spectroscopic observations are clearly the next logical step. Not only would they confirm the reality of the excess objects but they could perhaps tell us more about the source of the excitation. Also in the cases where there are many objects in one field they would give the kinematic properties of a cluster at a very early epoch. On 3 observing runs from the spring of 1987 to the spring of 1988 we tried to use the FOGS spectrograph on the MMT to make these observations. A total of one night was clear but the seeing ranged from 3" to 5" making faint object work impossible. We did observe four of the quasars to confirm the redshifts and to measure the EW

Name	Z(MMT)	EW(MMT)	V-N(MMT)	V-N(Phot)	Comment
0731+65	3.025	640Å	1.4, 1.5	1.30	Clean continuum
UM148	2.989	240Å	.8, .9	.82	Clean continuum
BGKPN13	2.92	100-200Å	.5, .8	1.06	Uncertain EW due to Lyman α abs.
UM141	2.90	200-400Å	.7, 1.2	.85	Uncertain EW due to BAL

Table 3.3: Comparison of Spectroscopic and Photometric EW for Quasars

of the Lyman α and NV complex.

Table 3.3 gives the observed redshift and the EW of Lyman α for the quasars. It also gives both the expected $V - N$ color for that EW and the value observed using the narrow band photometry. In the cases where the EW is well measured the comparison is very good (0731+65 and UM148). For BGKPN13 the comparison is fair but the EW is difficult to measure since the Lyman α line and the continuum toward the blue are very heavily absorbed. UM141 is a broad absorption line quasar (BAL) making the EW very uncertain but the comparison between the expected and observed value is still rather good. From these observations it would appear that the EW is determined to about 10 or 20% from the photometry, even for quasars where the broad emission lines completely fill the narrow band filter.

3.4 Discussion

Of the 12 quasars observed 5 show no excess emission objects at $> 2\sigma$ other than the quasar (UM141, WEE94, 1623.5+15.5, 1062.8+1753 and WEE43). An additional 5

quasars show a few excess objects associated with each quasar (BGKPN13, UM148, 1615.1+1713, UM184 and h1504+106). Finally, 2 quasars have a large number of excess objects (0830+115 and BG5711). This is in marked contrast to the results of Hu and Cowie (1987) and Spinrad (1987) who have imaged a total of 50 quasars. Without details of the sensitivity limits of these surveys it is difficult to determine why they find no excess sources. Two possibilities come to mind; they only looked very near the quasar or they did not make detailed photometric observations of all sources. The first possibility is important because the excess objects do not seem to cluster tightly around the quasar. The second point is important because the excesses of most sources are small and cannot be seen by simply "blinking" of images. In the rest of this section we will look at the properties of these objects and compare them to those that would be expected from starforming galaxies.

Let us begin by looking at the distribution of EWs since it is independent of cosmology. Figure 3.4 shows the distribution of $V - N$ colors which is related to EW by figure 3.2. The peak of the distribution ($V - N = .8$) corresponds to 50\AA in the rest frame at $z=3$. For $V - N < .5$ ($\text{EW} < 30\text{\AA}$) we become incomplete since our photometry is not accurate enough to differentiate these objects from neutral colored objects but there should be no limit to the maximum value of $V-N$. Figure 3.5 demonstrates how the distribution of $V - N$ colors is affected by photometry errors. The distribution is skewed toward larger values since we do not detect the sources which are scattered toward smaller values. The distribution is consistent

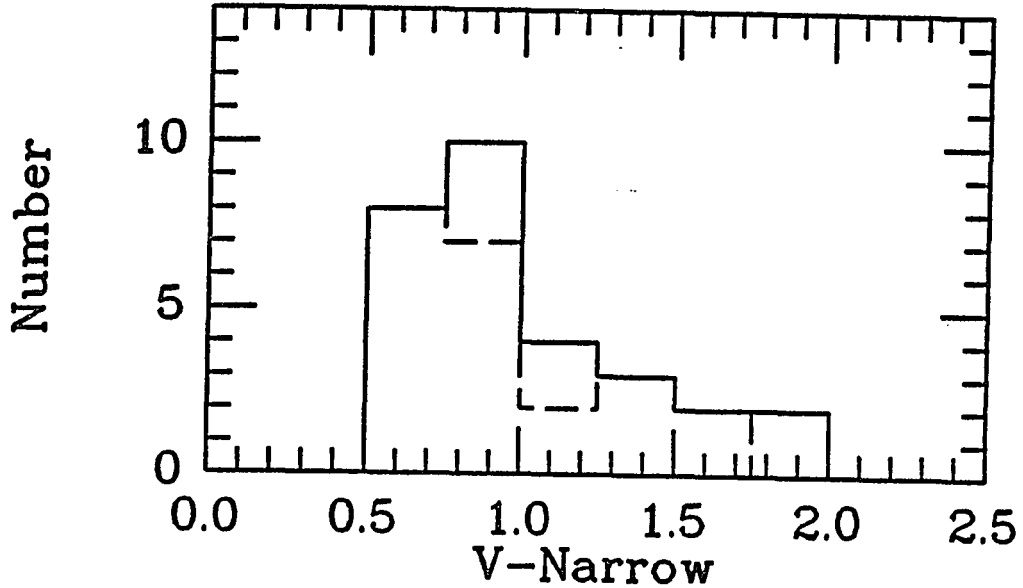


Figure 3.4: The distribution of $V - N$ colors for the excess objects found around the 12 quasars in this study. The solid line is for all objects while the dashed line is for objects with $V < 24$. The cut-off for low values is a selection effect since photometric errors prevent the differentiation of such objects from neutral colored objects. The distribution is much broader than would be expected from a model with constant star formation lasting longer than 10 million years and case B recombination. This is probably due to Lyman α absorption flattening the distribution to lower values.

with all $V - N$ colors being between .6 and 1. The maximum $V - N$ is rather uncertain due to scatter in the observations but is probably less than about 1.6 or an EW of about 150\AA in the rest frame. Having a peak value of 150\AA is close to what figure 3.2 would indicate is a reasonable value for case B and an IMF slope near 1.

The distribution of $V - N$ (Figure 3.4) is different from what would be expected from a simple constant star formation rate model (Figure 3.2). In the simple model one would expect most objects to be clustered strongly around the asymptotic

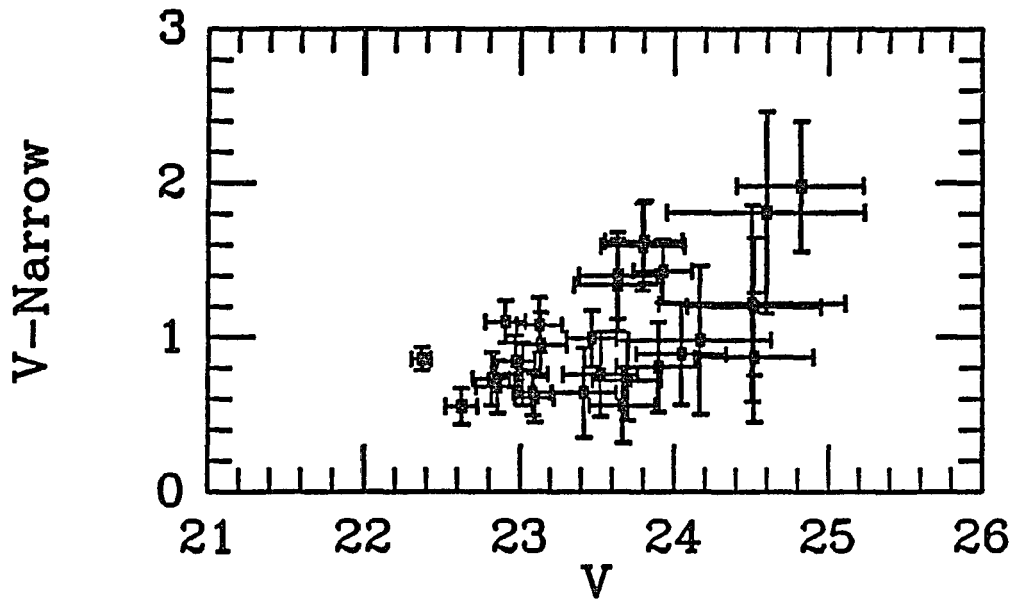


Figure 3.5: The color-magnitude diagram for narrow band excess objects found in the survey. The distribution of $V - N$ colors becomes very asymmetrical at faint levels due to the loss of objects which are scattered to small values of $V - N$. The distribution of $V - N$ colors is consistent with a range of $V - N$ from .5 to 1 at all V magnitudes.

value of the EW (about 100\AA). Our distribution is much broader and drops much more slowly at large $V - N$ than the simple model. One possible explanation of this would be large variations in the IMF slope from object to object. But observations of nearby galaxies (Freeman 1985) do not indicate much variation in the IMF of massive stars making this a rather ad hoc model. I suggest that the simple model is violated because of absorption of the Lyman α emission. Without absorption the EW of Lyman α for the asymptotic value should be about 100\AA but variable amounts of extinction broaden the narrow peak toward smaller EWs. This would imply that the observed Lyman α flux is a factor of 2 to 3 below the case B value for most objects, which is in agreement with nearby star forming galaxies with strong Lyman α (Hartman et al. 1988). In any event the inferred EW of Lyman α for these objects seems completely consistent with star formation being the ionizing agent.

Figure 3.6 presents the histogram of the rough V magnitudes for the excess objects detected. Once again we are incomplete below V of about 24. At $z=3$ the V filter samples the continuum at 1400\AA where the light will be dominated by the shortlived young stars. If we adopt a cosmology ($q_0=0, h=.5$) we can compute the source luminosities and the rough star formation rates (equation. 3.1). With this very large cosmology V of 23 corresponds to a star formation rate of $300M_{\odot}yr^{-1}$ while V of 24 corresponds to $100M_{\odot}yr^{-1}$. For a small cosmology ($q_0=.5$ and $h=.8$) these rates would be reduced by a factor of 9. Once again I stress that this calculation

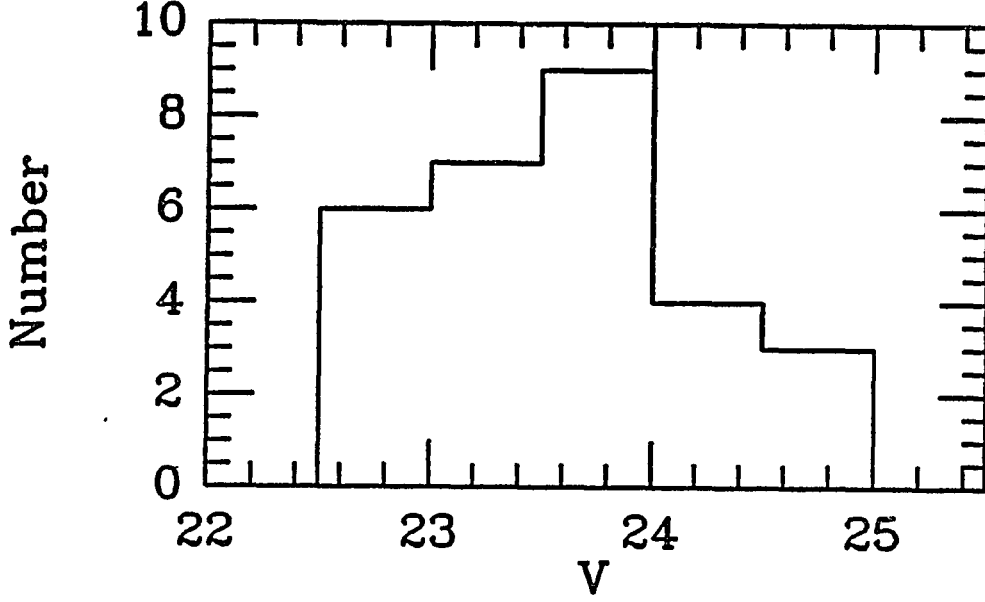


Figure 3.6: The distribution of V magnitudes for the narrow band excess objects detected during the survey. The survey is not complete below V of 24.

is very sensitive to the IMF. Similarly we can look at the Lyman α luminosities and use them to predict the star formation rate (Figure 3.7). To compute the luminosity we multiplied the predicted Lyman α EW (eqn. 3.5) by the flux at V assuming the spectrum is flat from V (eqn. 3.6) to the Lyman α line.

$$EW = 188\text{\AA} \left(10^{\frac{V-N}{2.5}} - 1 \right) \quad (3.5)$$

$$S(Ly\alpha) = EW(4.6 \times 10^{-9})10^{\frac{V}{-2.5}} \quad (3.6)$$

A Lyman α luminosity of $10^{44} \text{ erg sec}^{-1}$ gives a star formation rate of $50 M_{\odot} \text{ yr}^{-1}$ ($\alpha = -1$) and $130 M_{\odot} \text{ yr}^{-1}$ ($\alpha = -1.5$). These rates are 2 to 3 times smaller than those given by the continuum flux, which is not surprising since we argued that the Lyman α flux is probably a factor of 2 to 3 lower than the case B value due to

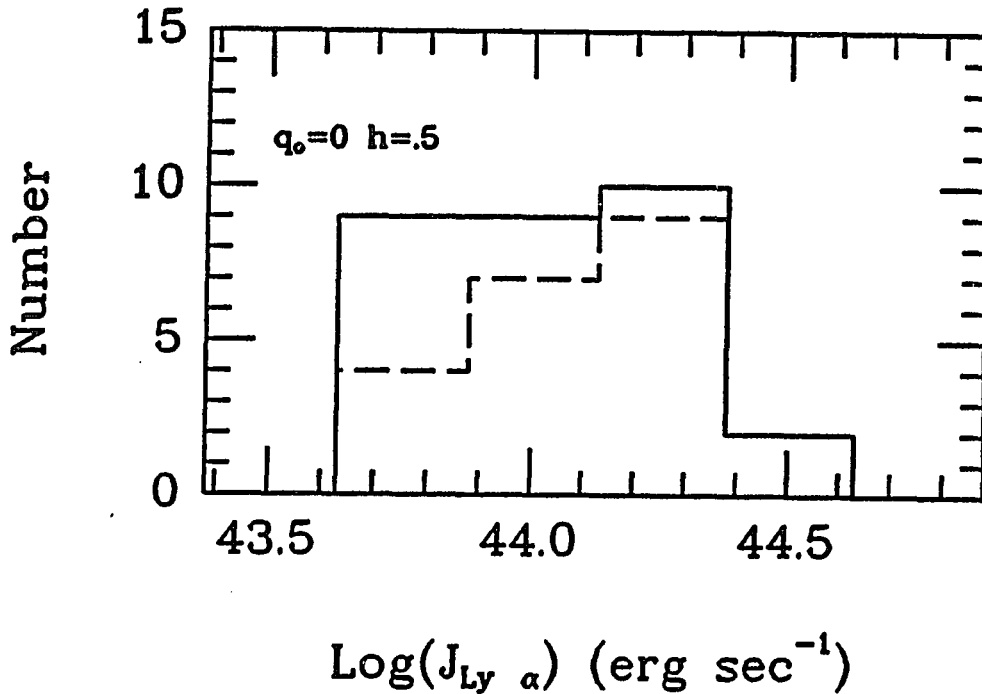


Figure 3.7: The distribution of Lyman α luminosity derived from the $V - N$ color and the V flux assuming a $q_0=0$, $h=.5$ universe. A cosmology with $q_0=.5$ and $h=.8$ would reduce the luminosities by a factor of 9. The solid line is for all objects and the dotted line is for all objects brighter than 24.

Lyman α trapping. Thus, the brightness and the Lyman α flux seem consistent with star formation rates of a few $100 M_{\odot} \text{yr}^{-1}$.

How do these star forming objects fit into the picture of galaxy formation? As discussed in the previous section strong Lyman α emission is not observed from star forming dwarfs with metallicities greater than .1 solar. If the star forming regions in these galaxies have properties similar to those of local galaxies then we would expect Lyman α emission from them only during the early stages of their formation. Since we lack a detailed understanding of why the metallicity correlates so strongly with Lyman α intensity, this assumption may not be valid for high star formation rates

in a large galaxy at high redshift when the UV background was possibly higher than today. But since the star formation rate per unit area is roughly the same for these objects as for the dwarfs we will assume their Lyman α flux correlates with metallicity in the same way as it does in the dwarfs. Thus, we assume that these objects are in an early stage of their formation having not yet processed enough metals to make them opaque to Lyman α emission. To test this one could try to measure the metallicity directly using the ratio of $H\beta$ to O[III]5007 emission in the near IR.

A further complication for understanding these objects is our lack of knowledge of the geometry of space. Here we shall discuss two extreme cosmologies; A large cosmology with $q_0=0$ and $h=.5$ and a small cosmology with $q_0=.5$ and $h=.8$. These cosmologies give luminosities and thus star formation rates which differ by a factor of 9. Also the time scales are different by a factor of 2. With the large cosmology star formation rates of $400M_{\odot}yr^{-1}$ are derived giving a time scale for forming $10^{11}M_{\odot}$ stars of a few times 10^8 years. The small cosmology gives a star formation rate of $50M_{\odot}yr^{-1}$ making the time scale for formation a few Gyrs. Given these two alternatives we will discuss if it is more plausible that we are seeing young disks beginning their formation or spheroids forming at $z=3$.

The star formation rate in the small cosmology is only a few times the current star formation rates of disks (Kennicutt 1983). Observationally, the past star formation rates of disks are thought to be a few times larger than the current rates (Twarog

1980, Kennicutt 1983). Thus, with slowly decreasing star formation rates it seems that these could be the disks we see today starting their lives 7Gyrs ago. This seems consistent with estimates for the disk age (Twarog 1980 and Winget et al. 1987). In the large cosmology it does not seem likely that these could be forming disks unless the star formation rates in disks have decreased far more than is now believed. The problem is that the disks would use all their gas in a short time (10^8 years) while the time from $z=3$ to today is 7Gyrs in this cosmology.

An alternative is that we are seeing spheroids in the process of forming. In the large cosmology the high star formation rates allow the spheroids to form in a short time completing their star formation at a redshift above 2 ($4 \times 10^8 yrs$ after $z=3$). This seems consistent with producing the stellar populations of current day elliptical galaxies (Wyse 1986). In the small cosmology it seems unlikely that these could be spheroidal galaxies forming. The problem is that the star formation rate is so low that the spheroids will still be forming at $z < 1$ even if the star formation rate does not decrease at all ($\tau_{form} = 2Gyrs$, star formation concludes at $z=.2$). This seems inconsistent with the stellar populations of current day elliptical galaxies and spheroids (O'Connell 1976, Pickels 1985 and Rose 1985).

Thus, without knowing the cosmology we have two plausible models for these galaxies involving the formation of either elliptical galaxies or disks. One final point is that the density of the Lyman α excess objects seems rather high in the case of 4 quasars. These could be young clusters. In this case it seems most likely that we are

seeing the formation of young spheroidal galaxies given the current day correlation between density and galaxy type (Dressler 1980b, Postman and Geller 1984). The observation by Butcher and Oemler (1984 and references there in) that blue galaxies do appear in cluster environments at relatively recent epochs ($z=.2$) could be due to these galaxies near the end of their star formation providing a means to produce spheroidal galaxies even in the small cosmology. A better understanding of the origin of the blueing in the Butcher Oemler clusters would elucidate this point better.

We now turn our attention to the environments of the quasars in this sample. As noted in the introduction the environments of quasars may provide clues into how and why the quasar population evolves. At low redshift ($z < .4$) Yee and Green (1984) find that quasars are found in regions of higher than normal galaxy density but not in clusters of Abell richness class 1 or larger. Furthermore, at moderate redshift ($z=.5$) the environments of radio loud quasars become rich (Yee and Green 1987). For these $z=3$ quasars we have a range of environments from fields with no Lyman α companions to fields with many companions probably indicating they are in rich environments. Once again we are beset by the incompleteness of a Lyman α search since probably only a small fraction of the objects are Lyman α bright, but they do give a lower limit to the richness of the environment. Basically, of the 12 quasars observed 4 appear to be in fairly rich environments with 4 or more Lyman α companions (BGKPN13, 0830+115, UM184 and BG5711).

Since the environments of low redshift quasars and the properties of metal ab-

sorption line systems near the quasar redshift at high redshift seem to correlate with radio properties we have tried to find radio observations of our quasars (Table 3.1). Some radio data was found in the literature and all the source locations were examined on the 6 cm sky flux survey map of Condon and Broderic (1986) which has a flux limit of 150mJy. Two of the sources are near large clusters of galaxies (Coma and Hercules) and will be excluded from the analysis since they could be badly contaminated by radio emission from cluster members in the low resolution map of Condon (Coma and 1602.8+1753). Additionally, h1504+106 may be detected in the Condon survey but only at a level of 100mJy which is below the survey limit of 150mJy so it will be classified as radio quiet. The result is that 2 of the four objects in rich environments are radio loud with a flux of more than 150mJy at 6 cm (0830+115 and UM184) while no objects in poor environments are detected. This is very suggestive that the same segregation of environments between radio loud and radio quiet quasars found at $z=0.5$ may exist at $z=3$ and that the associated metal absorption line systems are indeed due to clusters. Since the detected quasars are near the flux limit of the Condon maps it will be necessary to make more sensitive radio observations to test how good the correlation is. To further strengthen this correlation we note that the radio loud quasars 2016+112 and PKS1614+051 may be in a rich environments (Schneider et al. 1987, Djorgovski et al. 1987a).

The inverse effect is the observed decrease in the number of Lyman α forest absorption line systems as one approaches the redshift of the quasar (Weymann et

al. 1981, Murdoch et al. 1986 and Tytler 1987). One explanation of this effect is that the UV radiation from the quasar increases the ionization of the Lyman α forest clouds near the quasar, decreasing their Lyman α optical depth (Bajtlik et al. 1987). The presence of clusters around radio loud quasars could also help explain why the inverse effect appears to be stronger around radio loud quasars (Bechtold 1986) but this may be due to the sample of radio loud quasars being more luminous. The Lyman α emitting galaxies in the cluster would tend to enhance the inverse effect because they could provide significant ionizing radiation. To get a rough feeling for this let us consider the case of 0830+115. If we assume that half of the Lyman continuum radiation from the Lyman α companions escapes then they contribute 100 times less ionizing flux than does the quasar. Thus, it would appear that the Lyman α companions do not provide a significant contribution to the UV radiation field near the quasar unless the Lyman α bright galaxies only comprise a very small fraction of all the star forming galaxies or that the galaxies have faded rapidly in their Lyman continuum flux after ionizing the Lyman α forest clouds at an earlier time. An alternative possibility is that since galaxies have formed they may have incorporated the Lyman α forest clouds into them.

Chapter 4

The Stellar Populations of Blue High Redshift Radio Galaxies

4.1 Introduction

At redshifts greater than about 1 the optical colors of radio galaxies show significant deviations from what would be expected for a passively evolving elliptical (Djorgovski and Spinrad 1985). Some become very blue with optical colors approaching those of a starforming Im galaxy at the same redshift. In general, high redshift 3C galaxies also have bluer optical to infrared colors than predicted by passively evolving galaxy models (Lilly and Longair 1984, Eisenhardt and Lebofsky 1987). Eisenhardt and Lebofsky (1987) and Lilly and Longair (1984) suggest that the large blue scatter in the optical to IR colors is due to bursts of star formation. Since the blue optical emission in these narrow line radio galaxies is extended we will assume it is due to a stellar component rather than an active galactic nucleus (Lilly et al. 1983, Djorgovski and Spinrad 1985). The blue galaxies also show large amounts of

luminosity evolution being up to 5 magnitudes brighter in the visual than a passively evolving galaxy. Some show extremely strong Lyman α emission (Spinrad et al. 1985). Here we will present detailed optical to IR SEDs to study the stellar populations of these objects.

The characteristics of these blue galaxies seem very similar to what would be expected from a galaxy forming large amounts of stars. The question we would like to address here is if the bulk of the stellar population in these galaxies is old or if it has just formed. Since the spectral energy distribution of an old population peaks in the near IR, observations in the near IR provide the best constraint on such a population. We have therefore obtained IR photometry for a sample of high redshift 3C radio galaxies with blue optical colors to try and place constraints on the significance of the young stellar population.

In the next section we will discuss the observations and the gross properties of the 3C galaxies observed. In section 3 we will discuss in detail the radio galaxy 3C256 which is the most extreme object found. Finally, in section 4 we will apply the formalism developed for 3C256 to the other radio galaxies.

4.2 Observations

The IR photometry for this study was observed as part of a larger complete study of 3C radio galaxies. Here we shall limit our discussion to those galaxies with published

4.2 Observations

The IR photometry for this study was observed as part of a larger complete study of 3C radio galaxies. Here we shall limit our discussion to those galaxies with published optical photometry (Djorgovski and Spinrad 1984, Lilly and Longair 1984). Though our IR photometry is much more extensive than the published optical photometry we opted not to obtain optical photometry since such observations have already been made but not reported by Spinrad and Djorgovski (1988).

The IR photometry was obtained using the LHe cooled InSb photometer on the MMT. Most of the observations were made using an 8.7'' aperture with a 10'' chopper throw. For a few objects, where contamination of the beam was a problem, a 5'' aperture was used with a 6'' throw. One of the primary sources of error in aperture photometry is contamination of the reference beam by other sources. To overcome this we made multiple observations of the source at different hour angles so that the parallactic angle rotation of the MMT would move the reference beam to a different patch of the sky. If the observations did not agree we would make further observations until consistency was achieved. Flux calibration was obtained by observing standard stars from Elias et al. (1982). Typically 3 or 4 standard stars were observed each night. The internal consistency of the standards was typically .02 magnitudes with excellent repeatability from night to night. Table 4.1 presents our IR photometry for the blue 3C galaxies. Also, in table 4.1 we present IR and

optical photometry of the same sources from the literature. In general the agreement is good except for a few points which will be discussed below. The optical to IR spectral energy distributions (SEDs) are presented in figure 4.1 along with the SEDs of a $z=1$ E galaxy and a star forming Im galaxy from Coleman et al. (1980).

Let us discuss the radio galaxies and look at the consistency of our photometry with previous studies.

3C256 has the flattest SED of the blue radio galaxies but the near IR colors are similar to what would be expected from an old stellar population. Our K observation and that of Lilly et al. (1985) differ, with ours being slightly more than 1σ fainter.

3C241, while having a very flat and blue optical SED, has a red SED from R to K typical of an old stellar population in an elliptical galaxy. The H measurement reported by Lilly and Longair (1984) is clearly in error.

3C238 has a SED that is very similar to that of 3C241, though the data are less complete for this object.

3C234 has a very odd SED that drops steadily from K to B . In particular the drop from R to B is very large and difficult to understand. Given the unlikely $B - R$ color, the optical photometry seems suspect. Two independent observations in R agree well leaving the B photome-

Table 4.1: Photometry of 3C Radio Galaxies with $z > 1$

Name	Z	Ref	B	$\sigma(B)$	V	$\sigma(V)$	R	$\sigma(R)$	I	$\sigma(I)$	Apt	Ref	J	$\sigma(J)$	H	$\sigma(H)$	K	$\sigma(K)$
3C256	1.819	DS	22.12	0.1	21.85	0.1	21.60	0.1	20.94	0.1	8.7"	LLA	20.15	0.25	18.95	0.15	18.43	0.24
		LF					21.57	0.1	20.91	0.2	8"						17.97	0.25
3C241	1.617	DS	23.92	0.1	23.19	0.1	22.93	0.1			8.7"	LL	19.21	0.18	18.22	0.24	17.34	0.17
		LL					22.9	0.21	22.33	0.25	10.8"				10.16?	0.34	17.29	0.15
3C238	1.405	DS	23.03	0.1	23.05	0.1	22.51	0.1			5"	LLA			18.34	0.14	17.71	0.24
											8"						17.57	0.25
3C324	1.206	DS	23.08	0.1			21.27	0.1			8.7"	LL POL	19.27	0.18	18.54	0.14	17.52	0.16
		LL					21.34	0.16			12"				18.07	0.17	16.84	0.18
											7.8"						17.29	0.20
3C368	1.132	D2	21.35	0.1	21.30	0.1	20.60	0.1			8.7"	LL POL	18.84	0.13	17.59	0.13	16.77	0.18
											7.4"				18.06	0.16	16.68	0.17
											7.8"				18.70	0.22	17.17	0.14
3C239	1.781	LL					21.96	0.3	21.25	0.3	5"	LL			18.56	0.18	17.32	0.12
											10.8"						17.67	0.25
3C469.1	1.336	LL					22.00	0.16			8.7"		19.67	0.18	18.45	0.16	17.63	0.15
		DS			22.15	0.5			22.32	0.5								
3C356	1.079	LF	22.73	.10			21.26	.10			5"	LL POL	18.44	.12	17.77	.12	16.53	.07
		LL					21.84	.22			12"				17.35	.13	16.75	.13
											7.8"				17.47	.36	17.09	.22

DS - Djorgovski and Spinrad, 1985. D2 - Djorgovski et al., 1987. LL - Lilly and Longair, 1984. LLA - Lilly, Longair and Allington-Smith, 1985. POL - Puschell, Owen and Laing, 1982. LF - Le Fevre et al., 1988.

try begging for confirmation. The K photometry of Lilly and Longair (1984) is too bright by .7 mag. Our K observation is in agreement with Puschell et al. (1982). With the exception of the large drop from B to R this object looks similar to an object with a blue SED similar to 3C256. Clearly, further optical observations should be made for this source since it may have a very unusual SED but for now we will not consider it further since it does not fit into the class of blue objects.

3C368 has a SED intermediate between 3C256 and 3C241. The J observation by Lilly and Longair (1984) seems to be too bright by .8 magnitudes compared to our observations and those of Puschell et al. (1982), but the K observations of Puschell et al. seems to faint by .4 magnitudes. Chambers et al. (1987) have imaged this galaxy at K and have found that the peculiar lumpy morphology observed by Djorgovski et al. (1987b) in the optical is also present in the near IR. This source is a good example of the alignment of optical isophotes with radio lobes (McCarthy et al. 1987, Chambers et al. 1987).

3C239 is the second highest redshift object in this sample and has very strong Lyman α emission. Unfortunately, the data on this object are rather incomplete but the SED is rather steep. This object will not be considered further here because it lacks adequate optical photometry.

3C469.1 has a SED that looks rather similar to 3C238 or 3C241.

3C356 is the lowest redshift object in the sample and has a fairly red SED similar to that of 3C241. The photometry is consistent with our H point being perhaps slightly too faint by $\approx 1\sigma$.

To summarize the results of the observations, we find that the blue galaxies have rather similar SEDs and can be ordered by the ratio of the flat blue optical continuum to the red near IR continuum. In order of descending prominence of the blue continuum component the galaxies are 3C256, 3C368, 3C469.1, 3C356, 3C328 and 3C241. 3C239 and 3C324 defy classification and need further observations. Since 3C256 is the most extreme example of a blue galaxy we will discuss it in detail next.

4.3 The Case of 3C256

The radio source 3C256 was identified as a $z=1.819$ radio galaxy by Spinrad and Djorgovski (1984). Subsequent observations by Spinrad et al. (1985) revealed that it has strong Lyman α emission. Djorgovski and Spinrad (1985) found 3C256 had very blue colors in the optical (table 4.1) and is some 6 magnitudes brighter at V than a nonevolving giant elliptical galaxy. Also, Djorgovski and Spinrad (1985) found 3C256 to be extended with only a small color gradient, with the nucleus being slightly redder, which indicates it is not dominated by an active nucleus but rather

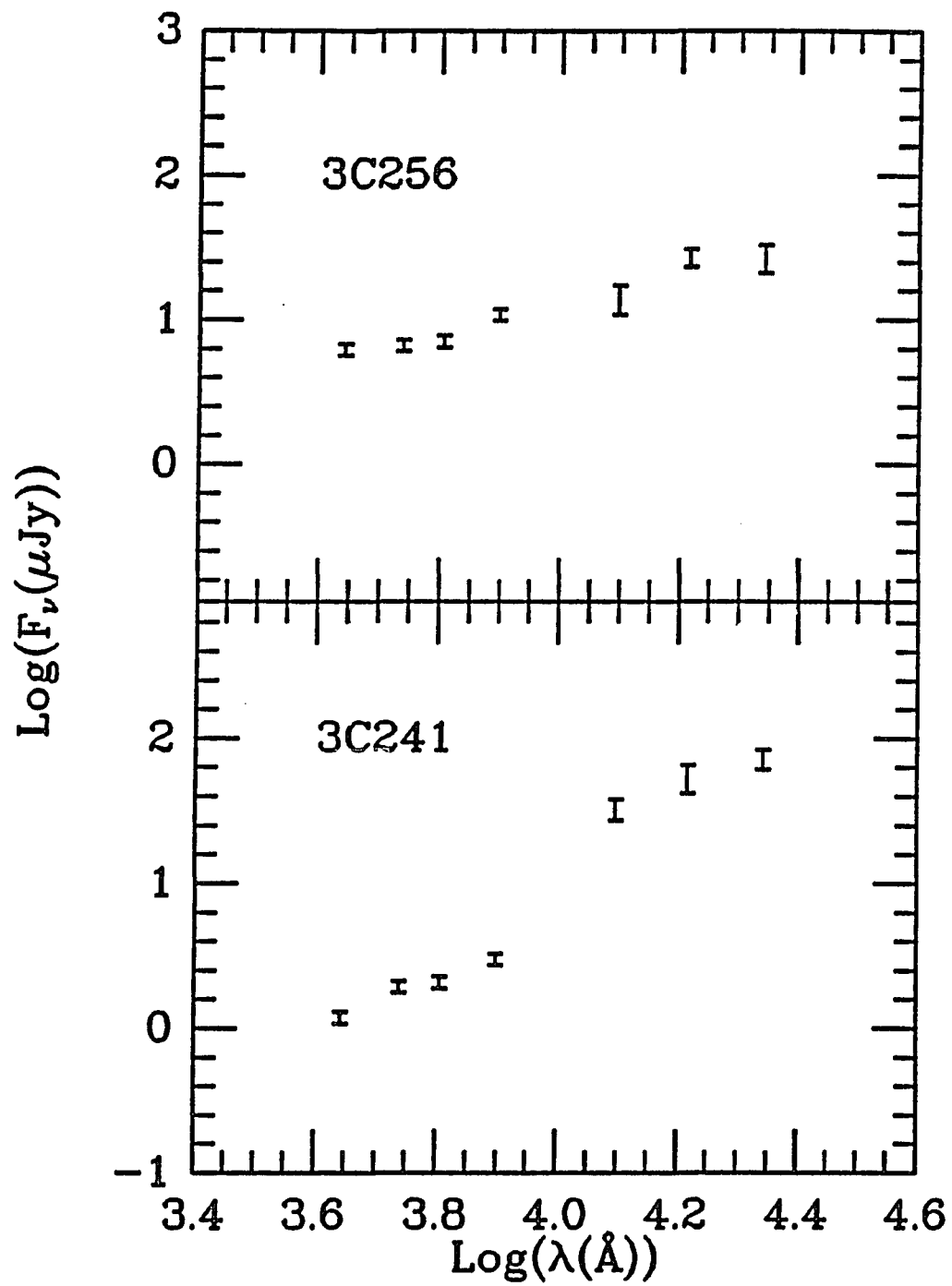


Figure 4.1: The observed spectral energy distributions of 3C radio sources from the optical to the IR.

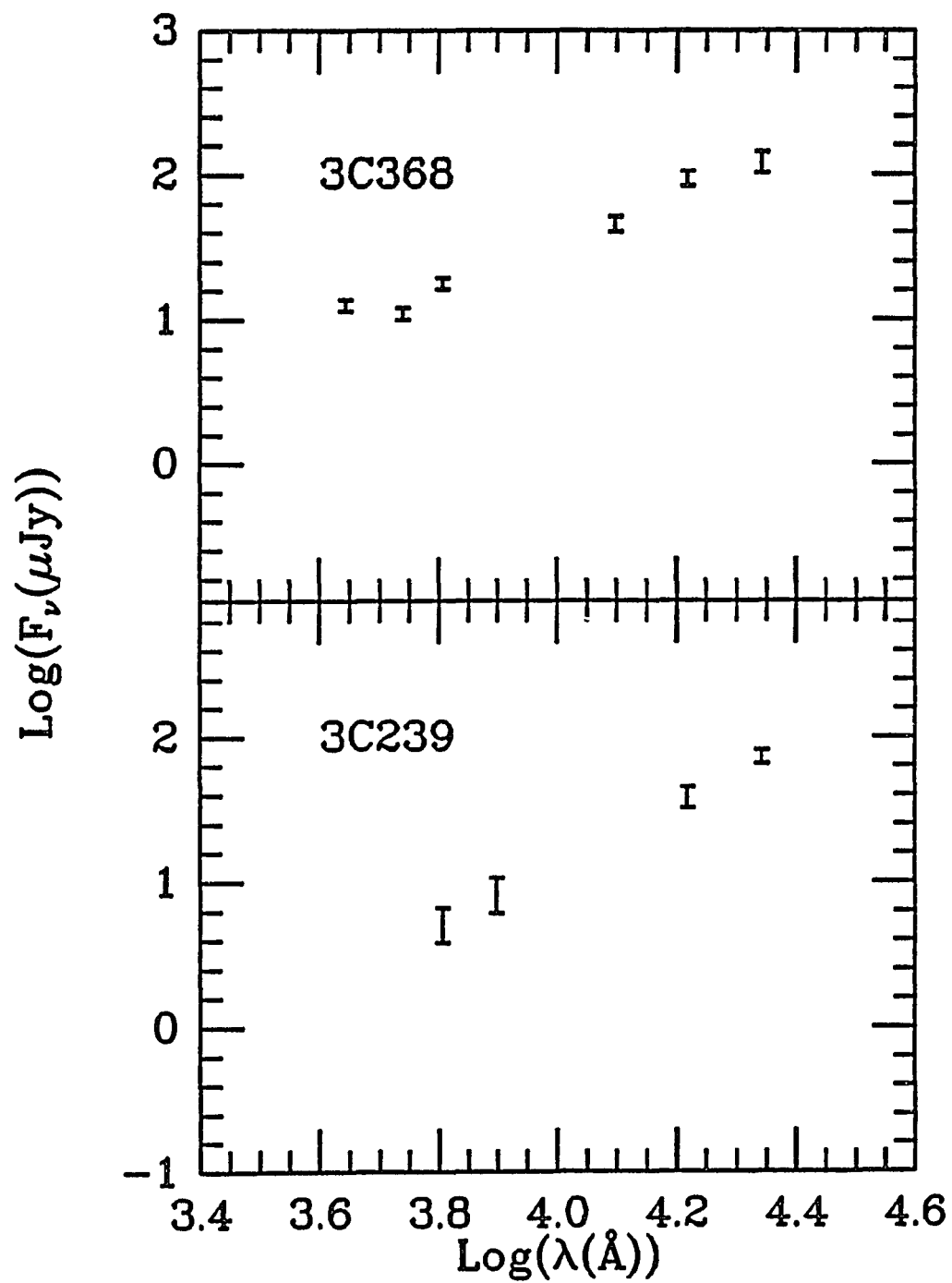


Figure 4.1: The observed spectral energy distributions of 3C radio sources from the optical to the IR.

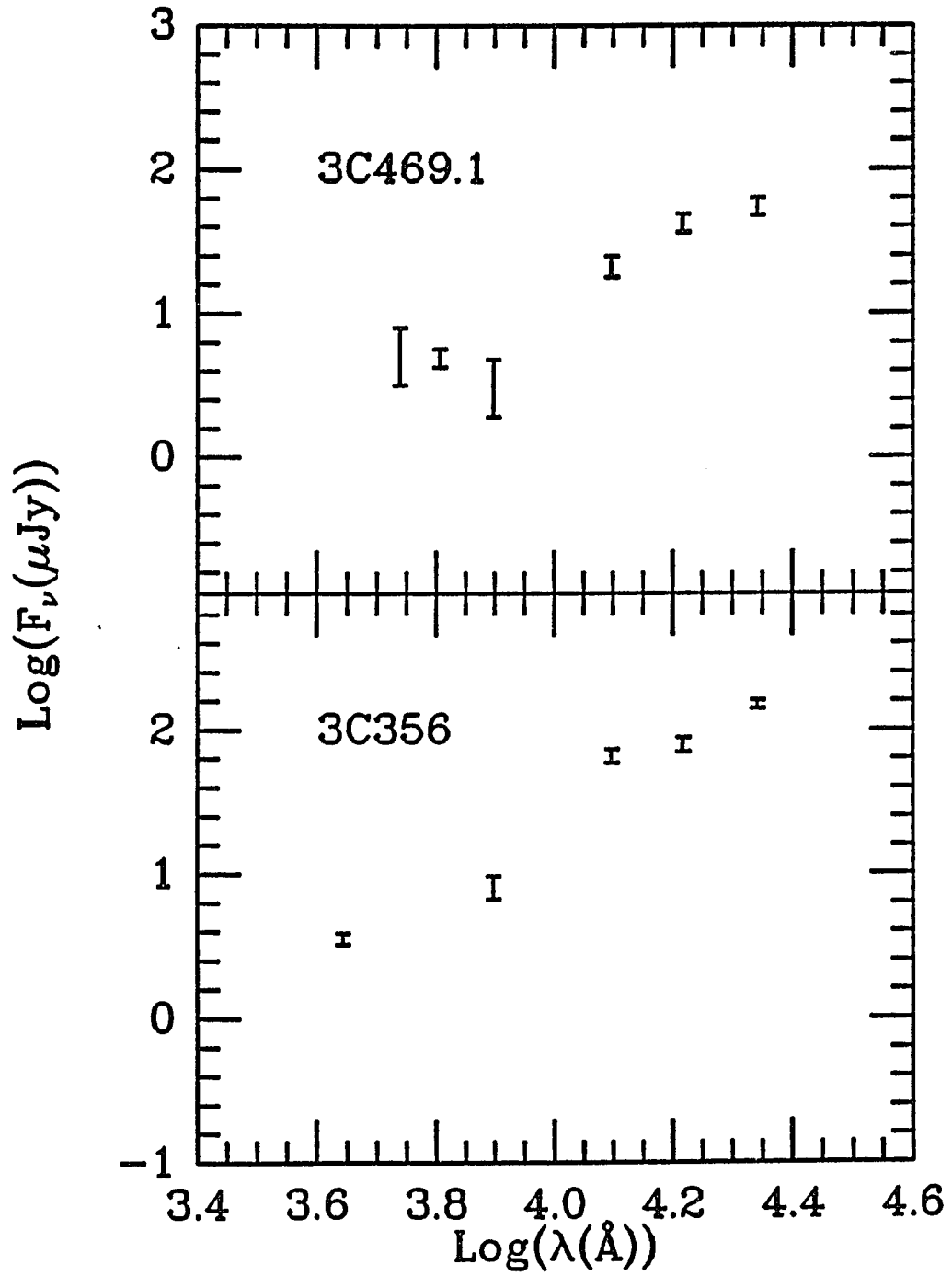


Figure 4.1: The observed spectral energy distributions of 3C radio sources from the optical to the IR.

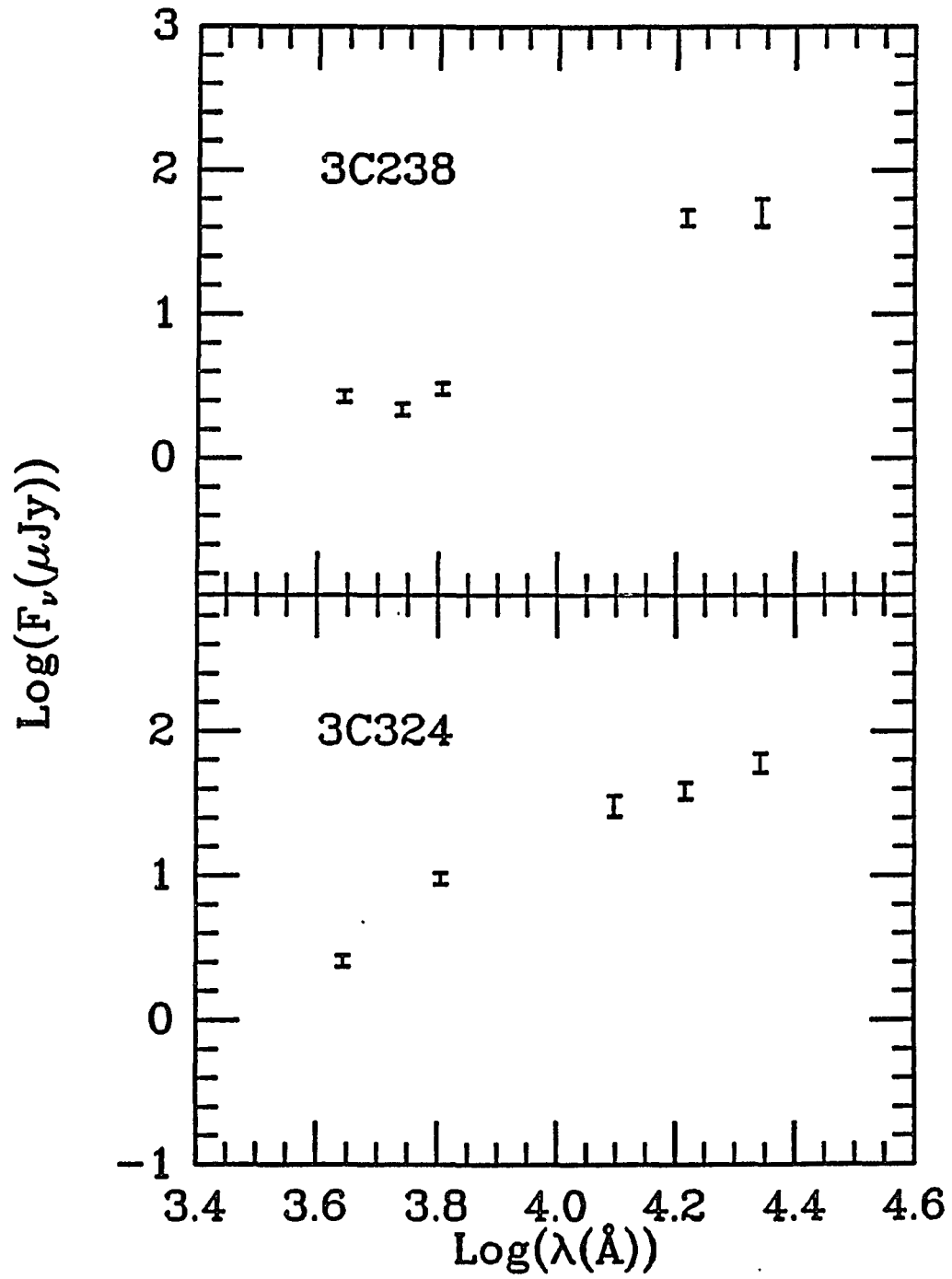


Figure 4.1: The observed spectral energy distributions of 3C radio sources from the optical to the IR.

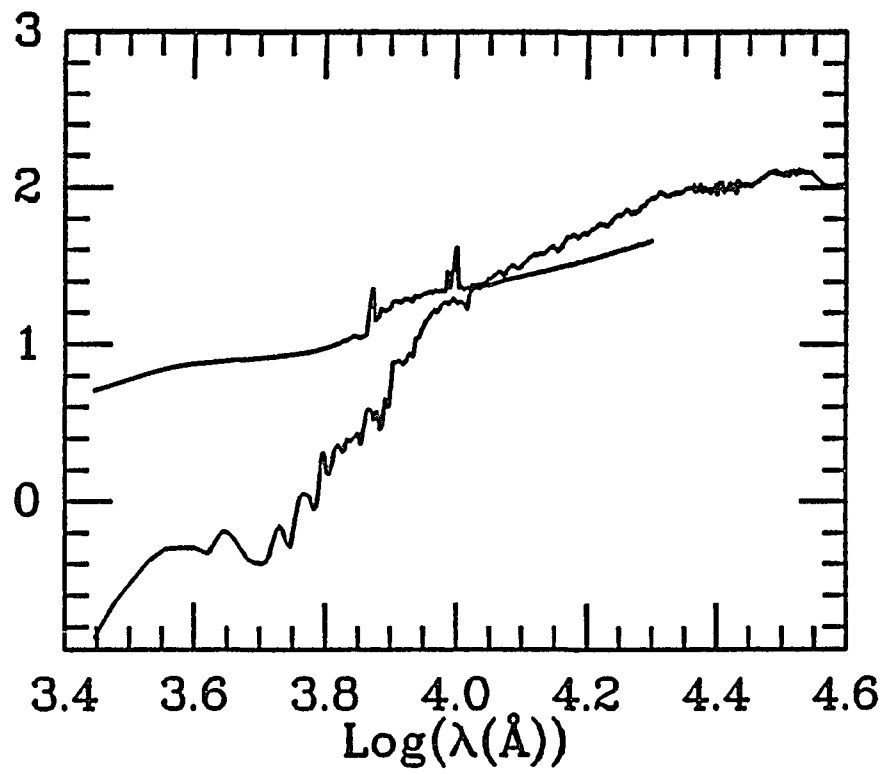


Figure 4.1: The spectral energy distributions of an elliptical galaxy and an Im galaxy from Coleman et al. (1980).

by star formation taking place over its total extent.

Let us consider some corrections to the photometric observations. Due to the high galactic latitude and small HI column no galactic extinction correction is applied. Since 3C256 has a very rich emission line spectrum, we used the observed line ratios of Spinrad et al. (1985) and the total Lyman α flux given by Spinrad (1987) to remove the line flux from the broad band observations. For the near IR we assumed the ratio of $Ly\alpha/H\beta$ was 23 (case B) and that [OIII]3727 and [OII]5007 had ratios of 3 and 10 to $H\beta$ respectively. Using these values a serious problem occurs in the B and H bands because it is predicted that nearly all the flux comes from the lines. There are several possible reasons for this; The total Lyman α flux is over estimated, the ratio of Lyman α to the high ionization lines is in error, or there is an excitation gradient with the high ionization lines being weaker further out in the object. We note that the uncertain value of the total Lyman α flux given by Spinrad (1987) seems rather large implying an EW for Lyman α of about 4000Å which is much larger than the value given in Spinrad et al. (1985) of about 2000Å. Assuming that the total Lyman α flux is overestimated by a factor of 4 gives corrections of : -.31, -.14, -.15, -.11, -.03, -.31 and 0 for the $BVRIJHK$ bands. Assuming a factor of 3 gives : -.43, -.19, -.20, -.14, -.04, -.44 and -.02. Since the correction is uncertain we shall just note that the largest corrections will be made to the B and H bands and are probably a few tenths of a magnitude.

4.3.1 The Current Star Formation Rate and the Optical Spectra

We shall use the prediction for Lyman α equivalent width derived in chapter 3 (figure 3.2) to test if young stars are a plausible source of ionization. The observed equivalent width of the Lyman α is 4000\AA averaged over the entire source (Spinrad 1987), but a value of 2000\AA may be more appropriate as discussed above. This gives a rest frame EW of about 1000\AA . Such a large EW cannot be produced by a normal continuous IMF unless it is very flat. Thus, the stellar UV does not seem to dominate the hydrogen photoionization and the Lyman α flux can not be used to derive the current star formation rate.

Even if one does not accept that the ionization is produced by stellar UV one can still derive a SFR using the B or V flux (1600\AA in the galaxy frame). Since this galaxy shows no strong color gradient we shall assume that all the UV flux comes from star formation. The observed B or V flux of $6 \times 10^{-29} \text{erg cm}^{-2} \text{sec}^{-1} \text{Hz}^{-1}$ gives a 1600\AA luminosity of $10^{30} \text{erg sec}^{-1} \text{Hz}^{-1} h^{-2}$ ($q_0=0$). From equation 2.6 we derive a star formation rate of $200 M_{\odot} \text{yr}^{-1}$ ($h=.5$). Once again we stress that this estimate is very sensitive to the IMF and the cosmology. Going to a small cosmology with $q_0 = .5$ and $h=.8$ would reduce this by a factor of 6.

Finally, we can place a limit on the mass of ionized gas in 3C256 from the Lyman α flux. Assuming case B recombination and that the ionized gas has a filling factor

of 1 we can place an upper limit of about $5 \times 10^{11} M_{\odot} h^{-2.5}$ with a mean density of $.3 \text{ cm}^{-1} h^{.5}$ which is insensitive to cosmology. A filling factor less than 1 could greatly reduce the gas mass. A filling factor of .1, which may be more appropriate for a narrow line region, would reduce the mass by a factor of 100 to $5 \times 10^9 M_{\odot}$. From the star formation rate derived above and assuming an efficiency of star formation of 5% we can estimate the maximum life time of this star forming phase is less than about 10^8 years but for a smaller filling factor it could be reduced to 10^6 years.

4.3.2 The Ratio of Past to Current Star Formation

While the UV constrains the current star formation rate, it places no constraint on the past star formation history. The past star formation history is best constrained by the IR observations where the low mass giant stars emit most of their flux. Here we shall consider 2 cases: 1) That the observed SED is completely dominated by the young stellar population, 2) That the observed SED has significant flux from both an old and a young stellar population. The first case will allow us to place a firm upper limit on how long the current star formation has been continuing. The second case will place a lower limit on how much mass the young stellar population contributes relative to an older underlying population.

Let us consider the case where the SED is dominated by the young stellar population. The observed SED of 3C256 was compared with several model SEDs of various ages (Figure 4.2) from Bruzual (1983), for a star forming burst lasting 10^9

yrs with a constant star formation rate (C model) and a Miller/Scalo IMF. The best fitting SED is one with an age of 4×10^8 yrs. For older times the light from giants begins to dominate the SED and it reddens rapidly. For younger ages the light from the most massive short lived stars dominates. Wyse (1986) and Chokshi and Wright (1987) have also produced model galaxies which include an evolving AGB and carbon star population which were not included in the models by Bruzual. As the result of this additional population these models redden more rapidly than those of Bruzual, reaching the observed SED before 10^8 years. Thus, it seems safe to conclude that the young stellar component of the 3C256 SED is at most about 10^8 years old but for modeling we will assume it is represented by the 4×10^8 year old Bruzual SED. This conclusion is still true if one considers declining star formation rates or models with older underlying populations since these models have more low mass stars which tend to redden them at an earlier time.

A young stellar population is initially very luminous. Thus, it is possible that a small mass of young stars could dominate the light from an older stellar population even though the mass is dominated by the old stars. The old stellar population in the galactic bulge is thought to be older than about 10Gyrs (Frogel and Whitford, 1987). Given the look back time to the current burst of star formation in 3C256, $6.3 \text{ Gyrs } h^{-1}$ ($q_0=0$), such an old population would be a few Gyrs old in 3C256. Model SEDs were constructed of such a composite stellar population using the Bruzual C model with a Miller/Scalo IMF. One component is an "old" population which is formed

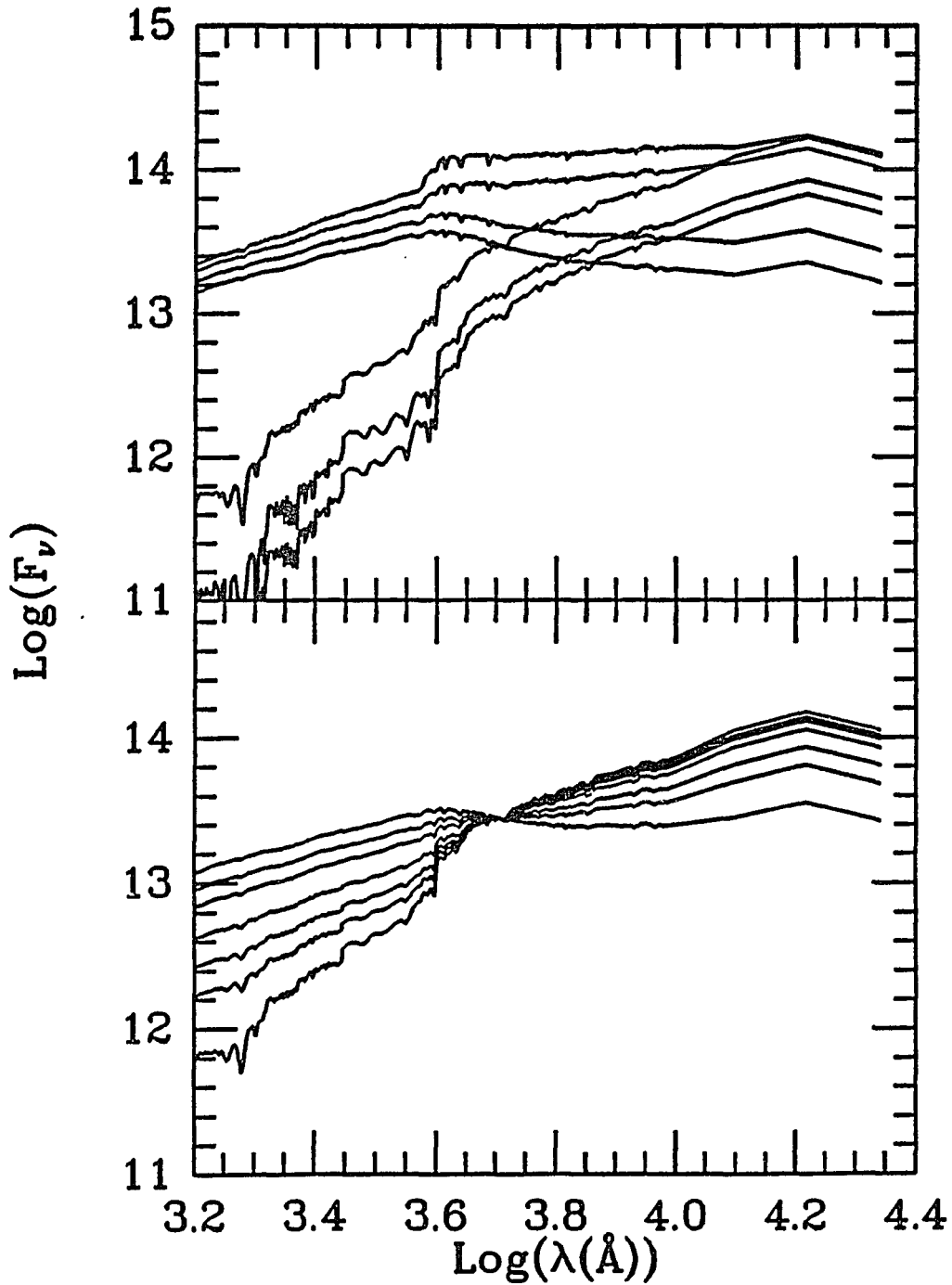


Figure 4.2: The top panel shows the SED for a Bruzual (1983) 'c' model with constant star formation for the first 10^9 years with a Miller-Scalo IMF. The top four SEDs are during the starforming phase at times of 10^9 , 4×10^8 , 10^8 , and 5×10^7 years from top to bottom. The lower three SEDs are after starformation has ceased at times of 4×10^9 , 10^{10} and 1.4×10^{10} years. The lower panel has the SEDs for a composite population composed of a 3×10^9 year old 'c' model and a 5×10^7 year old 'c' model. From top to bottom the SEDs have ratios of 50%, 30%, 10%, 5%, 1%, .5% and .05% of the young population to the old population.

in a constant SFR burst beginning 4×10^9 years before the epoch of observation and lasting 10^9 with no star formation for the following 3×10^9 yrs. Various mass ratios of a "young" population which has undergone constant star formation for 4×10^8 years were then added to make the composite SED. It appears that models with much more than half the mass in an older population can be excluded but the observed SED is consistent with no older population present at all, since the 4×10^8 year old population matches the SED.

In the previous case of a combined stellar population we placed a limit on the mass in an old stellar population assuming that the SED was completely dominated by the young stellar population. It is also possible that the SED is not completely dominated by the young stellar population but has significant contributions from both the old and the young stellar populations. These other possible star formation histories would have a stellar population younger than the age limit of 4×10^8 yrs and a larger old population to contribute the red light. There exists a whole family of these solutions. As the duration of the young star burst is reduced the ratio of the mass in the old population to the mass in the young population must increase. In effect we are replacing the light of the older red stars in the 4×10^8 yrs SED with the light from giant stars in the old population. As an example, to find what the minimum mass in the young population is, a young population with a constant star formation rate for 5×10^7 years would require an old stellar population with about 20 times the mass of the young stellar population (Figure 4.2). This result is

generally true for young populations with ages less than a few times 10^7 years since the stars which dominate the optical and near UV light are longer lived than this.

Neither solution can be discounted by the SED alone. Even if the SED has significant contributions from both an old and the young stellar population it still appears that the young population is very significant, contributing at least 5% of the mass. We can use the predicted star formation rate and the upper limit on the young population age to predict the mass of stars formed to be $2 \times 10^{10} M_{\odot}$. This is a few percent of the mass of a giant elliptical. Thus, the model with a small young population and a large old population seem to be the most consistent.

Finally, it is interesting to ask what 3C256 would look like today given its observed stellar population at $z=1.8$. In the galaxy rest frame 3C256 has a V magnitude of about $-23.3 + 5 \log h$ ($q_o=0$) or $-22.4 + 5 \log h$ ($q_o=.5$). Figure 4.3 shows models for the V band for various ratios of stellar mass formed in a constant star formation rate burst lasting 2×10^8 years and an old population formed 3×10^9 years earlier. These predictions were derived by integrating the population fading predictions of Wyse (1986). For just the old population we would expect 1.1 magnitudes of fading. For a 5% and 50% young stellar population the fading will be 1.6 and 3.8 magnitudes respectively. Therefore, the current V magnitude would be about -23.2 and -21.0 respectively (for $q_o=0$, $h=.5$). Models with larger young populations produce a less luminous galaxies at the current epoch since the young population fades more rapidly. If this object is to be the progenitor to a current day giant elliptical

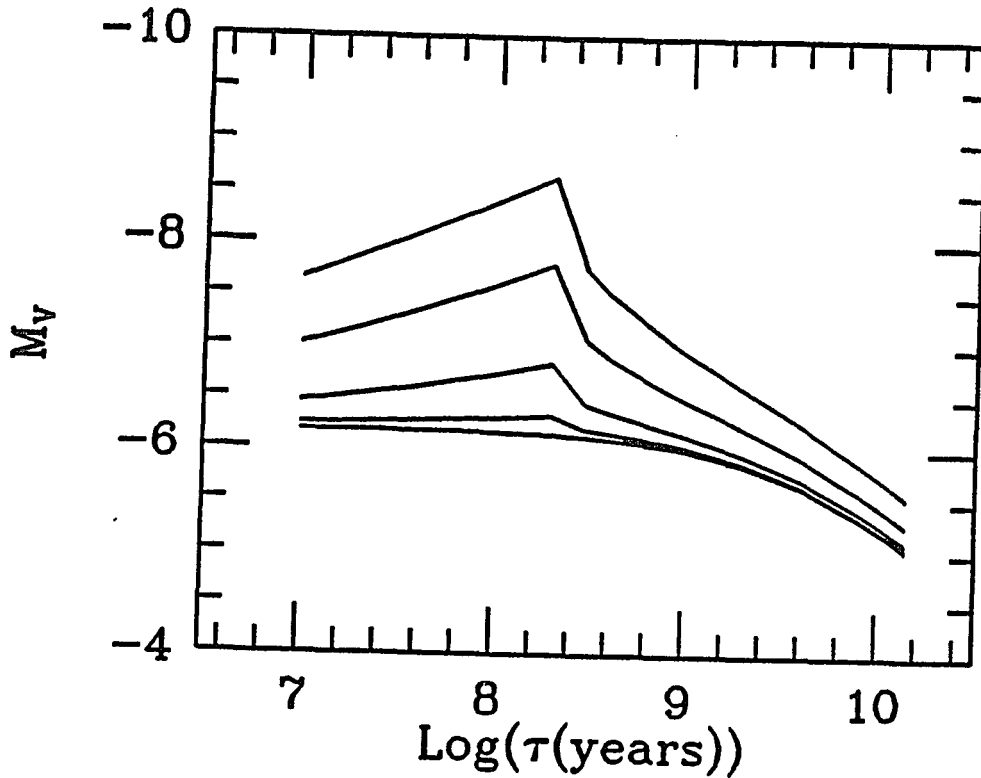


Figure 4.3: The V magnitude for a population with a 2×10^8 year burst of star formation and a 4×10^9 year old population which has had no star formation for the previous 3×10^9 years. From top to bottom the ratio of mass in the young and the old population in 50%, 30%, 10%, 5%, 1% and 0%.

galaxy, similar to current epoch radio galaxies, then a population dominated by the old stellar mass is required and only a few percent mass contribution by the young population is allowed.

To summarize this section, the SED of 3C256 indicates a large young stellar population. Unfortunately, the SED can not differentiate a moderately old star formation episode (4×10^8 years) from a composite population with a very young (10^7 years) and an old population. But a firm age limit of less than a few times 10^8 years can be placed on the young population; moreover, it must contribute

more than 5% of the total stellar mass. Two indirect arguments involving the star formation rate and the fading of the population suggest that a small young stellar population, a few percent of the total mass, may be preferred.

4.4 Discussion

In the previous section we showed that the SED of 3C256, the most extreme object in our sample, indicates it has a large young stellar population with an age less than 10^8 years contributing more than about 5% of the total mass. The current star formation rate is about $200 M_{\odot} \text{yr}^{-1}$ suggesting that the young population does contribute a few percent of the total stellar mass and that this object could be the progenitor of a giant elliptical galaxy. Since this is the most extreme object, similar but lower limits on young stellar components can be place on the other sources in the sample. Let us now look at all the sources in the sample in the context of a model with an old stellar population which dominates the IR while a small young stellar population dominates the optical and UV.

First, let us compare the IR colors of these galaxies to those of an old stellar population. Figure 4.4 shows the near IR color color diagram for the blue galaxies. The galaxies have slightly bluer IR colors than would be expected from the SED of a current day elliptical galaxy with their redshifts but the colors are very similar and show a small dispersion. The predicted IR colors are only accurate to .1 or

.2 magnitudes but the difference appears significant. If the slight blueing is real it can be attributed to the contribution of a blue continuum from the young stellar population and emission line contamination by O[II]3727 and O[III]5007 in the J and H bands. Thus, the IR SED seems consistent with being dominated by the light of an old population with a small amount of blueing due to a small young component. The lack of scatter in the IR colors of the blue galaxies is similar to that observed by Lilly and Longair (1984) in their sample of 3C radio galaxies but the observed shift in IR color is not noted by them. The small scatter is in contrast to the large amount of observed scatter for the IR colors of radio galaxies observed by Puschell et al. (1982) which may be due to large observational errors.

Also, we note that blue galaxies are not very over-luminous in the IR compared to the passively evolving prediction. We looked for correlations between the absolute K magnitudes of the galaxies with both the optical to IR colors and the redshifts assuming $q_o = 0$ and .5. We find no correlation between the optical to IR color and the K magnitude. Thus, we find that the young population does not contribute significant amounts of light at K which is expected since the near IR colors are not significantly perturbed. For both cosmologies the absolute K magnitude does correlate with redshift indicating luminosity evolution. About 1 magnitude of brightening does occur between $z=1$ and 2 which is consistent with passive evolution models (Tinsley, 1980). We also note, since the high redshift 3C galaxies are not over luminous in the near IR, then gravitational lensing does not seem to be a viable

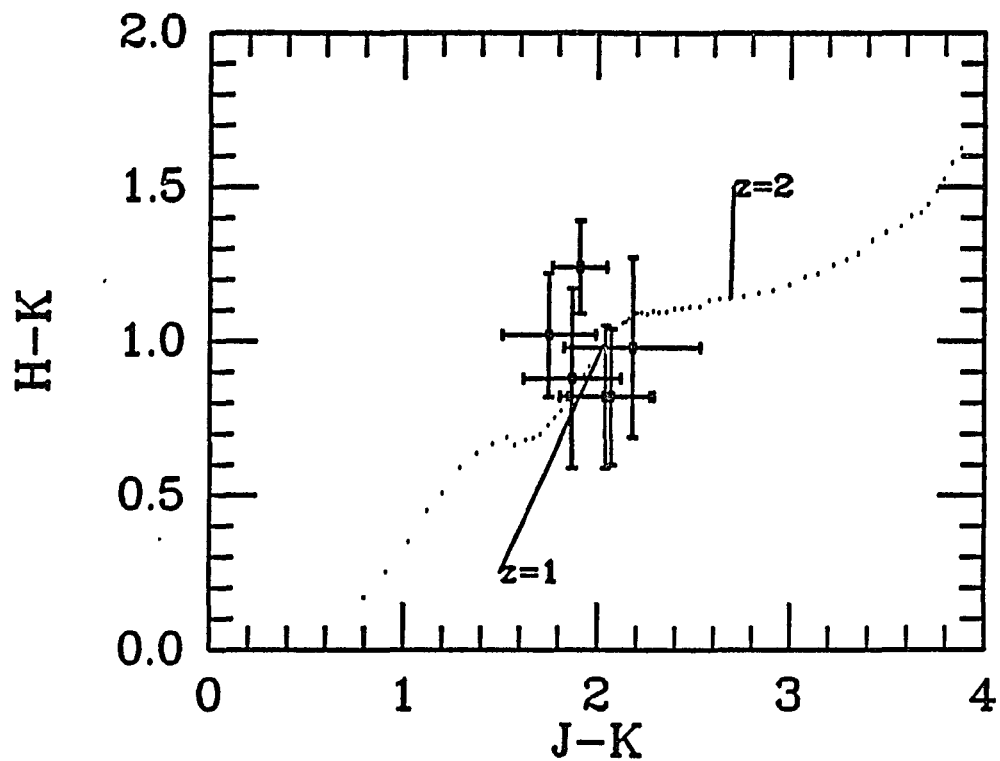


Figure 4.4: The infrared color color diagram for high redshift radio galaxies. The dotted line is the expected colors for an elliptical galaxy for redshifts between 0 and 3 at intervals of .05. The IR colors are slightly bluer than that expected from the nonevolving galaxy.

explanation for the extreme luminosity of these sources in the optical (Le Fever et al. 1988 and Hammer et al. 1986). The extreme optical luminosity is more simply explained by a small young stellar population.

A comparison with the 'c' models of Bruzual (1983) (Figure 4.2) indicates that no model with a single epoch of star formation can match these SEDs. The problem is that the observed SEDs are too blue from the UV to the optical while being red in the optical to IR. Thus, multiple generations of stars seem to be required to match the SEDs. The sequence of galaxies arranged by optical to IR colors is driven by the ratio of the young blue population to the old red population. The fundamental driving force of this sequence is the star formation rate which is approximately proportional to the UV luminosity. The bulk of the objects can be fit by a dominant population 4×10^9 years old with a small young stellar population contributing less than 1 to 2 percent of the total mass. The implied star formation rates range from $200 M_{\odot} \text{year}^{-1}$ (3C256) to about 10 or $20 M_{\odot} \text{year}^{-1}$ (3C238) ($q_0=0$, $h=.5$).

The object with the reddest optical to IR color is 3C241 ($z=1.617$) and it cannot be matched by the above composite populations since the 4×10^9 year old SED is too blue for this object. 3C241 is best matched by a 10^{10} year old Bruzual model plus a small amount of current star formation. The formation age of the old population is an uncomfortably long time before $z=1.6$ and is actually only barely possible if the Hubble constant is both very small $h \leq .5$ and the universe is very open $q_0 = 0$. The simplest explanation is that the SEDs by Bruzual become red too slowly due

to their lack of an evolving giant branch. With more complete galaxy models this object could provide an interesting upper limit on the epoch of galaxy formation given its high redshift and red optical to IR colors.

The mechanism triggering the observed star formation is not clear. The complex morphology of some of these sources has been interpreted as being due to mergers (Djorgovski et al. 1987b). For 3C368, where the IR morphology is also complex (Chambers et al. 1987), the fact that the IR colors are consistent with being dominated by an old population would imply that galaxies with large old stellar populations are merging. The major difficulty with the merger interpretation is the alignment between the radio lobes and the optical isophotes (Chambers et al. 1987, McCarthy et al. 1987). This would seem to imply that the radio lobes are somehow responsible for extended morphology. An interpretation would be that the extended IR emission and the slightly bluer IR colors are due to star formation, nonthermal emission from the hot spots or line emission associated with the radio lobes interacting with the ISM. The best test of this would be to obtain IR images to look for color gradients.

What is certain, is that for these objects we are witnessing the formation of a large intermediate age population which would be about 6-8 Gyrs old at the current epoch. This would support the view of O'Connell (1976), Pickles (1985) and Rose (1985) that spectral synthesis indicates large intermediate age populations in some nearby elliptical galaxies. Once again, the major difficulty in interpreting these

observations in the more general context of all elliptical galaxies is that we do not understand if these properties are related to the radio nature of these objects.

Chapter 5

Concluding Remarks

The point of departure for this thesis was to investigate the star forming periods of galaxies. In the preceding 3 chapters we have described three surveys for rapidly star forming galaxies and all three have found promising candidates. The IR survey described in chapter 2 was the most general of these and should have been able to detect luminous star forming galaxies at redshifts up to 25. This survey found no luminous galaxies ($K < 18$) at redshifts greater than 5. This would indicate that there is no luminous initial phase of galaxy formation when star formation rates exceed several $1000 M_{\odot} \text{year}^{-1}$. There appears to be no simple means of avoiding this limit except to raise the formation epoch above 25, to make the star forming galaxies very spatially extended, or to prolong the formation phase. This would exclude weakly dissipative rapid formation models such as Partridge and Peebles (1967). The lack of a very high luminosity star formation burst is the first conclusion of this work.

Using the IR data we did locate several objects which could be PGs at redshifts

less than 4. The best studied of these objects appears to show both a Lyman limit and Lyman α forest absorption suggesting a redshift near 4. If the redshift can be confirmed its luminosity indicates a star formation rate of several $100M_{\odot}year^{-1}$. More generally, we have found a large population of blue objects for which we have no redshift information. While one can argue that these objects contribute a significant portion of the present metals this type of analysis is rather uncertain (a factor of 10) due to the small numbers of objects and the uncertainties in the conversion of metals into luminosity and in the current metal density of the universe. Redshifts are needed to determine the star formation rates of the objects and to try and infer if we are seeing the formation of disks or spheroidal populations.

We have also tried to use quasars as sign posts for galaxies at $z=3$. This survey has found a large number of objects which show Lyman α emission characteristic of a star forming galaxy with a star formation rate of about $100M_{\odot}year^{-1}$. Here we have the additional knowledge of the redshift but it is still difficult to determine if we are witnessing young disks or spheroids forming.

Finally, we looked at the stellar populations of distant 3C radio galaxies. In these objects we have found evidence for star formation bursts with rates up to $100M_{\odot}year^{-1}$ in objects with large old stellar populations. These galaxies seem destined to become giant elliptical galaxies. Interpreting this result in terms of the formation of elliptical galaxies is dangerous since there seems to be a relation between the extraordinary radio nature of these objects and their stellar distributions.

Thus, the second conclusion of this study is that we have observed galaxies with redshifts between 1 and 4 which seem to be forming stars at the rate of about $100M_{\odot}year^{-1}$. The difficulty is to resolve whether we are observing the formation of spheroids, disks or a combination of these populations. To resolve this we need better knowledge of cosmology and a more complete understanding of the stellar populations of these objects. Techniques similar to those used in the study of the 3C galaxies should be very useful for determining if there are old stellar populations in these objects.

The fundamental question we asked at the beginning of this thesis was "are there short periods of time when galaxies form the bulk of their stars?". With the observed star formation rates of a few $100M_{\odot}year^{-1}$ it would take 10^9 years to form a galaxy mass of stars. This is indeed a short time compared to the Hubble time. But uncertainty in cosmology could decrease the star formation rate by a factor of almost 10 making the formation time similar to the Hubble time. This uncertainty in the time scale is the cause of the uncertainty in whether we are observing the formation of disks or spheroids. A long timescale implies that star formation would continue until the current epoch and thus it seems most likely that we are seeing galaxy disks.

We have also produced some interesting results not directly associated with the formation of galaxies. In the IR survey we have found a group of luminous red galaxies at redshifts near 1. These objects have optical to IR SEDs similar to

current day ellipticals but have luminosities which are as high as those of giant ellipticals. Their highly uncertain space density is perhaps 10^4 times higher than giant ellipticals. The origin of objects like these seems very difficult to explain since their SED are dominated by an evolved population and they must fade by 1 or 2 magnitudes more than other galaxies for this population to vanish by the current epoch. It does seem that light from AGB stars may play a role in these objects since the UV to optical portions of the SEDs are blue while the optical to IR portions of the SEDs are red.

The observation of possible clusters of galaxies near several $z=3$ quasars has important implications for the formation of structure in the universe and the shape of the perturbation spectrum. With more detailed observations we can compare the properties of these clusters (mass, velocity dispersion, radius) with those predicted by the scaling laws for the evolution of such properties (Kaiser, 1986). Also, a possible correlation between radio loud quasars and richer environments could have implications for the evolution of the quasar population, the nature of associated metal line systems and the origin of the exclusion effect for Lyman alpha forest absorption.

Not to break with long standing tradition we will finish this work by discussing what the next step in the progression of research should be. First priority should be given to obtaining optical spectra to secure redshifts for the blue objects found in the IR survey. Beyond this, the next step is to try and expand the sample of

objects so that reliable statistics can be compiled for blue objects and red luminous galaxies. Fortunately, IR array technology is progressing rapidly with the array area growing by a factor of 4 every year since this project began. Thus, larger surveys are attractive and a factor of 10 increase in sky coverage seems like a realistic next phase. These data will also provide the first infrared-selected galaxy sample large enough for studies of galaxy evolution and cosmology in a sample which is not biased by UV selection of distant objects.

This study has shown that quasars are reasonable sign posts for distant galaxies. Optical spectroscopy of the objects found in this way seems to be the next phase. This would provide confirmation of the objects, velocity dispersions of the clusters and clues to the metallicities of the galaxies. Also, complete optical to IR SEDs would provide useful constraints on any old population in these objects. Finally, radio observations (mJy level) of the quasars will be needed so that the natural bifurcation of the quasars into radio loud and radio quiet can be seen. Future studies should also try to expand the sample of quasars for better statistics and to probe the evolution of the populations at different redshifts.

LIST OF REFERENCES

- Azzopardi, M., Lequeux, J. and Westerlund, B.E., 1985, *Astro. Ap.*, **144**, 388.
- Bahcall, N.A., 1977, *Ann. Rev. Ast. and Astrophys.*, **15**, 503.
- Barnes, J. and Efstathiou, G., 1987, *Ap. J.*, **319**, 575.
- Baron, E. and White, S.D., 1987, *Ap. J.*, **322**, 585.
- Bajtlik, S., Duncan, R.C. and Ostriker, J.P., 1988, *Ap. J.*, **327**, 570.
- Bechtold, J., 1987, in *Third IAP workshop "High Redshift and Primeval Galaxies"*, Edited by J. Bergeron, D. Kunth, B. Rocca-Volmerange and J. Trans Thanh Van, (Paris:Editions Frontieres) p. 397.
- Bhavsar, S.P. and Barrow, J.D., 1985, *MNRAS*, **213**, 857.
- Blanco, V.M., 1988, *A. J.*, **95**, 1400.
- Boughln, S.P., Saulson, P.R. and Uson, J.M., 1986, *Ap. J.*, **301**, 17.
- Brown, G.S. and Tinsley, B.M., 1974, *Ap. J.*, **194**, 555.
- Bruzual, G.A., 1981, *Ph. D. thesis, Astronomy Department, University of California, Berkely.*
- Bruzual, G.A., 1983, *Ap. J.*, **273**, 105.
- Butcher H.R. and Oemler, A., 1984, *Ap. J.*, **285**, 426.
- Chokshi, A. and Wright, E.L., 1987, *Ap. J.*, **319**, 44.
- Chambers, K.C., Miley, G.K. and van Breugel, W., 1987, *Nature*, **329**, 604.
- Coleman, G.D., Wu, C. and Weedman, D.W., 1980, *Ap. J. Suppl. Ser.*, **43**, 393.
- Condon, J.J. and Broderick, J.J., 1986, *A 140Mhz Sky Atlas Covering $-5 < dec < +82$* , National Radio Astronomy Observatory.
- Cornell, M.E., Aarronson, M., Bothum, G. and Mould, J., 1986, *Ap. J. Suppl. Ser.*, **64**, 507.
- Couch, W.J., Ellis, R.S., Kibblewhite, E.J., Malin, D.F. and Godwin, J., 1984,

MNRAS, **209**, 307.

Cowie, L., 1987, in *The Post-Recombination Universe*, ed. N. Kaiser and A. Lasenby (NATO Advanced Science Institute Series).

Cowie, L.L., Lilly, S.J., Gardener, J. and McLean, I.S., 1988, *Ap. J.*, **332**, L29.

Cowie, L., 1985, (private communication cited in Koo 1986).

Cutri, R.M. and McAlary, C.W., 1985, *Ap. J.*, **296**, 90.

Davis, M. and Huchra, J., 1982, *Ap. J.*, **254**, 437.

Davis, M, 1980, in IAU Symp. No. 92 *Objects at High Redshift*, ed. G.O. Abell and P.J.E. Peebles, Riedel: Dordrecht, p. 57.

Deharveng, J.M, Joubert, M. and Kunth, D., 1986, in First IAP Meeting on *Star-Forming Dwarf Galaxies and Related Objects*, Ed. D. Kunth, T. X. Thuan and J.T.T. Van (Paris:Editions Frontieres) p. 431.

Djorgovski, S., Spinrad, H., McCarthy, P. and Strauss, M.A., 1985, *Ap. J.*, **299**, L1.

Djorgovski, S. and Spinrad, H., 1985, preprint.

Djorgovski, S., Strauss, M.A., Perley, R.A., Spinrad, H. and McCarthy, P., 1987a, *A. J.*, **93**, 1318.

Djorgovski, S., Spinrad, H., Pedelty, L., Rudnick, L. and Stockton, 1987b, *A. J.*, **93**, 1307.

Dressler, A., 1980, *Ann. Rev. Astr. Ap.*, **22**, 185.

Dressler, A., 1980, *Ap. J.*, **236**, 351.

Eggen, O.J., Lynden-Bell, D. and Sandage, A., 1962, *Ap. J.*, **136**, 748.

Eisenhardt, P.R.M. and Lebofsky, M.J., 1987, *Ap. J.*, **316**, 70.

Elias, J.H., Frogel, J.A., Matthews, K. and Neugenbauer, G., 1982, *A. J.*, **87**, 1029.

Ellis, R., 1987, in IAU Sym. No. 124 *Observational Cosmology*, ed. by A Hewitt, G. Burbidge and Li Zhi Fang, Dordrecht: Reidel, p. 367.

- Ellis, R.S., 1983, in *The Origins and Evolution of Galaxies*, ed. B.J.T. Jones and J.E. Jones, Dordrecht: Reidel, p. 255.
- Elston, R., Rieke, G.H. and Rieke, M.J., 1988, *Ap. J. (Letters)*, **331**, L77.
- Efstathiou, G., Ellis, R.S. and Peterson, B.A., 1988, *MNRAS*, **232**, 431.
- Ferland, G. and Netzer, H., 1979, *Ap. J.*, **229**, 274.
- Foltz, C.B., Weymann, R.J., Peterson, B.M., Sun, L., Malkan, M.A. and Chaffee, F.H., 1986, *Ap. J.*, **307**, 504.
- Frogel, J.A. and Whitford, A.E., 1987, *Ap. J.*, **320**, 199.
- Freeman, K.C., 1970, *Ap. J.*, **160**, 811.
- Freeman, W.L. , 1985, *Ap. J.*, **299**, 74.
- Groth, E.J. and Peebles, P.J.E., 1977, *Ap. J.*, **217**, 385.
- Gunn, J.E., Hoessel, J.G. and Oke, J.B., 1986, *Ap. J.*, **306**, 30.
- Hamilton, D., 1985, *Ap. J.*, **297**, 371.
- Hammer, F., Nottale, L. and Le Fever, O., 1986, *Astr. Ap.*, **169**, L1.
- Hartman, L.W., Huchra, J.P., Geller, M.J., O'Brien, P. and Wilson, R., 1988, *Ap. J.*, **326**, 101.
- Hazard, C., Morton, D.C., McMahon, R.G., Sargent, W.L.W. and Terlevich, R., 1986, *MNRAS*, **223**, 87.
- Hogan, C.J., 1987, *Ap. J. (letters)*, **316**, L59.
- Hoyle, F., 1949, in *Problems of Cosmical Aerodynamics*, Dayton Ohio: Central Air Documents Office, p. 195.
- Hu, E. and Cowie, L.L., 1987, *Ap. J. (letters)*, **317**, L17.
- Hubble, E.P and Tolman, R.C., 1935, *Ap. J.*, **82**, 302.
- Iben, I. Jr. and Renzini, A., 1983, *Ann. Rev. Astron. Ap.*, **21**, 271.
- Kaiser, N., 1986, *MNRAS*, **222**, 323.

Kennicutt, R.C., 1983, *Ap. J.*, **272**, 54.

Kennicutt, R.C., 1988, personal communication.

Kormendy, J., 1977, *Ap. J.*, **218**, 333.

Koo, D.C. and Kron, R.G., 1987, in IAU Sym. No. 124 *Observational Cosmology*, ed. by A Hewitt, G. Burbidge and Li Zhi Fang, Dordrecht: Reidel, p. 383.

Koo, D.C., 1986a, *Spectral Evolution of Galaxies*, ed. C. Chiosi and A. Renzini, Dordrecht: Riedel, 419.

Koo, D.C., 1986b, *Ap. J.*, **311**, 651.

Koo, D.C., 1985, (cited in Koo, 1986).

Koo, D.C. and Kron, R.G., 1980, *PASP*, **92**, 537.

Koo, D.C., Kron, R.G., Nanni, D., Trevese, D. and Vignato, A., 1986, *Astron. and Astrophys.*, **91**, 478.

Kron, R.G., 1980, *Physica Scripta*, **21**, 652.

Kunth, D. and Sargent W.L.W., 1986, *Ap. J.*, **300**, 496.

Kurucz, R.L., 1979, *Ap. J. Supl. Ser.*, **40**, 1.

Larson, R.B., 1986, *MNRAS*, **218**, 409.

Larson, R.B., 1974, *MNRAS*, **166**, 585.

Larson, R.B., and Tinsley, B.M., 1978, *Ap. J.*, **219**, 46.

Leach, R. and Lesser, M., 1987, *PASP*, **99**, 668.

Lebofsky, M.J. and Eisenhardt, P.R.M., 1986, *Ap. J.*, **300**, 151.

Le Fevre, O., Hammer, F., Nottale, L., Mazure, A. and Christian, C., 1988, *Ap. J.*, **324**, L1.

Le Fevre, O., Hammer, F. and Jones, J., 1988, *Ap. J. (letters)*, **331**, L73.

Lequex, J., Maucherat-Joubert, M., Deharveng, J.M. and Kunth, D., 1981, *Astron. Astrophys.*, **103**, 305.

- Lilly S.J., 1987 , *MNRAS*, **229**, 573.
- Lilly S.J. and Longair, M.S., 1984, *MNRAS*, **211**, 833.
- Lilly, S.J., Longair, M.S., and McLean, I.S., 1983, *Nature*, **301**, 488.
- Lilly, S.J., Longair, M.S. and Allington-Smith, J.R., 1985, *MNRAS*, **215**, 37.
- Loh, E.D. and Wilkinson, D.T., 1979 (see private comm. in Davis 1980)
- Lonsdale, C.J., Person, S.E., and Matthews, K., 1984, *Ap. J.*, **287**, 95.
- Mackey, 1985, (Cited by Koo 1986a).
- Matsumoto, T., Akiba, M., and Murakami, H., 1988, *Ap. J.*, **332**, 575.
- McCarthy, P.J., van Breugel, W., Spinrad, H. and Djorgovski, S., 1987, *Ap. J.*, **321**, L29.
- Meier, D.L., 1976, *Ap. J.*, **207**, 343.
- Meier, D.L., and Terlevich, R., 1981, *Ap. J. (letters)*, **246**, L109.
- Melnick, J., 1986, in *First IAP Meeting on Star -Forming Dwarf Galaxies and Related Objects*, Ed. D. Kunth, T. X. Thuan and J.T.T. Van (Paris: Editions Frontieres) p. 171.
- Mould, J., 1986, in *Stellar Populations*, ed. C. Norman, A. Renzini and M. Tosi, Cambridge University Press, p. 29.
- Murdoch, H.S., Humstead, R.W., Pettini, M. and Blades, J.C., 1986, *Ap. J.*, **309**, 19.
- Norris, J., 1986, *Ap. J. Supl.*, **61**, 667.
- O'Connell, R.W., 1976, *Ap. J.*, **206**, 370.
- Oke, J.B., 1974, *Ap. J. Suppl.*, **27**, 21.
- Osterbrock, D.E., 1974, *Astrophysics of Gaseous Nebulae*, W.H. Freeman and Company: San Francisco.
- Partridge, R.B., 1974, *Ap. J.*, **192**, 241.

- Partridge, R. B. and Peebles, P.J.E., 1967, *Ap. J.*, **147**, 868.
- Pickles, A.J., 1985, *Ap. J.*, **296**, 340.
- Postman, M. and Geller, M.J., 1984, *Ap. J.*, **281**, 95.
- Pritchet, C. and Hartwick, D., 1988, *Toward Understanding Galaxies at Large Redshift*, Ed. R.G. Kron and A. Renzini, Kluwer Academic Publisher: Holland, 213.
- Puschell, J.J., Owen, F.N., and Laing, R.A., 1982, *Ap. J. (letters)*, **257**, L57.
- Renzini, A., 1986, in *Stellar Populations*, ed. C. Norman, A. Renzini and M. Tosi, Cambridge University Press, p. 213.
- Renzini, A. and Buzzoni, A., 1986, *Spectral Evolution of Galaxies*, ed. C. Chiosi and A. Renzini, Dordrecht: Reidel, p. 321.
- Rieke, G.H., Cutri, R., Black, J.H., Kailey, W.F., McAlary, C., Lebofsky, M.J. and Elston, R., 1985, *Ap. J.*, **290**, 116.
- Rieke, M.J., Rieke, G.H. and Montgomery, E.F., 1987, in *Infraed Astronomy with Arrays*, Ed. C.G. Wynn-Williams and E.E. Becklin, University of Hawaii: Institute for Astronomy, p. 213.
- Rose, J.A., 1985, *A. J.*, **90**, 1927.
- Salpeter, E.E., 1955, *Ap. J.*, **121**, 161.
- Sandage, A.R., 1972, *Ap. J.*, **173**, 485.
- Sandage, A.R., 1986, in *Stellar Populations*, ed. C. Norman, A. Renzini and M. Tosi, Cambridge University Press, p. 29.
- Sargent, W.L.W., Young, P.J., Boksenberg, A. and Tytler, D., 1980, *Ap. J. Suppl.*, **42**, 41.
- Schild, R.E., 1983, *PASP*, **95**, 1021.
- Schmidt, M.J, Schneider, P., and Gunn, J.E., 1986, *Ap. J.*, **310**, 518.
- Schechter, P., 1976, *Ap. J.*, **203**, 297.
- Schneider, D., Gunn, J.E., Turner, E., Lawrence, C., Schmidt, M., and Burke, B., 1987, *A. J.*, **94**, 12.

- Schweizer, F., 1982, *Ap. J.*, **252**, 455.
- Shanks, T., Stevenson, P.R.F., Fong, R. and MacGillivray, H.T., 1984, *MNRAS*, **206**, 767.
- Spinrad, H. and Djorgovski, S., 1984, *Ap. J. (letters)*, **285**, L49.
- Spinrad, H., Filippenko, A.V., Wyckoff, S., Stocke, J.T., Wagner, R.M., and Lawrie, D.G., 1985, *Ap. J.*, **299**, L7.
- Spinrad, H., 1986, *PASP*, **98**, 269.
- Spinrad, H., 1987, in Third IAP workshop *High Redshift and Primeval Galaxies*, Edited by J. Bergeron, D. Kunth, B. Rocca-Volmerange and J. Trans Thanh Van, (Paris:Editions Frontieres) p. 59.
- Spinrad, H. and Djorgovski, S., 1988, private communication.
- Stone, R.P.S., 1977, *Ap. J.*, **218**, 767.
- Stockton, A. and MacKenty, 1987, *Ap. J.*, **316**, 584.
- Struck-Marcell, V. and Tinsley, B.M., 1978, *Ap. J.*, **221**, 562.
- Tinsley, B.M., 1980, *Ap. J.*, **241**, 41.
- Terndrup, D., 1988, *A. J.*, **96**, 884.
- Toomre, A., 1977, in *The Evolution of Galaxies and Stellar Populations*, ed. B.M. Tinsley and R. Larson, New Haven: Yale Univ. Obs., p. 401.
- Twarog, B.A., 1980, *Ap. J.*, **242**, 242.
- Tyson, J.A., 1988, *A. J.*, **96**, 1.
- Tytler, D., 1987, *Ap. J.*, **321**, 49.
- Walsh, D., Lebofsky, M.J., Rieke, G.H., Shore, D. and Elston, R., 1985, *MNRAS*, **212**, 631.
- Wyse, R.G., 1985, *Ap. J.*, **299**, 593.
- Van den Bergh, S., 1975, *Ap. J. (letters)*, **198**, L1.

- Veron-Cetty, M.P. and Veron, P., 1984, *A Catalogue of Quasars and Active Nuclei*, ESO Scientific Report No 1.
- Warren, S.J., Hewett, P.C., Osmer, P.S. and Irwin, M.J., 1987a, *Nature*, **330**, 453.
- Warren, S.J., Hewett, P.C., Irwin, M.J., McMahon, R.G., Bridgeland, M.T., Bunclark, P.S. and Kibblewhite, 1987b, *Nature*, **225**, 131.
- Weedman, D., 1985, *Ap. J. Supl.*, **57**, 523.
- Winget, D.E., Hansen, C.J., Liebert, J., Van Horn H.M., Fontaine, G., Nather, R.E., Kepler, S.O. and Lamb, D.Q., 1987, *Ap. J.*, **315**, L77.
- Weymann, R.J., Williams, R.E., Peterson, B.M. and Turnshek, D.A., 1979, *Ap. J.*, **218**, 619.
- Weymann, R.J., Carswell, R.F. and Smith, M.G., 1981, *Ann. Rev. Astr. Ap.*, **19**, 41.
- Wynn-Williams, C.G. and Becklin, E.E., 1987, *Infrared Astronomy with Arrays*, University of Hawaii: Institute for Astronomy.
- Wyse, R. G., 1985, *Ap. J.*, **299**, 593.
- Yee, H.K.C. and Green, R.F., 1984, *Ap. J.*, **280**, 79.
- Yee, H.K.C. and Green, R.F., 1987, *Ap. J.*, **319**, 28.
- Young, P., Sargent, W.L.W. and Boksenberg, A., 1982, *Ap. J. Suppl.*, **48**, 455.
- Zinn, R., 1985, *Ap. J.*, **293**, 424.